ANALYSIS OF ANTIBODY REACTIVITIES IN LYSOZYME-IMMUNIZED MICE WITH PEPTIDE LIGANDS: A MODEL FOR EPITOPE-TARGETED VACCINE DESIGN

by

Melita Borg Irving
B.Sc., University of Waterloo, 1997

THESIS SUBMITTED IN PARTIAL FULFILLMENT OF
THE REQUIREMENTS FOR THE DEGREE OF

DOCTOR OF PHILOSOPHY

In the
Department
of
Molecular Biology and Biochemistry

SIMON FRASER UNIVERSITY

Spring 2006

APPROVAL

Name: **Melita Borg Irving**

Degree: Doctor of Philosophy

Title of Thesis: Analysis of Antibody Reactivities in Lysozyme-Immunized Mice with Peptide Ligands: A Model for Epitope-Targeted Vaccine Design

Examining Committee:

Chair: **Dr. Andrew Beckenbach**
Professor, Dept. of Biological Sciences
Department of Molecular Biology and Biochemistry

Dr. Jamie Scott
Senior Supervisor
Professor, Dept.of Molecular Biology and Biochemistry

Dr. Lynne Quarmby
Committee Member
Associate Professor, Dept. of Molecular Biology and Biochemistry

---

Dr. David L. Baillie
Committee Member
Professor, Dept. of Molecular Biology and Biochemistry

Dr. Margo Moore
Internal Examiner
Associate Professor, Dept. of Biological Sciences

Dr. John Schrader
External Examiner
Professor, British Columbia Research Centre, University of British Columbia

Date Approved: January 9, 2006

ABSTRACT

Many viruses evade antibody (Ab)-mediated clearance through the presentation of immunodominant, highly variable epitopes, and the masking of conserved ones. It has been proposed that vaccines incorporating peptides that cross-react with conserved epitopes could be used to target the production of Abs that protect against a range of viral isolates.

For this thesis the concept of *epitope-targeted vaccine design* is explored with the model protein hen egg lysozyme (HEL). The goals of the work are to develop peptide markers for murine anti-HEL Abs that can also be used as immunogen to amplify Ab production against target HEL epitopes. Three types of peptides are analyzed: (i) a peptide selected from a phage-displayed random peptide library (RPL) with the anti-HEL monoclonal Ab D1.3, (ii) peptides identified from RPLs with polyclonal (pc) Abs from the sera of HEL-immunized mice, and, (iii) peptides derived from the linear sequence of HEL.

A peptide selected with D1.3 Ab shares critical binding residues in common with its cognate discontinuous epitope but showed no reactivity with anti-HEL sera. A prime-boost immunization study, in which mice were primed with HEL to produce anti-HEL pcAbs, and boosted with the peptide to amplify the production of D1.3 or D1.3-like Abs, did not yield cross-reactive Abs. Thus, D1.3 Ab may not have been produced in the priming immunization because it is a rare specificity in the immune response to HEL. A peptide marker for an anti-HEL Ab commonly produced amongst mice was identified in a RPL screening with anti-HEL pcAbs. The commonly reactive peptide was also used in ELISPOT analysis to characterize epitope-specific B cell responses to HEL; the peptide-reactive cells represented less than 1% of IgG-producing B cells. The peptide was not recognized by anti-HEL IgG from rabbit, however, emphasizing the limitations of using animal models for developing epitope-targeted vaccines. Lastly, a set of 10-mer overlapping HEL peptides showed common patterns of reactivity with different murine anti-HEL sera. These findings indicate that common HEL epitopes are targeted amongst mice in the humoral immune response to HEL and that a prime-boost immunization strategy may succeed with a commonly reactive peptide marker.

Key Terms: Antibody, Vaccine Design, Epitope, Hen Egg Lysozyme, Phage-displayed random peptide libraries

DEDICATION

This thesis is dedicated to my husband James.

James, I am both grateful and glad that I made this journey with you by my side.

Thank you.

ACKNOWLEDGEMENTS

During my graduate studies at SFU I have had the pleasure of working with many wonderful and talented people who have truly enriched my life. I would like to thank my friends and colleagues Alfredo Menendez and Marinieve Montero for their advice and technical support, as well as for inviting me into their home for many delicious meals. Thanks also to my lab mates Sondra Bahr, Ruth Featherstone, Tannika Grant, Nienke van Houten, Martina Mai, Joanna Chodowska, Heather Sarling, Sampson Wu, Sonia Statsny, Dawn Armstrong, Xin Wang, Chao Wang, Mike Chow, Keith Chow, Oscar Pan, Juqun Shen, Brett Vanderkist, Jessie Yoon and Karina Shi for their camaraderie. I would also like to acknowledge the many other technicians and undergraduates who have been a delight to work with in the lab over the years.

My former roommate Himani Utkhede is a dear friend and I thank her for many fond memories as well as for her consideration during difficult times. Thanks also to other friends in the department who have been there to share in laughter and fun over the years.

Thank you to my supervisor Jamie Scott for accepting me into her lab, for her financial support, and for challenging me constantly, both as a person and as a scientist. Thanks to my committee members, Drs. Lynne Quarmby and Dave Baillie for their helpful discussions, support and guidance. Thanks to the other members of my examining committee, Drs. Margo Moore and John Schrader, for their time and effort in evaluating my research.

Lastly, I would like to thank my parents Keith and Sheila Hipel, and my in-laws, Sharon and Doug Irving, for their encouragement, love, and emotional support. Thanks also to my brothers Lloyd, Conrad and Warren, and my brother-in-law John for being a part of my life. Most importantly, thank you to my husband James for his unconditional love and support, for helping to keep me balanced, and for bringing so much adventure into my life; I look forward to many more travels abroad and back-packing trips, and all that the future holds for us.

TABLE OF CONTENTS

LIST OF FIGURES

LIST OF TABLES

ABBREVIATIONS

Ab	Antibody
ABTS	2,2;-azino-bis(3-ethylbenzthiazoline-6) sulfonic acid
Agn	Antigen
AMP buffer	9.58% 2-amino-2-methyl-1-propanol, 1mM $MgCl_2$, 0.01% Triton-X-405, pH 9.8
BCR	B cell receptor
Bio-	Biotinylated
BSA	Bovine serum albumin
D	Solid-phase screening
ds	Double-stranded
DTT	Dithiothreitol
ELISA	Enzyme-linked immunosorbent assay
ELISPOT	Enzyme-linked immunospot
f88-4 phage	f88 phage
Fab	Antigen binding fragment of an antibody
FBS	Fetal bovine serum
Fc	Comprises two, disulfide bonded, C-terminal halves of the two antibody heavy chains
Fv	Heterodimeric variable fragment of an antibody
GC	Germinal centre
Gln	Glutamine
h	Hours
H	Heavy chain
H1, H2, H3	Hypervariable loops 1,2 and 3 of the heavy chain
HEL	Hen egg lysozyme
HIV-1	Human immunodeficiency virus-type 1
HRP	Horse radish peroxidase
IC_{50}	Inhibitory concentration required to reduce ELISA signals to 50%
Ig	Immunoglobulin
ip	Intraperitoneal
Kd	Dissociation constant
L	Light Chain
L1, L2, L3	Hypervariable loops 1,2 and 3 of the light chain
LT	Lymphoid tissue
MAb	Monoclonal antibody
MBP	Maltose binding protein
ME	Mercaptoethanol
MHC	Major histocompatibility complex
min	Minutes
N	In-solution phase screening
NFDM	Non fat dry milk
Nt	Neutralizing
O.D.	Optical density
ON	Overnight

PBS	Phosphate-buffered saline
PBS/NFDM/Tw	Phosphate-buffered saline, 5% (w/v) non-fat dried milk, 0.2% (v/v) tween-20
pcAbs	Polyclonal Abs
PCR	Polymerase chain reaction
RT	Room temperature
sIg	Surface immunoglobulin
SA	Streptavidin
sc	Subcutaneous
ss	Single-stranded
Strep	Streptomyocin
TBS	Tris-buffered saline
TBS/BSA	Tris-buffered saline, 2% (w/v) bovine serum albumin
TBS/BSA/Tw	Tris-buffered saline, 1% (w/v) bovine serum albumin, 0.1% (v/v) tween-20
TCR	T cell receptor
TD	Thymus-dependent
Tet	Tetracycline
TI	Thymus-independent
Tw	Tween-20

CHAPTER 1 THESIS INTRODUCTION

1.1 Epitope-Targeted Vaccines

Antibody (Ab) is produced and secreted by specialized B cells called plasma cells. Ab helps defend against extracellular pathogens, such as encapsulated bacteria, and viruses in the extracellular phases of their life cycle by binding directly to proteins or glycoproteins on their surfaces. The region of an antigen (Agn) that is recognized by the binding site, or paratope, of an Ab molecule, is called an epitope. Through direct interactions with Agn, Ab functions by neutralizing (Nt), opsonizing and/or initiating activation of the complement system, and by activating other cells such as macrophages and mast cells. Although a broad range of Abs is typically elicited in response to infection or immunization, only some of them are 'functional' and capable of Nt the pathogen (1) (2). The remaining Ab specificities do not provide protection and, in some instances, have been shown to enhance infectivity or block the effects of NtAbs (3) (4) (5). The importance of Nt Ab production cannot be understated, as it is a feature common to most effective vaccines currently in use for humans; the vaccines against polio, measles, tetanus, diphtheria, pertussis and hepatitis B all protect *via* Nt Abs (6).

Most vaccines are designed to mimic natural infection without causing actual disease. This is accomplished by immunizing with attenuated or killed pathogen, or surface protein(s) derived from the pathogen (subunit vaccines). Although this approach has been successful for the design of many vaccines, none have been successfully developed against tuberculosis or leprosy, or against many parasitic diseases such as malaria, leishmaniasis and schistosomiasis. There are also no vaccines against many viruses, including human immunodeficiency virus (HIV), dengue, Epstein- Barr virus, cytomegalovirus, rotaviruses, respiratory syncytial virus and herpes simplex virus. Moreover, some antiviral vaccines currently in use, like those against measles and mumps, do not offer complete protection (7).

For this thesis, due to the complexity and extensive differences in the characteristics of various pathogenic agents (*i.e.*, their life-cycles, modes of infectivity *etc.*), vaccine design will be considered with respect to viral agents only. Also, although Nt Abs alone are not sufficient to control or eliminate many pathogens because they persist extra-lymphatically in neurons,

granulomas or epithelial cells (cytotoxic T cell-mediated effector mechanisms are required for clearance), this thesis focuses solely on Ab responses to immunization.

The recurring shortcoming in the immune system's defence against many viruses appears to be the lack of production of Abs that bind and Nt the pathogen - natural infections sometimes elicit poor functional Ab responses (8) (9). Persistent and annually recurring pathogens often evade immune clearance through the presentation of immunodominant, hypervariable or repeated epitopes that play little or no role in protection when targeted by the immune response (10). Also, sometimes the *conserved* Nt epitopes (*i.e.*, sites on a pathogen that are in common amongst mutants) are difficult targets for Abs because they are camouflaged by heavy glycosylation, or they are thermostably concealed and exposed only briefly during the infection process (11). For example, although the immune system rapidly generates many Abs in response to natural infection with HIV-1, few of them are Nt, or they are quickly rendered non-Nt by minor antigenic variations of the virus (12) (13) (14). The masking of conserved Nt epitopes, along with the rapid rate of mutation of HIV-1, helps HIV-1 to evade immune clearance by Abs.

For rapidly evolving pathogens such as HIV-1 that bear conserved Nt epitopes, developing a vaccine that specifically targets the production Nt Abs against these sites would be an important step in improving vaccine design. Such Nt Ab specificities could help in preventing HIV-1 infection, or help to attack potential escape mutants in a person already infected with the virus. This approach is called "epitope-targeted vaccine design". Major efforts are being undertaken by many labs, including our own, to develop a vaccine against HIV-1 that elicits Nt Abs against conserved epitopes on surface coat proteins and are thus effective against a wide spectrum of HIV-1 strains.

Remarkably, only five broadly Nt anti-HIV-1 Abs, b12, 2F5, 4E10, 2G12 and 447-52D, have been identified to date. The broadly NtAbs have been well characterized and they bind to either the exterior of the coat protein gp120 or to the transmembrane gp41 envelope glycoprotein (15) (13). Interestingly, four of the five of the broadly-Nt Abs are characterized by having long VH3 regions (described in section 1.3, page 5), a feature common in human Ab responses to viral infections (16), and they appear to be highly mutated from their germline genes (17). Although 2G12 does not bear a long VH3 region, it is considered an unusual Ab because there is "domain swapping" of the heavy and light chains (each heavy chain "twists" in order to interact with both light chains) (18). It is unknown when broadly-Nt Ab emerges during the course of HIV-1 infection but they are thought to be rare specificities. Research conducted in our lab has involved the identification, characterization and optimization of peptide ligands for the broadly-Nt anti-

HIV-1 Abs, b12, 2G12, 2F5 and 4E10 (19) (20). The peptide candidates identified have potential use in diagnostics, therapeutics and most significantly for epitope-targeted vaccine design. With the ultimate goal of producing epitope-targeted vaccines against relevant pathogens, the purpose of this thesis is to explore the concept of epitope-targeted vaccine design with the readily accessible and well-characterized model protein, hen egg lysozyme (HEL).

1.2 Peptide-based vaccines

The idea of developing peptide-based vaccines to specifically elicit Nt Abs was first introduced in the early eighties (21) (22). It was proposed that peptide mimics of Nt sites might provide a means of directing the production of Nt Abs against epitopes that may not be immunodominant in the context of the whole pathogen. It is not uncommon for Abs to cross-react with structurally similar but distinct antigenic molecules. In some instances the Ab binds with higher affinity to the cross-reactive molecule than the original immunogen; this phenomenon is called "heteroclitic binding" (23). Two molecules are defined as "cross-reactive" or "antigenic mimics" of one another if they are capable of binding to a common Ab specificity, and they are further characterized as "structural mimics" if they share the same mechanism of binding to the Ab (*i.e.*, they make the same atomic contacts with the all or part of the Ab paratope). Conversely, the Ab specificity can itself be described as cross-reactive because it binds to two different molecules. It is important to note, however, that although two molecules may be cross-reactive (*i.e.*, they bind to the same Ab), they are not necessarily "immunogenic mimics" of one another - even though two molecules bind a common Ab specificity, they may not both be capable of eliciting that Ab specificity *in vivo*.

A strategy for identifying peptides that could potentially elicit Abs capable of recognizing pre-specified sites on a target protein, is to use Nt monoclonal (M) Abs that have been raised against whole Agn to select cross-reactive peptides. These peptides can be identified from a panel of synthetic peptides derived from the sequence of the native Agn (24) or they can be selected from a gene-fragment library (randomly digested gene fragments of a pathogen's genome are recombinantly expressed on phage) (25) (26), or from phage-displayed random peptide libraries (RPL) (27). The cross-reactive peptides must then be tested for their immunogenic properties in the context of the proper carrier, adjuvant and animal model system. The Abs elicited by the cross-reactive peptide immunogen must be capable of Nt the pathogen *in vitro* and providing protection *in vivo*. In this way, the peptide lead is shown to be both cross-reactive and an immunogenic mimic of the target epitope: the peptide is cross-reactive because it

can bind to the same Ab as its cognate epitope and it is an immunogenic mimic by virtue of its ability to elicit Ab(s) that cross-react with its cognate epitope.

Thus far, there has been limited success in the application of peptide vaccines and although several peptide candidates have undergone clinical trials, as of yet, none are licensed for use as vaccines in humans (28). In the nineties, however, a peptide vaccine for canine parvovirus was developed that matched the efficacy of the classical vaccine (based on inactivated virus) (29). Moreover, others have identified cross-reactive peptide ligands with Nt MAbs against the measles virus (30), respiratory syncytial virus (31), murine coronavirus (32), herpes simplex virus 2 (33) (34), *Neisseria meningitidis* (35), and *Schistosoma mansoni* (36) that successfully conferred protection in mice against challenge with the native pathogen. Continued research efforts are needed to fully explore the potential of peptide-based vaccines, especially for major pathogens, such as HIV-1, for which traditional vaccine design has thus far failed.

There are several advantages of administering synthetic peptide vaccines over conventional ones including safety, cost, stability and relative ease of production. To effectively elicit an immune response, synthetic peptides are usually conjugated to a carrier protein, either recombinantly or *via* a chemical cross-linking agent. Classical carrier proteins, such as ovalbumin (OVA), tetanus toxoid and keyhole limpet hemocyanin, provide T helper (T_H) cell help needed for the affinity maturation of Ab responses, isotype switching, and memory B cell production. Interestingly, an individual B cell can receive help from T_H cells specific for different antigenic peptides (not derived from the Agn that BCR recognizes) as long as the B cell can present those determinants to the T_H cells. Mitchison and others (37) first demonstrated this phenomenon in the late 1960s and early 1970s in their studies of the immune response to haptens conjugated to carrier proteins. They observed that, in order to induce an optimal secondary Ab response against a hapten, the experimental animal must be primed and boosted with the same hapten-carrier conjugate, not just the same hapten. Their analysis of the cell populations ultimately showed that T_H cells recognize the carrier and B cells recognize the hapten. This principle is known as the "carrier effect" and it has implications in immunization strategies – for an optimal secondary Ab response, it may be important to hold T_H cell epitopes in common for the priming and boosting immunizations.

Recombinant filamentous phage particles have also been used as immunogenic carriers to induce anti-peptide Ab responses, even in the absence of adjuvant (38). Phage particles were first used directly as immunogens in the late eighties by de la Cruz *et al.* (39). In the early nineties, Schellekens *et al.,* showed that a peptide, derived from a RPL with a MAb specific for

glycoprotein G of herpes simplex virus type-1, could be used to confer protective immunity to infection in mice. Since then, other immunization studies have also demonstrated that recombinant phage can elicit Abs that cross-react with native Agn and provide protection *in vivo* (32) (33) (30).

An advantage of using phage over classical carrier proteins in immunization strategies is that B cell epitopes are mostly limited to 10-12 of the outer residues of the major coat protein (pVIII) and the approximately 350 residue outer domain of the minor coat protein (pIII) (40). Thus, phage particles elicit a somewhat restricted Ab response as compared to classical carrier proteins. A disadvantage, however, is that T_H cell help is also more limited with a phage carrier than a classical carrier protein such tetanus toxoid. This limitation, however, can potentially be overcome by cross-linking a promiscuous or 'universal' T cell epitope, such as peptide fragment 830-844 of tetanus toxoid (41) or a peptide derived from the circumsporozoite protein of the malarial parasite *Plasmodium falciparum* (42), to the phage carrier.

1.3 Antigen-antibody interactions

There are four major isotypes of secreted Ab, immunoglobulin (Ig) G, IgM, IgE, and IgA. IgG and IgM protect against Agns in the blood and lymphatic system, IgA protects on mucosal surfaces, and IgE triggers basophils and mast cells in skin and mucosae to release vasoactive and inflammatory mediators. The general features of the human IgG molecule are shown in Figure 1.1. IgG, the major Ab isotype found in the blood and lymphatic system, is composed of two identical polypeptide chains of about 450 amino acids (the heavy (H) chains) covalently linked through disulfide bridges to two identical polypeptide chains of approximately 250 residues (the light (L) chains). The L chain genes are generated by recombination of one κ or λ variable (V) gene with one joining (J) segment and a constant (C) region gene. The H chain gene involves an additional element, a diversity (D) gene segment. Each H chain has four domains of two anti-parallel beta sheets, VH found at the N-terminus, and CH1, CH2 and CH3. (A hinge region connects the CH1 and CH2 domains.) Each L chain has two domains, VL (found at the N-terminus) and CL (Figure 1.1).

Figure 1.1. The human IgG molecule.

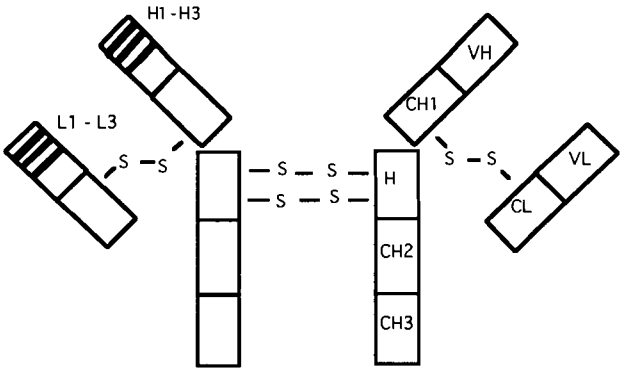

The IgG molecule comprises two identical H chains and two identical L chains linked to one another *via* disulfide bridges.

The surface of the Ab paratope (there are two paratopes per Ab molecule) is found at the N-terminus of the VH and VL domains, and is mainly composed of six hypervariable loops (H1-H3 and L1-L3) that are held in place by the framework of the Ig fold of the VH and VL domains (Figure 1.1) (43). The hypervariable loops roughly correspond to the complementary determining regions identified in the Ab sequencing studies of Wu and Kabat (44). The central paradigm of Ab-Agn interactions is that the three-dimensional structure of the six hypervariable loops binds to a chemically and structurally, complementary surface on Agn (45).

The hypervariable loops vary both in sequence and in length, with H3, the site of V-D-J recombination, bearing the greatest diversity. H3 and L3 normally dominate in terms of buried surface area and H3 usually forms the geometrical centre of the interface with Agn (46). With the exception of H3, all of the loops form a limited set of main-chain conformations that are called "canonical structures" (47). Residues important in defining the backbone of these structures usually do not participate in direct contact with Agn and are internally packed (47) (48). Interestingly, the surface topography of the Agn-binding site, which is defined by the combinations of its canonical structures, varies according to the size of the Agn - as the Agn becomes smaller the contact surface becomes more concave (46). Vargas-Madrazo *et. al.*, (49) showed that in some instances, common paratope topologies are determined by particular canonical-loop combinations, and that some canonical-loop combinations are associated with preference for certain type of Agn.

In general, the combining sites of anti-protein Abs are planar, whereas, those of anti-peptide Abs are groove-like and those of anti-hapten Abs are cavity-shaped (49) (50) (51). It has been observed that the recognition of proteins typically involves the apical region of all six loops, peptides tend to be contacted by internal residues of the paratope, and residues at the base of the Agn-binding site (buried in the VL:VH interface) interact with haptens (46). It has also been observed that Abs do not use L2 to contact haptens or peptides (52) (53) (54) and it is quite common for a peptide to bury itself deeply as a beta-turn motif in the Ab combining site (55).

1.3.1 Peptide cross-reactivity with anti-protein antibodies

Basic structural and functional rules are emerging for the basis of protein recognition by Abs (*i.e.*, protein-protein interactions), as are principles defining the cross-reactivity of peptides. Ab usually binds protein *via*: (i) shape complementarity between the epitope and the paratope (ii) a large number of lower energy contacts that define the surfaces of the epitope and paratope, and (iii) a few high-energy contacts that confer a large component to the energy of binding (24) (56). Residues involved in these high-energy contacts or "hot spots" are called critical binding residues (CBRs).

The location of CBRs on the polypeptide chain defines whether an epitope is continuous or discontinuous (57). CBRs located within a contiguous stretch of polypeptide sequence form continuous epitopes, whereas, discontinuous epitopes are formed by CBRs, distally located on the polypeptide sequence, that are juxtaposed on the Agn surface by protein folding. Abs binding to both a continuous and a discontinuous protein epitope are depicted in Figure 1.2.

Figure 1.2. Continuous *versus* discontinuous protein epitopes.

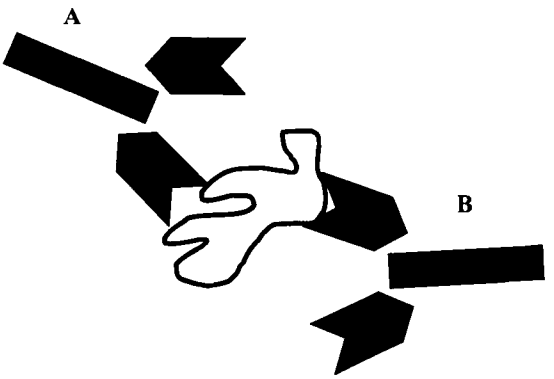

Ab "A" is binding to a discontinuous epitope and Ab "B" is binding to a continuous epitope.

The strength of an Ab-Agn interaction is influenced by a number of factors including shape complementarity between the two interfaces, the number and types of contacts (*e.g.*, hydrophobic interactions, Van der Waals interactions, solvent mediated and direct hydrogen bonding, and salt bridges) made between the paratope and the epitope, and by the thermodynamics of the bound complex *versus* the free Ab and Agn structures in solvent. Studies have shown that Agn-Ab interfaces are rich in aromatic residues, especially Tyr and Trp, as well as the charged residue Arg, but they are depleted in the charged residues Asp, Glu and Lys (58). Arg and aromatic residues often make up thermodynamic 'hot spots' in the binding interface, probably due to their ability to make multiple favourable interactions (23).

Amino acid substitution studies such as Ala replacement scans (the replacement of individual amino acids with Ala), of the epitope and/or the Ab paratope, along with affinity studies, are used to characterize protein-protein interactions and define CBRs. Interestingly, it has been shown that solvent-accessible residues involved in hydrogen bonding, that would be predicted to constitute a large source of binding energy, can sometimes be energetically neutral, as their interactions can be replaced by hydrogen bonds *via* water molecules that move into the gaps created in the mutated interface between the paratope and the epitope. Conversely, residues with no direct contact with the paratope can make unpredictably large contributions to the binding energy of the Agn-Ab interaction (59, 60) (61) (23).

Aside from conducting Ala replacement scans in conjunction with crystallographic studies, it is impossible to accurately predict which of the cross-reactive peptides' residues directly contact the Ab paratope and/or contribute to the binding energy of the interaction (62). A residue replaced with Ala, which results in a loss of binding to Ab, could have a role in direct contact with the paratope, or it could serve to maintain the structural integrity of the peptide (it helps to orient other amino acids for contact with the paratope). Both of these types of residues are considered CBRs, the former playing a functional role, and the latter playing a structural role, in contacting the paratope. Thus, to determine the mechanism of Agn-Ab binding, both functional (*i.e.*, Ala replacement scans) and structural data are required. By comparing these data, to a side-by-side analysis of a cross-reactive peptide:Ab complex, one can deduce if there is a shared mechanism of binding (*i.e.*, structural mimicry) between the cognate epitope and the cross-reactive peptide. Such structural and functional studies of cognate protein and cross-reactive peptide are important for ascertaining if there is any correlation between structural mimicry and immunogenic mimicry.

Although studies have demonstrated that peptides that cross-react with Abs against continuous protein epitopes can be used as immunogens to elicit Abs that cross-react with target Agn, the nature of such cross-reactive Abs (*i.e.*, the gene usage and the structure of the Ab in complex with peptide), as well as the properties of the peptides capable of inducing them have been poorly characterized (63, 64). It remains difficult to predict which protein epitopes will make effective targets for peptide-based vaccines, and Abs raised against peptides usually bind with high affinity to the peptide but only weakly to its cognate protein. Conversely, Abs raised against native Agn usually bind with lower affinity to peptide fragments of that Agn than to the whole Agn (65). This may be due to the absence in the peptide of a portion of the antigenic determinant, conformational differences between the protein and the peptide, flexibility of the peptide, and/or to the absence in the peptide of long-range effects (*e.g.*, electrostatic) that may be present in the context of the native protein. Much work is needed to further elucidate the mechanism of cross-reactivity of peptides with protein epitopes and to characterize the nature and breadth of the cross-reactive Abs.

1.4 B cell development and activation

In adult mice, lymphocytes are generated in the bone marrow (BM), a primary lymphoid tissue, and subsequently migrate into peripheral, secondary lymphoid tissues where they respond to antigenic stimulation. Within the BM, developing B cells recombine genes encoding H and L

chains. The earliest B cell that can be identified is one that has both its heavy and light chain variable regions in germline configuration. The maturational subsets of B cells can be broken into various stages based on Ig gene rearrangement and expression, as well as by the presence of various cytoplasmic proteins and surface markers. These stages take place within the BM and will not be discussed (66) (67).

After B cells have matured, they leave the BM for peripheral lymphoid tissues, including the spleen, lymph nodes and other non-encapsulated lymphoid tissue such as the mucosal- and gut-associated lymphoid tissues. Lymphocytes circulate between the secondary lymphoid tissues until they encounter Agn. After being activated by Agn, lymphocytes are thought to "home" preferentially to tissues similar to those in which the activating Agn was initially encountered. In addition, some return to the BM where they persist in the absence of Agn for extended periods of time (68) (69) (70) (71). Migration of B cells is mediated by binding of chemokine receptors on the lymphocyte surface to their ligands on specialized postcapillary venules of the target organ, as well as by binding to tissue-specific adhesion molecules (1, 2).

B cells undergo complex differentiative pathways and can be separated into distinct B cell subsets that are histologically, phenotypically and functionally distinct from one another. Mature B cells have been divided into two major subsets, B1 and B2 cells. B1 cells are dominant during fetal development but are only present as only a minor population in adults. They are an important part of the innate B cell response to bacterial Agns and typically produce Abs of a restricted repertoire that are low affinity, polyreactive, and mostly of IgM isotype. B1 cells produce and secrete Ab in the absence of T_H cell help and they arise primarily from self-renewing populations in the pleural and peritoneal cavities (1, 2, 67).

B2 cells arise from stem cells in the BM and are precursors of the thymus-dependent (TD) immune response - CD4+ T_H cells are required for their activation. CD4+ T_H cells have been divided into different subsets depending on their cytokine profiles. $CD4^+$ T cells that produce interleukin (IL)-2, IFN-γ but not IL-4 are designated T_{H1} cells. T_{H1} cells are mostly involved in delayed type hypersensitivity reactions and help to produce IgG2α but not much IgG1 or IgE in the mouse. $CD4^+$ T_H cells that produce IL-4 and IL-5 but not IL-2 or IFN-γ are designated T_{H2} cells. T_{H2} cells are very efficient helper cells for Ab production. CD4+ cells with cytokine profiles intermediate between T_{H1} and T_{H2} are known as T_0 cells (72).

Unlike B1 cells, B2 cells adapt in response to Agn exposure and they typically produce Abs of higher affinity than B1 cells. B cells involved in a TD response require two signals for activation. The first signal is received from the specific binding of the BCR to Agn; the Agn can

be soluble, but usually it is captured and presented by an antigen-presenting cell (APC). The second signal comes from direct cell-cell contact with an Agn-activated T_H cell, and/or from secreted stimulatory cytokines, such as interleukin IL- 4 or 5 (for mice) (67) (73) (74) (75). The central specific interaction of B cells and activated T_H cells is between the MHC class II-peptide complex on the B cell surface and the T cell receptor (TCR). This interaction is augmented, however, by other direct cell contacts. The interaction of the B cell surface molecules B7-1 and B7-2, with CD28 on T_H cells, for example, causes the stabilization of mRNA for IL-2 and other cytokines and thereby prolongs the delivery of activation signals to B cells. The most potent activating signal to B cell is mediated through the interaction of CD40 and CD40 ligand that is transiently expressed on activated T cells (76).

During the initiation of an acquired immune response to Agn, specialized microenvironments called germinal centres (GCs) form in the secondary lymphoid tissues (Figure 1.3). Five important events, dependent upon T_H cell help, take place within the GCs: (i) the clonal expansion of Agn-specific B cells and the apoptosis of non-binding B cells, (ii) isotype switching, (iii) somatic mutation, mostly within the hypervariable loops of BCRs, (iv) affinity maturation of BCRs, and (v) the differentiation of B cells into memory and plasma cells (77) (78) (79) (80) (81). Some plasma cells remain within the secondary lymphoid tissue where they can secrete Ab, while others circulate throughout the body. After memory B cells leave the GC they re-circulate or home to draining areas of the spleen and lymph nodes. During secondary antigenic stimulation, memory B cells rapidly divide and differentiate into plasma cells. This generates ten times more plasma cells than in the primary response (82).

Immune responses to blood-borne Agn typically take place in the spleen, and immune responses to Agn that has entered tissue are usually manifest in local lymph nodes. The secondary lymphoid tissues provide specialized microenvironments in which APCs, T cells and B cells localize and can interact with one another. APCs migrate throughout the body in search of Agn. Agn that is captured by APCs is processed and displayed as short peptide fragments *via* MHCII receptors. As APCs travel through T-cell rich regions of secondary lymphoid tissue those that display Agn will become trapped. This localization of migrating APCs, in a region through which naïve T cells constantly circulate, is critical because it enables their encounter with a T_H cell bearing a TCR that recognizes the particular peptide-MHCII complex. Naïve B cells also pass through these T cell rich regions and those that have bound Agn on their BCRs become trapped. This enables Agn-binding B cells and activated T cells of cognate Agn-specificity to interact and mutually stimulate one another.

The first phase of the primary humoral immune response involves the formation of a "primary focus" of clonal expansion that results from the interaction of an Agn-binding B cell with an armed T_H cell of cognate specificity – both types of lymphocytes rapidly proliferate at this site. After several days, the primary focus involutes and plasma cells (resulting from some of the proliferating B cells) migrate to other regions of the secondary lymphoid tissue where they secrete large amounts of Ab. Other B cells and T cells that proliferate in the primary focus migrate into follicles found in B-cell rich zones of secondary lymphoid tissue, where they proliferate to form GCs.

GCs are composed mainly of proliferating B cells but T_H cells make up about 10% of the population. GCs are divided into a dark zone and a light zone. As depicted in Figure 1.3, the dark zone is the site of centroblast (B cells with low surface (s)Ig expression) expansion and diversification of the BCR *via* somatic hypermutation (step 1). The light zone is the site of centrocyte (B cells that have increased sIg expression but reduced rates of division) selection and differentiation into memory B cells (step 2). The light zone is marked by the presence of follicular dendritic cells (FDCs) that localize whole Agn in the form of Agn:Ab:complement complexes bound to Fc and complement receptors. The role of this Agn depot is not known but it could be to maintain long-lived plasma cells. The memory B cells produced in the light zone either differentiate into Ab-secreting plasma cells or they remain non-secreting precursors for secondary challenge with Agn (step 3). Centrocytes can also migrate back to the dark zone and undergo another cycle of diversification. Cells that do not receive antigenic stimulation are eliminated by apoptosis (step 4) in the light zone.

Figure 1.3. Maturation of B cells in the germinal centre.

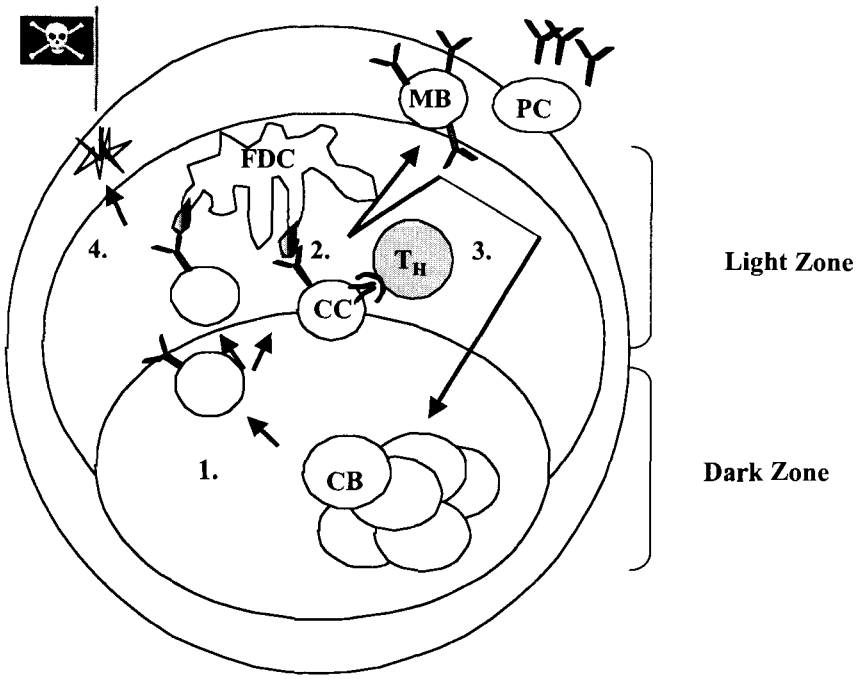

MB = memory B cell, PC = plasma cell
FDC = follicular dendritic cell, T_H= T helper cell
CC =centrocyte, CB = centroblast,

CB cells divide and diversify in the dark zone (1), then enter into the light zone where as CCs they either receive stimulation (2) and differentiate into memory B cells or plasma cells (3), or they are eliminated by apoptosis (4).

As shown in Figure 1.4, the antigenic stimulation of memory B cells can result in: (A) their division into more B cells, or, (B) their differentiation into plasma cells. The differentiation of memory B cells into plasma cells involves several phenotypic changes, including the down-regulation of the BCR and the surface marker B220, and the upregulation of the surface marker CD138 (for mice) (83, 84) (85) (86). Fluorescent Abs against these markers and others can be used to identify and isolate specific types of B cells from the spleen, blood or lymph nodes *via* fluorescence-based, cytometric analysis (87-89) (90).

Figure 1.4. Effects of antigenic stimulation on memory B cells.

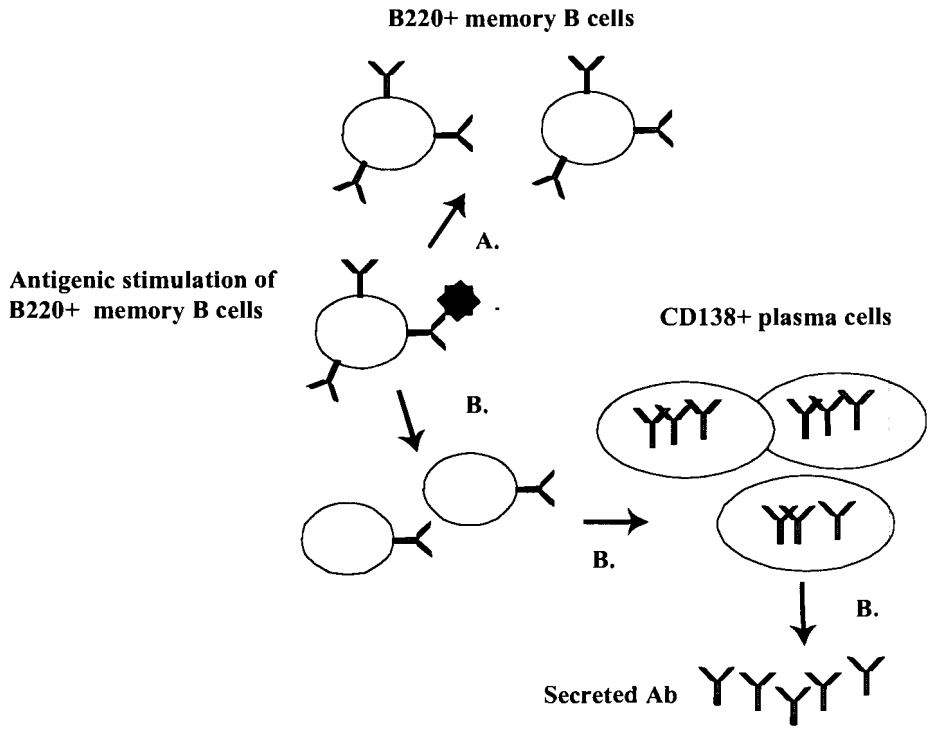

Antigenic stimulation of B220+ memory B cells results in: (A) the division of those cells and, (B) the differentiation of those cells into CD138+/B220- Ab-secreting plasma cells.

1.5 Immunoglobulin diversity and bias

The diversity of the BCR repertoire is immense and arises as a result of several processes, including: (i) combinatorial events (the permutations generated by recombination of various V, D and J gene segments), (ii) junctional events (the processing of the ends of the recombining variable regions elements through exonuclease activity and by N and P nucleotide addition), (iii) alternative joining of D gene segments, and (iv) the process of somatic mutation following clonal selection by Agn (91). Interestingly, however, the expressed repertoire does not reflect the diversity that would be expected from such processes and the so-called "holes in the repertoire" can arise from the deletion or receptor editing of cells that bind to self-proteins with high affinity (92). The non-random rearrangements of Abs are also influenced by chromosomal location of gene segments, as well as polymorphisms in recombination signal sequences (RSS) flanking each segment; RSSs comprise conserved heptamer, nonamer and spacer sequences, and are located 3' to each V segment, 5' to each J segment and on both sides of each D segment.

The relative positions of the murine IgH subgroups have been deduced by deletion mapping studies of the rearranged loci of murine, pre-B and B cell lines, and the number of genes per subgroup have been estimated form Southern Blot and hybridization studies (93) (94) (95). Figure 1.5, adapted from the IMGT website (http://imgt.cines.fr/), depicts the organization of the murine heavy chain gene segments (the number of genes per VH family is not shown). Studies indicate that for murine Ab sequences, there is a bias towards the usage of V genes located at the 3' end of the IgH locus (96). This observed 3' bias led to the "chromosomal proximity hypothesis" that states that rearrangement is enhanced for genes that are located in close proximity to one another in the genome (97).

The 81X gene (in the VH5 family) is the most 3' functional V_H gene in the murine V_H locus and rearranges frequently early in ontogeny and also in adult bone marrow. In the adult human repertoire (unlike the human fetal repertoire), a 3'V_H bias is not observed. In the human repertoire, however, certain gene segments, such as IGHV4-34, 59 and 23, are more commonly utilized than others (98). Such bias in gene usage may influence Abs elicited in response to natural infection or immunization. If, for example, a Nt Ab against a conserved epitope is highly represented in the naïve B cell repertoire due to bias, and the "germline form" of the Ab also binds the conserved epitope, it may be an excellent candidate in an epitope-targeted vaccine strategy.

Figure 1.5. Organization of murine heavy chain gene segments.

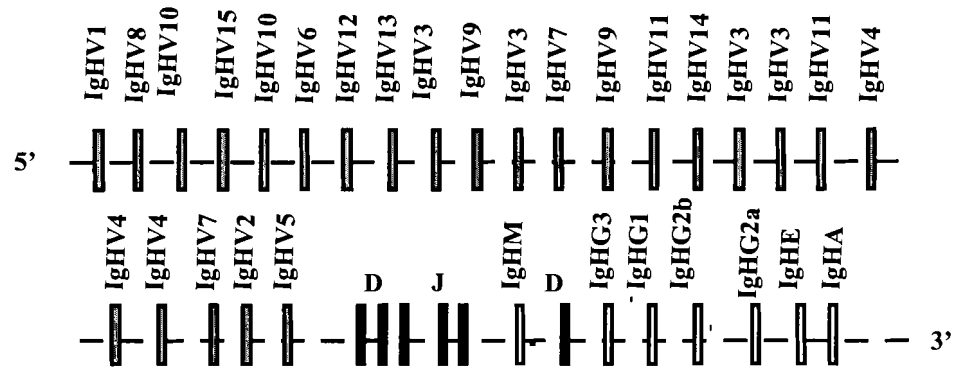

The murine H chain gene segments comprise 15 different VH families, D and J segments, and genes encoding the constant region of the H chain that dictates Ab isotype.

1.6 Considerations for the development of peptide-based, epitope-targeted vaccines

As previously stated, the concept of developing "epitope-targeted vaccines", in which the goal of an immunization is to elicit a Nt Ab response against a conserved epitope, is gaining wider attention for pathogens that elicit poor functional humoral responses to natural infection, but for which rare Nt Abs have been identified against conserved epitopes. Thus, a potential vaccine could be designed to: (i) target the production of a particular, pre-specified Nt Ab specificity, or, (ii) target the production of other Abs against a conserved epitope to which broadly Nt Ab(s) have been mapped. There are several important considerations regarding the feasibility of these two approaches. With regard to targeting the production of a particular Ab specificity, the characteristics of that Ab, such as its gene usage (are the genes commonly used?) and its level of somatic mutation (it may be more difficult to recapitulate a highly mutated Ab) may influence the probability of eliciting that Ab in an immunization strategy. With respect to eliciting other Ab specificities against the target epitope, there may be limitations in the number and diversity of Abs, due to bias and limitations in the repertoire, which can be generated against an individual epitope. It may, however, be possible to elicit Abs that overlap with part of the defined Nt epitope and are also protective.

A further complication regarding the design of epitope-targeted vaccines with peptide ligands relates to the striking difference in the topologies of anti-protein *versus* anti-peptide Abs. Immunization with a cross-reactive peptide may elicit a strong "anti-peptide-like" Ab response (*i.e.*, Abs with groove-like paratopes) but few, if any, "anti-protein-like" Abs (having flat paratopes) that bind to the cognate protein epitope. One means of potentially circumventing this obstacle is to prime with whole Agn to elicit anti-protein Abs, including the target Ab, and boosting with the cross-reactive peptide to amplify the production of the target Ab specificity (19) (99) (100). This vaccine strategy is called a "prime-boost immunization" and is depicted in Figure 1.6.

Figure 1.6. Prime boost immunization with whole antigen and a cross-reactive peptide ligand to amplify Ab production against a target epitope.

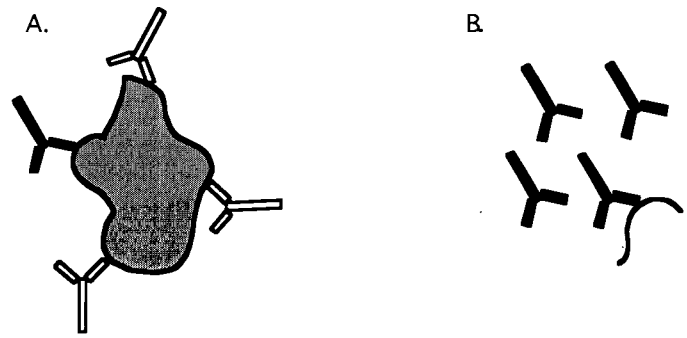

For the prime boost immunization, pcAbs, including Ab against the target epitope, are elicited in the priming immunization with native Agn (A). In the boosting immunization (B) with a cross-reactive peptide ligand, Ab against the target epitope is specifically amplified.

1.7 Hen egg lysozyme as a model antigen for exploring epitope-targeted vaccines

Lysozyme is an anti-bacterial protein that was first identified in 1922 by Alexander Fleming, the discoverer of penicillin. Remarkably, lysozyme is present in every living organism in the plant and animal kingdoms. In vertebrates it is mainly found in biological secretions such as tears, and in birds it is very abundant in egg whites. Lysozyme is a small, secreted enzyme of 129 amino acids, which folds into a compact globular structure. The protein is approximately ellipsoidal in shape and has 8 Cys residues that make 4 disulfide bridges that are critical for enzymatic activity. Lysozyme is comprised of an alpha+beta fold consisting of five to seven alpha helices (this varies depending on the species) and a three-stranded antiparallel beta sheet.

There is a large catalytic cleft (the principal catalytic residues are Glu 35 and Asp 52) which functions to hydrolyze the beta (1-4) glycosidic bond between residues of N-acetyl glucosamine and N-acetyl muramic acid of certain polysaccharides comprising the cell walls of bacteria. Bacteria become susceptible to osmotic lysis when lysozyme denatures their rigid cell walls (101).

HEL is the lysozyme from chicken egg whites. Its primary structure is shown in Figure 1.7. Since its discovery, HEL has emerged as a major model protein for a range of applications including protein-protein interactions, antigen presentation, Ab design by genetic engineering, and vaccine development. HEL is an ideal protein for exploring epitope-targeted vaccine design because it has been thoroughly characterized with respect to structure, antigenicity and immunogenicity. It is also practical for studying immune responses because, although it is highly immunogenic, it is non-toxic *in vivo* and is therefore unlikely to cause unwanted, non-specific effects in immunized animals (101).

For this thesis, the concept of epitope-targeted vaccine design is explored with the model protein HEL and cross-reactive peptide ligands. The goals of the thesis are to develop peptide markers that can be used to follow Ab and B cell responses to HEL immunization and, under appropriate immunization conditions, be used to amplify the production of Abs against a target HEL epitope. Section 1.7.1 provides background information regarding the antigenicity and immunogenicity of HEL and section 1.7.2 describes the anti-HEL MAb D1.3. The filamentous phage and phage-displayed random peptide libraries are described in section 1.8 and an overview of the thesis is presented in section 1.9.

Figure 1.7. The primary structure of HEL.

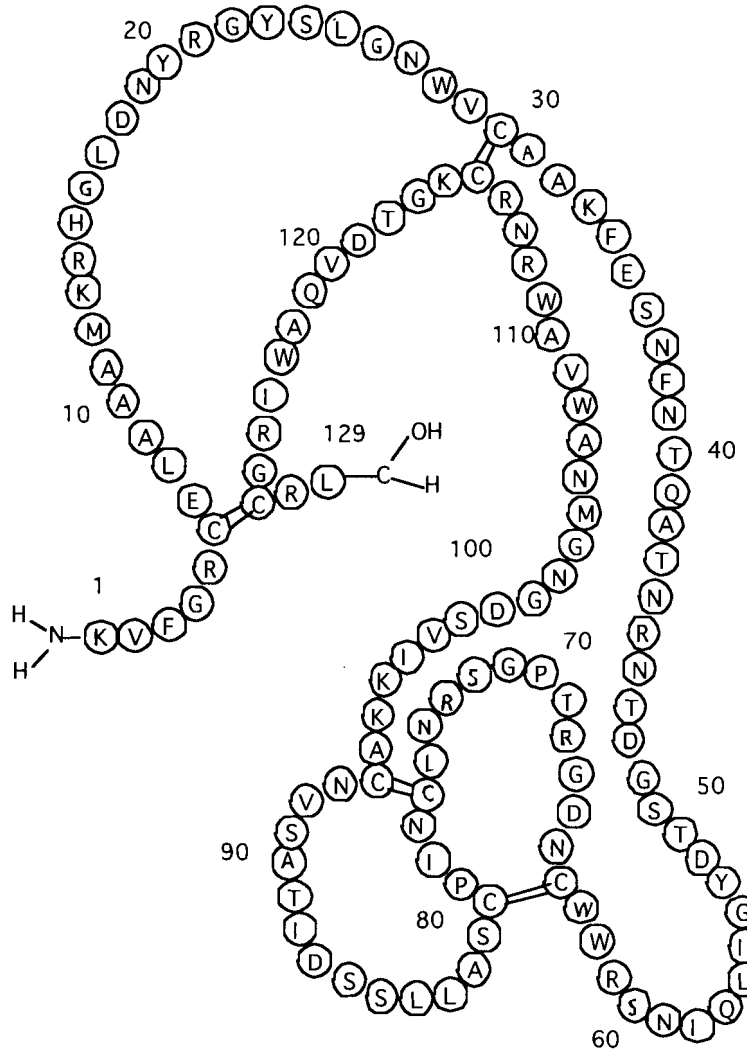

1.7.1 The antigenicity and immunogenicity of HEL

The humoral immune response to HEL has been characterized in several animal models including rabbits, goats, sheep, guinea pigs and mice. Early studies revealed that HEL undergoes an almost complete loss in antigenicity upon denaturation and that there is little or no cross-reactivity between native and denatured HEL (*i.e.*, the Abs against native HEL do not bind to denatured HEL). It was also shown that denatured HEL is itself immunogenic but that the resultant Ab does not bind to the native protein (101). These findings indicate that the majority of

B cell determinants on HEL are discontinuous, and dependent upon the native spatial conformation of the protein, rather than continuous.

Immunization with HEL elicits a diverse pcAb response and there are differences in the strength and the breadth of Ab specificities generated against the protein, not only in different animal species (*i.e.*, rabbits *versus* mice), but also between various strains of inbred animals. There are many factors that influence the nature of an Ab response including genetic differences in B cell, T cell and MHC receptor repertoires, intrinsic properties of the protein itself (such as surface charge), conditions under which the immunization is conducted (age of the animal, type of adjuvant used, route of administration *etc.*), and pre-exposure of an individual to other Agns. Although several mouse strains, for example, produce strong Ab responses to HEL, some are virtually non-reactive to immunization with the protein. Hill *et al.*, analyzed the plaque forming cell (PFC; this protocol is described in the Introduction of Chapter 4) response to HEL with spleen cells of different HEL-immunized strains of H-2 haplotype mice and showed that BALB/c mice ($H\text{-}2^d$) yielded 106 PFCs per 10^6 spleen cells, the highest responders were A/J mice ($H\text{-}2^a$) at 2220 PFCs per 10^6 cells, whereas, C57BL/6 and two other $H\text{-}2^b$ haplotypes tested were poor responders (only 13 of 200 C57BL/6 mice responded to HEL) (102).

Determinants on HEL have been elucidated through protein cleavage and the characterization of fragments that maintain antigenic and immunologic activity. Studies have shown that the majority of anti-HEL MAbs do not react with peptides that do not include disulfide bridges, further supporting the notion that most B cell epitopes are conformational (101). Remarkably, Metzger *et al.* (103), found that of 44 MAbs generated against HEL in $H\text{-}2^a$ mice, only six bound to HEL peptides "NC" (residues 1-17, linked by Cys6-Cys127, to 120-129), "L2" (13-105), or "L3" (106-129) (104), which together encompass the entire protein. From these studies, it appears that the small, compact, and globular nature of HEL results in mostly conformational epitopes being targeted by murine Abs. It is also possible that some of these peptide fragments, when taken out of the context of the native protein, adopt different and/or abnormally flexible structures that inhibit reactivity with Abs that may map to these linear regions in the context of the native structure.

With respect to antigenically and immunogenically defined regions on HEL, the continuous and flexible region consisting of residues 38-54 has been shown to bind Abs from HEL-immunized rabbits, goats and sheep. A small fraction of anti-HEL Abs from various mouse strains have also been characterized as reactive against this region of HEL, and the peptide conjugated to carrier has been used to elicit Abs in rabbits, goats and some strains of mice, that

cross-react with HEL. It is thought that the "flexibility" of this region in the context of native HEL enables this antigenic as well as immunogenic cross-reactivity (105) (106) (107) (108) (109).

Another well-characterized cleavage product of HEL comprises residues 64-80, and is commonly referred to as "the loop" because it includes a disulfide bridge between Cys64 and Cys80. Immunization of rabbits and goats with "the loop" peptide, conjugated to carrier, was the first example of using a completely synthetic Agn to elicit Abs that cross-react with a native protein (110) (111). Interestingly, this region of the protein reacts with Abs from HEL-immunized rabbits and goats, but it does not react with Abs from certain strains of HEL-immunized mice. In the early seventies, Mozes *et al.,* (112) immunized eleven different mouse strains with HEL or "the loop" conjugated to carrier. Only one of the strains (C57BL/6) did not respond strongly to HEL immunization, but three of the strains were poor responders to "the loop" region (SJL, BALB/c and C3HeB/Fe), even though the peptide was conjugated to an immunogenic carrier. In their study they demonstrated that mouse strains able to produce Abs against "the loop" could do so whether it was present within the native protein or conjugated to a synthetic carrier molecule. Single amino acid substitutions within "the loop" further revealed that not all residues contribute equally to antigenicity, Arg68 has a major role in its specificity, and antigenicity depends upon an intact conformational structure (*via* a disulfide bond) (113). Thus, studies with HEL have demonstrated that an entire protein, or region of a protein, that is immunogenic in one species or strain may be virtually nonimmunogenic in another.

In the early nineties, Newman *et al.*, (114) tested 49 BALB/c anti-HEL MAbs, from seven time-points after single and multiple immunizations with HEL, for patterns of specificity and avidity. They analyzed localization by dividing the surface of HEL into four antigenic "regions", based on binding interactions with previously characterized MAbs, and corresponding to structural domains defined by the tertiary structure of HEL (115). Complementation group I was defined by competition with HyHEL 8, 10 and 26, group II by HyHEL 5 and 7, group III by HyHEL 9,11,12,15 and D1.3, and group IV by HyHEL 16. (Abs in the same complementation groups block each others binding to HEL, whereas, Abs from different groups do not.). They showed that the Ab epitopes covered at least 80% of the protein surface and that virtually the entire surface of HEL is a "continuum of overlapping epitopes". Based on their panel of 49 MAbs, generated at different time points in the immune response to HEL, they also concluded that specificity patterns against the protein change during the transition from primary to secondary immune response. Group III Ab (the group including D1.3), for example, was present

throughout the primary and secondary immune response to HEL, whereas, group II Ab emerged in the secondary Ab response. There was no single MAb specificity that was immunodominant at any stage of the immune response.

Interestingly, the average relative avidity of the MAbs, as measured by endpoint titration assays of the different MAbs, did not increase over the course of immunization, as may be expected for Ab specificities that have undergone affinity maturation over the course of immunization. Similarly, Goldbaum *et al.*, (116), using a plasmon resonance technique, analyzed the affinities (K_a) and association (K_{on}) rate constants of 23 BALB/c mouse anti-HEL MAbs (prepared as Fab) obtained after few and multiple immunizations (mice were immunized with 50 – 100 μg HEL) and found that there was no correlation between time or dose of immunization and either of the values. (The affinities ranged from 1.1×10^7 to, 1.4×10^{10} M^{-1}). There was also no correlation between the accumulation of mutations in the MAbs and the length and dose of immunogenic challenge. This contradicts the orthodox view of immune maturation that: (i) Ab mutations accumulate over time *via* hypermutation in the immunoglobulin loci and (ii) favourable mutations drive affinity maturation. Work in the late 1960s by Eisen and Siskind as well as Weigert provided the first evidence for affinity maturation. Eisen and Siskind made quantitative measurements of Ab affinity for hapten (Ab affinity increased over the course of the immune response) and Weigert identified somatic mutations in mouse lambda chains (117) (118). Further corroborating the findings of Newman *et al.*, and Goldbaum *et al.*, relating to affinity maturation, is work from (i) Scharff's group showing discrepancies between somatic mutation and increases in affinity for Ab responses from cryptococcal infections (119) and (ii) Zinkernagel's laboratory on the murine response to vesicular stomatitis virus infection, that likewise, does not show evidence of affinity maturation (120) (121).

If the long-term goal is to elicit Nt Abs that do require significant affinity maturation in order to bind their target epitope, this apparent lack of affinity maturation may render HEL a poor model protein for exploring the feasibility of epitope-targeted vaccine design. It may, for example, be possible to elicit an Ab that does not undergo affinity maturation after a short period of immunization, but eliciting an Ab specificity that has undergone significant affinity maturation may require a prolonged immunization period. Nevertheless, HEL has long served as an important model protein for investigating immune specificity and, from another perspective, the apparent lack of affinity maturation of the anti-HEL Ab response may make it a good starting model for epitope-targeted vaccine design.

Studies with HEL, reviewed in (101), strongly support the "multideterminant regulatory model" of the humoral immune response. This regulatory model proposes that: (i) most of the accessible surface of any globular protein is potentially immunogenic, (ii) sites can be defined as immunogenic only with respect to an individual responder and, (iii) the total antigenic structure of a protein is the sum of all sites recognized by a large variety of responding individuals and species. This is in contrast to the view that proteins contain a limited number of sites that are intrinsically immunogenic, irrespective of the individual or species responding to the Agn. The multideterminant regulatory hypothesis, however, does not preclude the possibility that some sites on a protein are intrinsically more immunogenic within an individual than others due to properties of the epitope itself such as amino acid type, surface location and flexibility, *etc.*, or due to the random repertoire of all potentially responsive B cells circulating at the time of immunization.

1.7.2 The anti-HEL MAb D1.3

HEL and D1.3 MAb is one of the most thoroughly characterized protein-protein interactions (56). Extensive crystallographic studies, along with site-directed mutagenesis and affinity analyses, have been conducted for HEL and D1.3 (122) (123) (61) (60). Such work has elucidated the mechanism of binding for D1.3 and HEL, and has made a significant contribution towards our current understanding of protein-protein interactions. HEL and D1.3 is thus a useful model system for studying the feasibility of peptide-based, epitope-targeted vaccine design.

The D1.3 MAb originated from the secondary immune response of a HEL-immunized BALB/c mouse; the mouse was immunized subcutaneously with 100 μg of HEL in Freund's complete adjuvant, given a second injection of 100 μg in Freund's incomplete adjuvant 15 days later, and given a third injection of 50 μg HEL in PBS intravenously on day 36 (124). The VH region of D1.3 is a member of the VH2 family. Together, the VH and VL chains have a total of ten somatic mutations from their germline genes; five of the mutations are silent and the remaining five are amino acid replacements. The replacement somatic mutations in VL and VH of D1.3 are shown in Figure 1.8. Only one of the somatic mutations, VLTyr50 makes direct contact with HEL (125).

Figure 1.8. Heavy and light chain gene sequences of D1.3 MAb.

	FR1	CDR1 31-35	FR2
VH	QVQLKESGPGLVAPSQSLSITCTVSGFSLT	GYGVN	WVRQPPGKGLEWL
VH germline	QVQLKESGPGLVAPSQSLSITCTVSGFSLT	GYGVN	WVRQPPGKGLEWL

CDR2 50-65	FR3	CD3 95-102	JH2
GMIWGDG**N**TDYNSALKS	RLSISKDNSKSQVFLKMNSL**H**TDDTARYYCAR	ERDYRLDY	WGQGTTLTVSS
GMIWGDGSTDYNSALKS	RLSISKDNSKSQVFLKMNSLQTDDTARYYCAR	ETDYRFDY	WGQGTTLTVSS

	FR1	CDR1 24-34	FR2
VL	DIQMTQSPASLSASVGETVTITC	RASGNIHNYLA	WYQQKQGKSPQLLVY
VL germline	DIQMTQSPASLSASVGETVTITC	RASGNIHNYLA	WYQQKQGKSPQLLVY

CDR2 50-56	FR3	CD3 89-97	JK1
YTTTLAD	GVPSRFSGSGSGTQYSLKINSLQPEDFGSYYC	QHFWSTPRT	FGGGTKLEIKR
NAKTLAD	GVPSRFSGSGSGTQYSLKINSLQPEDFGSYYC	QHFWSTPRT	FGGGTKLEIKR

Shown are the germline and somatically mutated VH and VL sequences of D1.3 Ab. The sequences are arranged in framework (FR1-3) regions and complementary determining regions (CDR1-3) and joining regions (J). From (125).

The structure of the D1.3 heterodimeric variable fragment (Fv) in both its liganded (*i.e.* bound to HEL) and unliganded states (126) has revealed that residues from all six CDRs, as well as two framework residues contact HEL, and that this contact is made by up to 20 hydrogen bonds and 44 van der Waals contacts. D1.3 binds to a discontinuous epitope on the surface of HEL. The interface between D1.3 and HEL is tightly packed with 16 HEL and 17 Ab residues making close contact. The three-dimensional structure of HEL and the D1.3 Fab fragment (122) showed that the interface is an area of about 30 by 20 Å. The D1.3 paratope is an irregular, but fairly flat surface, and it has a small cleft, between the H3 and L3 loops, that accommodates the side chain of the CBR Gln121, of HEL.

Several groups have determined the K_d for HEL and D1.3 MAb. England *et al.* reported a K_d, with the BIAcore apparatus, of 11.5+/- 1.9 nM for HEL and D1.3, and a Kd of 669 nM for HEL and the "germline" Ab of D1.3 (all residues were reverted to "wild-type") (125). By constructing a series of D1.3-based Abs, with each somatic mutation individually reverted to wild-type, they concluded that the affinity maturation of D1.3, which resulted in a 60-fold improvement of affinity over the germline Ab, was due to a decrease in the rate of dissociation

(K_{off}); because point mutations in the Ab paratope do not significantly change the hydrophobicity and electrostatic charge (important for long-range forces affecting K_{on}) but have a strong effect on short-range interactions such as van der Waals forces and hydrogen bonds (which affect K_{off}).

Hawkins *et. al.,* (127) reported a similar K_d of 3.3 nM for D1.3 Ab and HEL by fluorescence quench titration. In their study, they also displayed D1.3 Fv wild-type mutants on phage and determined their affinities with HEL, and they built a library of 2 x 10^6 phage clones displaying mutants of D1.3 Fv. Interestingly, they found that much of the energetics of the interaction between HEL and D1.3 are driven by contacts near a small linear epitope made up of residues Gly117, Thr118, Asp119, Val120, and Gln121. Each of these amino acids makes multiple contacts with the Ab, while others towards the periphery make only one contact each. None of the mutations in their library clones that resulted in improved affinity were found in the contact interface. Their findings suggest that a few residues at the contact interface are responsible for the majority of the binding affinity between D1.3 Ab and HEL, but that these interactions can be modulated by residue changes outside of the binding site.

In a comprehensive study, including Ala scan replacement and X-ray crystallography, Dall'Acqua *et. al.*, also characterized the interface between HEL and D1.3 Ab (128). Similar to Hawkins *et al.*, they found that a small patch of contiguous residues dominates the energetics of D1.3 binding to HEL. By individually substituting 12 of the 13 nonglycine contact residues (determined by X-ray crystallography) on HEL to Ala, and measuring differences in coupling energies to D1.3 ($\Delta\Delta G = \Delta G_{mutant} - \Delta G_{wild\text{-}type}$), they showed that only four residues, Asp119, Gln121, Ile124 and Arg125 are critical for binding (*i.e.*, they had a $\Delta\Delta G$ greater than 1kcal/mol). Residues with differences in coupling energies between 0.7 and 0.9 included Ser24, Lys116, Tyr118, and Val120. Interestingly, their analyses also revealed that some replacements predicted to be disruptive to binding interactions actually resulted in low $\Delta\Delta G$ values due to the stable addition of water molecules in the interface. For example, the replacement of Asp18 with Ala, resulting in the loss of one hydrogen bond and seven Van der Waals contact, yielded a $\Delta\Delta G$ -0.3 kcal/mol. This work is very important because it demonstrates that direct protein-protein contact is not evidence of a productive interaction between the participating amino acids.

One of the strongest arguments for using HEL and D1.3 as a model system for exploring epitope-targeted vaccine design is based on the work by Goldbaum *et al.* (129). Following the network theory of Jerne and others (130), they used the D1.3 MAb to establish an anti-idiotypic network. An idiotypic network is depicted in Figure 1.9: the anti-Id is a "mirror image" of the Id and the anti-anti-Id is the image of the Id and reacts with the Agn used to elicit the Id. In a

crystallographic analysis Goldbaum *et al.*, showed that anti-anti-idiotypic MAbs, produced in mice using rabbit polyclonal anti-Id Abs against D1.3, bound to both HEL and an anti-Id MAb *via* many of the same contacts as the D1.3 paratope. Further, the V-gene usage of the anti-anti-Id MAbs was very similar to that of D1.3. The affinity of the anti-anti-Id MAbs, however, was two orders of magnitude greater for the anti-Id (the "epitope mimic") than for HEL. The authors were unable to find structural evidence for an internal image of HEL in the anti-Id, but the epitope on HEL, however, is an alpha-helix, which is unlikely to be found in the CDR region of an Ab. Importantly, however, this study demonstrated that it is possible to produce Abs similar in sequence to D1.3 (*i.e.*, "D1.3-like" Abs) that also bind HEL.

Figure 1.9. Illustration of an idiotypic network.

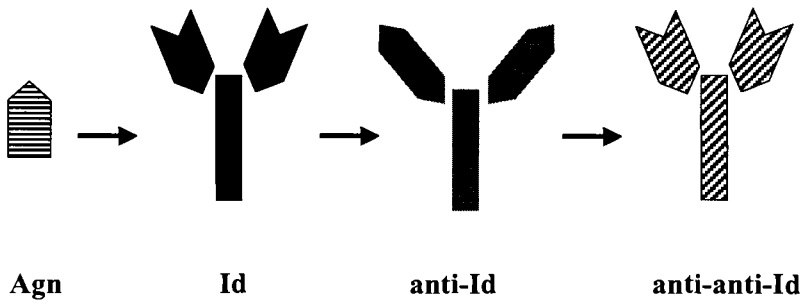

1.8 Phage-displayed random peptide libraries for the identification of peptides that cross-react with anti-protein antibodies

The filamentous phage, depicted in Figure 1.10, resemble long, flexible rods and are composed of four minor, and one major, coat protein, that encapsulate a single-stranded DNA genome. The major coat-protein, pVIII, is present in just under three thousand copies and is arranged in an overlapping, shingle-like, array along the length of the phage particle (131). The minor coat proteins are found at the tips of the phage particle.

Figure 1.10. The major and minor coat proteins of recombinant filamentous phage.

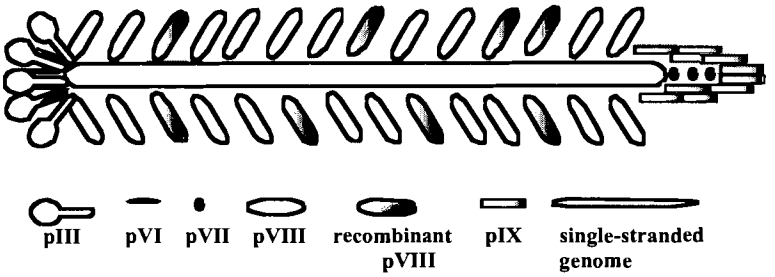

The Ff class of filamentous phage has been most thoroughly characterized and is specific for *Escherichia coli* containing the F plasmid because it uses the tip of the F conjugative pilus as a receptor during infection. The life cycle of Ff phage, including infection, replication and assembly is described here briefly. Phage infection is initiated by binding of its pIII protein (present in 3-5 copies at one end of the phage particle) to the tip of the F pilus of *E. coli*, which subsequently contracts and disassembles into the bacterial membrane. The major coat protein pVIII, as well as the pVII and pIX minor coat proteins are then believed to also disassemble into the host cytoplasmic membrane as the phage DNA is translocated into the cytoplasm of the host cell (131). Once the viral (+) strand has entered the cytoplasm, the complementary (-) strand is synthesized by bacterial proteins and the DNA is assembled into covalently closed, supercoiled, DNA called the parental replicative form (RF). The (-) strand of the RF is then used as a template for transcription, and the resultant mRNAs are translated into phage proteins. New viral DNA strands are synthesized *via* a "rolling circle" mode of replication using bacterial proteins, and these are in turn are converted into RF DNA. The synthesis of RF DNA ensues until the phage protein pV reaches a critical concentration and binds to single-stranded (+) DNA, thus preventing its conversion to RF. Phage protein pV forms dimers that interact with the viral (+) DNA (about 800 pV dimers per single-stranded viral DNA molecule) and thereby prepares viral DNA for packaging into virions.

Phage assembly occurs at the inner membrane of the host cell where the phage coat proteins are located. Assembly is initiated by pVII and pIX that together, with the first set of pVIII molecules, interact with the phage DNA packaging signal (MOS) on the cytoplasmic side of the inner membrane. As the phage particle elongates by moving through the inner membrane, pV dimers interacting with the (+) viral DNA are replaced by pVIII proteins. When the terminus of the (+) viral DNA is reached, the assembly process ends with the addition of pVI and pIII (132) (133). The Ff phage does not kill its host during productive infection but infected cells

grow more slowly than uninfected ones. About 1000 phage particles are produced in the first life cycle after infection, and 100-200 particles per generation thereafter.

Although all of the phage coat proteins have been used to display recombinant peptide, the ones most commonly used are pVIII and pIII (134) (135) (136). In general, the minor coat protein, pIII, is used to accommodate libraries of longer peptides (or small protein fragments), whereas, the major coat protein, pVIII, is used to display shorter inserts but at a higher copy number than is possible for pIII libraries (137) (138) (139) (140). For peptide inserts greater than six to eight residues, a copy of the wild-type pVIII coat protein is also required to enable phage assembly (38). Such phage particles are called "hybrids" because they comprise both wild type and recombinant pVIII proteins. The ratio of recombinant pVIII protein *versus* wild-type pVIII protein varies for different phage clones, and is dependent mostly upon the sequence and length of the recombinant peptide (131) (141) (142).

The screening of RPLs is a relatively straightforward and efficient means of identifying peptide ligands, for Abs against protein or non-protein Agns, amongst millions of peptide candidates. In a typical screening: (i) the target molecules, such as a MAb, are incubated, either in solution or on a solid support, with the RPL(s), (ii) washes are conducted to remove non-binding phage, and, (iii) target-binding phage are amplified in male *E. coli* cells carrying an F plasmid. These steps are repeated for several "rounds" to enrich target-binding phage, after which individual phage clones are isolated, amplified and tested for binding to the target molecules in binding assays, such as enzyme-linked immunosorbent assays (ELISAs) (143). Increasing the stringency of the screenings, such as using a lower concentration of the screening Ab, or shorter incubation periods between the Ab and the RPLs, can promote the selection of tighter-binding phage clones. Sequences of the phage-displayed peptides identified in a screening can be obtained with ease by sequencing the region of the phage genome that encodes the peptide insert (144).

The production RPLs requires the design and synthesis of a degenerate oligonucleotide that encodes the random peptide sequences to be displayed. Each variable residue of the peptide is encoded by a degenerate codon, either NNK or NNS (where N represents A, G, C or T, K represents G or T and S represents G or C). NNK and NNS both encode all 20 amino acids and one stop (amber) codon. The degenerate oligonucleotide is then cloned into DNA encoding the phage-display genome vector. This enables the production of phage that display a foreign peptide encoded by the genome it carries. (Each phage particle bears multiple copies of a single

recombinant peptide sequence.) *E. coli* cells transfected with the ligated viral DNA produce the RPL, with library sizes typically ranging between 10^8 and 10^9 phage clones (144).

It is not possible to determine *a priori* what type of library will yield a ligand for a given MAb or pcAbs (19, 145) (20). Thus, screenings typically include several RPLs that may vary in: (i) the type of display (pIII *versus* pVIII), (ii) the length of the peptide insert, and, (iii) the presence of constraints such as fixed Cys residues that may form intramolecular disulfide bonds, or other fixed residues. Libraries with fixed Cys residues are structurally constrained and have proven particularly useful in the identification of peptides that cross-react with MAbs of discontinuous protein epitopes (19, 146). The fixed Cys residues likely decrease the flexibility of the peptide and thereby stabilize its structure (147).

Subsequent to the selection of Ab-binding peptides, it is often necessary to "optimize" the peptide ligand by increasing the number of contact or stabilizing residues on the peptide to improve the apparent affinity of the peptide-Ab interaction. Optimization can be carried out through the construction of two types of sublibraries. One type of sublibrary, referred to as a "consensus sublibrary", involves fixing the consensus residues (residues found in common in multiple Ab-binding peptides) identified in the screenings and randomizing all others. The other type of sublibrary is an "NNK-doped sublibrary", so named because the oligonucleotide codons are encoded with 50% wild-type codon (*i.e.*, encodes the residue of the parental peptide sequence) and 50% degenerate NNK codon (148). For NNK-doped sublibraries, every codon can be doped, or codons for the consensus sequence can be doped while all nonconsensus residues are completely randomized. The advantage this type of sublibrary is that by not fixing any residues one is able to identify which consensus residues are not absolutely required for binding (*i.e.*, their replacement with an alternative residue may still enable strong target-ligand interactions). In Chapter 2, both a consensus sublibrary and an NNK-doped sublibrary were constructed and screened to optimize a peptide ligand for binding to the anti-HEL MAb D1.3.

1.9 Overview of thesis

For this thesis, HEL is used as a model Agn, for exploring the concept of peptide-based, epitope-targeted vaccine design. The goals of the thesis are to develop and optimize peptide ligands to be: (i) used as markers to analyze anti-HEL Ab specificities and B cells from individual BALB/c mice and, (ii) under appropriate immunization conditions, be used as immunogen to focus Ab production against a target HEL epitope. Three types of peptide ligands are used in the

thesis: (i) a peptide that cross-reacts with the anti-HEL MAb D1.3, (ii) peptides selected from RPL screenings with pc anti-HEL Abs, and (iii) both long and short peptides derived from the linear sequence of HEL.

The thesis is divided into three chapters of data. Chapter 2 describes the identification, optimization, and antigenic and immunogenic characterization, of an RPL-derived peptide that binds D1.3 MAb. Although the phage-displayed peptide ("E3") was shown by an Ala replacement scan to bear CBRs in common with its cognate HEL epitope it showed no reactivity with serum from HEL-immunized mice, nor was it able in a direct immunization, to elicit Abs that cross-react with HEL. Thus, the E3 peptide is an antigenic but not an immunogenic mimic of its cognate HEL epitope. A prime-boost immunization with HEL and the E3 peptide also failed to target the production of D1.3 or D1.3-like Abs.

The purpose of the work in Chapter 3 was to identify a peptide ligand for an Ab commonly produced amongst BALB/c mice in the immune response to HEL and to characterize anti-HEL Ab specificities in individual mice with peptide ligands. RPLs were screened with pcAbs from HEL-immunized mice and one "commonly-reactive" peptide "3D" was identified. The remaining cross-reactive phage clones bound only to one of the three screening Abs used in their selection. Serum samples from HEL-immunized mice were also tested for reactivity with three longer HEL peptide fragments (38-54, 64-80 and 76-100) and a set of 10-mer overlapping HEL peptides covering the entire sequence of HEL. Although there was no binding of anti-HEL serum to the three longer peptides, there was binding to a variety of the 10-mer peptides. Moreover, binding patterns were very similar amongst anti-HEL serum samples suggesting that common HEL epitopes are targeted by the Ab response in different mice.

The final data chapter, Chapter 4, describes the development of assays to identify HEL+ and 3D+ B cells (*i.e.*, B cells that produce Ab against these Agns), amongst pools of spleen cells from HEL-immunized mice. In this way, the serum Ab response against HEL and the cross-reactive 3D peptide can be correlated to the B cell response. Three assays, flow cytometry, the *in vitro* culture of spleen cells and enriched B cells, and ELISPOT analysis are described. With the ELISPOT analysis it was shown that 3D+ B cells represent approximately 1% of total IgG+ B cells.

Lastly, Chapter 5 is an overall discussion of the findings in each of the three data chapters, and provides direction for future work needed to further explore the concept of epitope-targeted vaccine design.

CHAPTER 2 IDENTIFICATION AND CHRACTERIZATION OF A PEPTIDE THAT CROSS-REACTS WITH THE ANTI-LYSOZYME MONOCLONAL ANTIBODY D1.3

2.1 Introduction

Epitope-targeted vaccines have been proposed as a means of defending against infectious agents that elicit poor functional Ab responses during natural infection but for which "rare" Nt Abs have been identified. If the Nt Abs are rare because they are produced against conserved epitopes that are not immunodominant in the context of the native Agn, then immunization with whole protein from the pathogen is unlikely to elicit these specificities. Moreover, an alternative strategy, of immunizing with an Agn fragment may also not be feasible if the target epitope is discontinuous and comprises residues that are distant in the linear sequence of the protein (21, 101, 149, 150). In these instances, cross-reactive peptides might be a way of representing the epitope and, under appropriate immunization conditions, targeting the production of Ab specificities against the conserved, target epitope.

In this chapter, the protein HEL and the well-characterized MAb D1.3 (described in Chapter 1, sections 1.7.1 and 1.7.2) are used as a model system for exploring epitope-targeted vaccine design. The goals of this chapter are to: (i) screen RPLs to identify a peptide that specifically binds D1.3 MAb, (ii) characterize the antigenicity of the cross-reactive peptide, (iii) use the peptide as a marker to detect D1.3 or D1.3-like Abs in sera from HEL-immunized mice, and (iv) under an appropriate immunization strategy, use the peptide to elicit or enhance D1.3 or D1.3-like Ab production in mice.

To identify peptides that cross-react with the D1.3 epitope, 15 RPLs were screened with D1.3 MAb. Two consensus sequences emerged from the screening and were used to design two sublibraries. Several optimized peptides were identified in the screening and one of them, the "E3" peptide, was chosen for characterization. Competition ELISA showed that the E3 peptide cross-reacts specifically with HEL for binding D1.3 Ab, and an Ala replacement scan of the recombinantly displayed peptide revealed CBRs in common between E3 and its cognate HEL epitope. No reactivity, however, was observed with sera from HEL-immunized mice against the

peptide. This suggests that either D1.3 is not commonly elicited amongst HEL-immunized mice, or D1.3 is present, but at too low a titre for detection *via* ELISA analysis. The anti-HEL sera also failed to react with optimized peptides from an NNK-doped E3 sublibrary.

All immunization strategies attempted with the E3 peptide failed to elicit D1.3 or D1.3-like Abs. Sera from mice immunized with recombinant E3 phage reacted with both the E3 peptide and f88 phage but no binding to HEL was observed. The peptide was further tested in a prime-boost immunization strategy in which mice were primed with HEL and boosted twice with recombinant E3 phage. This strategy was based on the assumptions that D1.3 Ab is elicited in the priming immunization with HEL, albeit at a very low titre, and that the cross-reactive peptide could be used in the boosting immunizations to amplify the D1.3 Ab response. Although there was no reactivity of anti-HEL sera against the E3 peptide, because D1.3 Ab is so close in sequence to its germline genes (125), and the mice are inbred, it was assumed that D1.3 is in fact commonly produced by BALB/c mice, but only at low titres. ELISA analysis of sera from mice primed with HEL and boosted with peptide, however, failed to show evidence of Abs that cross-react with HEL and the E3 peptide. Thus, most likely D1.3 is not a commonly produced Ab specificity in the immune response to HEL and the E3 peptide is not an immunogenic mimic of its cognate HEL epitope.

2.2 Materials and Methods

2.2.1 Reagents

The *E. coli* strain K91 (Hfr-Cavelli) was used to amplify phage. Phage particles were amplified in the presence of tetracycline (Tet) and IPTG (isopropyl-beta-D-thiogalactopyranoside) (GibcoBRL, Burlington, ON). Polyethylene glycol (PEG) and solid cesium chloride (C-3139), used for phage purification, were purchased from Sigma-Aldrich (St. Louis, MO). The 12 mL, quick-seal polyallomer tubes used for CsCl density gradient purification of phage were purchased from Beckman Instruments Inc. (#342413, Palo Alto, CA).

Eleven of the RPLs used were constructed in the Scott lab (144), and the four 'Cys' libraries were a gift from Dr. G.P. Smith (University of Missouri, Columbia) (Table 2.1). D1.3 Fab and IgG were gifts from Dr. Roy Mariuzza (University of Maryland Biotechnology Institute, Rockville, MD). Additional D1.3 IgG was kindly provided by Dr. Richard Willson (University of Houston, Houston, Texas).

Table 2.1. pVIII -displayed RPLs used in screenings with D1.3 Ab.

Library	Sequence
X6	X_6
X15	X_{15}
X8CX8	X_8CX_8
X15CX	$X_{15}CX$
XCX15	XCX_{15}
LX-8	XCX_8CXGG
LX10	$XCX_{10}CXGG$
LX12	$XCX_{12}CXGG$
Cys3	$X_5CX_3CX_5$
LX-4	XCX_4CX
Cys4	$X_4CX_4CX_4$
Cys5	$X_4CX_5CX_4$
Cys6	$X_4CX_6CX_4$
LX-6b	XCX_6CX
LX6	XCX_6CX

'X' represents random residues.
'C' represents a fixed Cys.

RPL screenings were conducted with streptavidin (SA)-coated magnetic beads (Dynabeads M-280, Dynal, Lake Success, NY) and a Dynal magnet or a 96-well filtration plate along with a vacuum manifold (1.2 μM, MABV N12, Millipore, Billerica, MA). NHS-LC-biotin (Pierce) was used for the biotinylation of IgG, Fab and HEL (Sigma-Aldrich). Centricon® Centrifugal filter units were used to wash and concentrate protein (Millipore). For bio-IgG and bio-Fab, 30 and 10 NMWL kDa filter units were used, respectively. For bio-HEL, 3 NMWL kDa filter units were used.

The electrocompetent *E. coli* strain MC1061 was used for phage sublibrary production. For sublibrary construction, VENT and Klenow fragment DNA polymerases were purchased from GibcoBRL. The restriction enzymes, *PstI* and *HIND III*, as well as reagents required for the Ala replacement scan of the phage-displayed E3 peptide, including buffer, bovine serum albumin (BSA), adenosine triphosphate (ATP), T4 DNA ligase and T7 DNA polymerase, were purchased from New England Biolabs (NEB, Beverly, MA). PCR products were purified with QIAquick PCR purification columns (Qiagen, Mississauga, ON). Ligation products were concentrated and desalted using a 10 NMWL kDa Ultrafree®-MC Centrifugal Filter Device (Millipore).

Recombinant peptides in the 55E3 and 55C4 sublibraries have the amino acid sequences 5' -A X_3 N C X G X_2 C X R X_2 - 3' and 5' X C X P Q (T/S/A) (T/S/A) X_5 C X 3', respectively. X is a fully randomized amino acid encoded by NNK, in which N is A, C, G or T and K is G or T.

The E3 (ASQPNCDGLVCNRWHPAEGGK-bio) and C4 (TCYPQTSTTPPHCDPAEGGK-bio) peptides, both with and without a biotin-modified Lys residue at their amino terminus, were synthesized by Dr. B.P. Gangadhar at Simon Fraser University (SFU, Burnaby, BC). The residues PAE (underlined) were included because they are found at the carboxy terminus of the displayed peptide in the context of recombinant pVIII and may influence binding by D1.3 to the peptides. The two Gly residues form a flexible spacer. The bio-Lys residue was included for immobilization of the peptides in ELISA analysis *via* SA. Additional, unbio-E3 peptide was synthesized at the Nucleic Acid Protein Service Unit at the University of British Columbia (NAPS Unit, UBC, Vancouver, BC). All peptides were amidated at their carboxy termini and cyclized. The peptides were HPLC-purified to greater than 95% purity.

For ELISA experiments, 96-well, microtiter, high-binding plates were purchased from Corning Inc. (Corning, NY). Recombinant streptavidin (SA), used in ELISA analysis to immobilize bio-peptide was purchased from Roche (Manheim, Germany). HRP-conjugated-goat-(anti-mouse IgG-H+L)-Ab, and HRP-conjugated-goat- (anti-mouse IgG-Fc)-Ab were purchased from Pierce (Rockford, IL). [Fc consists of the C-terminal halves of two heavy chains disulfide-bonded to each other by the hinge region.] HRP-conjugated neutravidin (NA) and HRP-conjugated protein A were also purchased from Pierce. Dialyzed BSA, dithiothreitol (DTT), and 2, 2'-azino-bis(3-ethylbenzthiazoline-6-sulfonic acid) (ABTS) were purchased from Sigma-Aldrich. Tween-20 (Tw) was purchased from ICN Biomedicals Inc. (Irvine, CA). Plate washings were conducted in an EL-403 plate washer or by hand and ELISA plate readings were made done with an EL312e Bi-Kinetics Reader (Bio-Tek Instruments Inc., Winooski, VT).

The pMal-X vector was modified from the maltose-binding protein (MBP) fusion vector, pMal-p2 (NEB) by L.L.C. Bonnycastle (151). All reagents used in transferring the E3 peptide to the amino-terminus of MBP, and the amylose columns used for purification of the MBP fusion protein, were obtained from NEB. XL-1 Blue *E. coli* cells were used for MBP fusion protein expression. Amicon centriprep-30 concentrators (Millipore) were used to concentrate the fusion protein and the Bio-Rad Protein Assay was used to determine its concentration according to the manufacturer's instructions.

Cy5-conjugated-goat- (anti-mouse-IgG-H+L)-Ab, for Kd determination using the KinExA instrument (Sapidyne Instruments Inc., Boise, ID) was purchased from Jackson ImmunoResearch Laboratories, Inc. (West Grove, PV).

The oligonucleotides encoding for the phage-displayed E3 peptides bearing single Ala substitutions (underlined) have the sequences: 5'- CC ATC ACA ATT AGG CTG *AGC* AGC GGC AAA GCT TAG C-3', 5'- CC ATC ACA ATT AGG AGC ACT AGC GGC AAA GC-3', 5'- CA AAC CAA ACC ATC ACA ATT AGC CTG ACT AGC GGC AAA G -3', 5'- C CAA ACC ATC ACA AGC AGG CTG ACT AGC G-3', 5'- CA AAC CAA ACC ATC AGC ATT AGG CTG ACT AGC-3', 5'- CG ATT ACA AAC CAA ACC AGC ACA ATT AGG CTG ACT AG -3', 5'- CA ACG ATT ACA AAC CAA AGC ATC ACA ATT AGG CTG AC-3', 5'- CCA ACG ATT ACA AAC AGC ACC ATC ACA ATT AGG-3', 5'-GG ATG CCA ACG ATT ACA AGC CAA ACC ATC ACA ATT AGG-3', 5'-GG ATG CCA ACG ATT AGC AAC CAA ACC ATC AC-3', 5'-GC AGG ATG CCA ACG AGC ACA AAC CAA ACC ATC AC-3', 5'-C TGC AGG ATG CCA AGC ATT ACA AAC CAA ACC-3', 5'-CC TTC TGC AGG ATG AGC ACG ATT ACA AAC CAA AC-3'. The oligonucleotides were 5' phosphorylated.

Oligonucleotide encoding for the E3 doped sublibrary were prepared following the two-column method of Glaser *et al.* (148). The E3 doped sublibrary oligonucleotide has the sequences: 5'-ATC ACC TTC TGC AGG ATG CCA ACG ATT ACA AAC CAA ACC ATC ACA ATT AGG CTG ACT AGC GGC AAA GCT TAG CAT AGG AAC-3' with each codon (except those encoding the E3 peptide's two Cys residues; underlined) doped with 50% the E3 encoding codon and 50% NNK degenerate codon. Two columns were used during the synthesis. For each codon in the E3 sequence (except those encoding the two Cys residues) the E3 encoding codon was synthesized on one column and the NNK degenerate codon on the other. The contents of the two columns were then mixed and divided between the two columns. This was repeated for each codon. All oligonucleotides were synthesized on an ABI 392 synthesizer at SFU.

Female BALB/c mice were used for all immunization studies (Charles River Laboratories, Wilmington, MA). They were immunized with Adjuvax adjuvant (Alpha-Beta Technology, Worcester, MA; this adjuvant is no longer commercially available) or the Ribi adjuvant system (Sigma-Aldrich), and HEL (L777-3, Sigma-Aldrich) or HEL conjugate. HEL conjugate was prepared with the cross-linking agent glutaraldehyde (Sigma-Aldrich).

Sequencing was performed using either the Thermo Sequenase Radiolabeled Terminator Cycle Sequencing Kit (USB, Cleveland, OH) or the Thermo Sequenase II Dye Terminator Cycle Kit (Amersham Biosciences, Piscataway, NJ) following the manufacturer's instructions. Sequencing was carried out at SFU or at the Centre for Molecular Medicine and Therapeutics (CMMT) at the UBC (Vancouver, BC). DNA fragments generated using the radiolabeled kit were developed on Fuji Medical X-ray film and analyzed manually. DNA fragments generated

using the Dye kit (Amersham Biosciences) were resolved on an ABI 373 sequencing apparatus and analyzed using the EditView 1.0.1 software.

2.2.2 Phage production and PEG precipitation

Phage particles were produced in *E. coli* strain K91 following the procedures of Bonnycastle *et. al.*, (144). Briefly, 1.5 x 10^8 starved K91 cells (152) were infected with 10^6 phage particles diluted in 10 µL of Tris-buffered saline (TBS; 50 mM Tris-HCl (pH7.4), 150 mM NaCl). The infection was incubated at room temperature (RT) for 10 minutes (min) and 160 µL NZY media supplemented with 0.2 µg/mL Tet (NZY/Tet medium) was added for 30 min at 37°C with shaking to induce Tet resistance. Without selection for Tet resistance encoded by the phage vector, the cells would cure themselves of the phage.

Infections were plated at various dilutions onto agar containing NZY and 40 µg/mL Tet (NZY/Tet plates). Following overnight (ON) incubation at 37°C, individual colonies were inoculated in 2 mL NZY supplemented with 15 µg/mL Tet and 1 mM IPTG (NZY/Tet/IPTG medium). IPTG induces the *tac* promoter, which drives the expression of the recombinant pVIII protein. The phage cultures were incubated in test tubes on a shaker (250 rpm) ON at 37°C for approximately 20 h. The phage cultures were transferred to microfuge tubes and centrifuged for 15 min at 15,000 x g to pellet bacterial debris. All centrifugations were performed at 4°C. The culture supernatants (approximately 1.3 mL) were transferred to fresh microfuge tubes and the phage precipitated for a minimum of 4 h at RT, or ON at 4°C, with 0.15 volume 16.7% (w/v) PEG and 3.3 M NaCl (PEG/NaCl). The microfuge tubes were centrifuged for 40 min at 15,000 x g to pellet the PEG/NaCl-precipitated phage. Phage pellets were resuspended in 50 µL TBS and heated to 70°C for 15 min to kill any remaining bacteria. The microfuge tubes were centrifuged at 15, 000 x g to pellet any debris and the phage supernatant transferred to a fresh tube.

Phage concentration was estimated by 0.8% agarose gel electrophoresis of lysed phage particles (along with a control of well 10^{10} f88 phage particles) and visualization of viral DNA using ethidium bromide staining and UV light. Phage clones were stored at 4°C, typically at a concentration of 1 x10^{10} phage particles/µL.

2.2.3 Large-scale phage production and purification on CsCl density gradient

Two litres NZY/Tet/IPTG medium, were inoculated with a single colony of K91 cells infected with phage, and then shaken at 250 rpm for 21 h at 37°C. The culture was centrifuged at

4500 x g for 10 min at 4°C (all centrifugation steps were conducted at 4°C) to pellet the cells. The supernatant was centrifuged again at 11 000 x g for 10 min to clear the supernatant. To precipitate the phage, the supernatant was mixed well with 0.15 volumes PEG/NaCl and incubated ON at 4°C. The PEG/NaCl-precipitated phage were pelleted by centrifugation at 11, 000 x g for 40 min. The supernatant was discarded and the pellet resuspended in 100 mL PBS (23 mM NaH_2PO_4, 77 mM Na_2HPO_4, 150 mM NaCl, pH 7.4). The resuspended phage were cleared of any residual bacteria by incubation in a 70°C water bath for 15 min, followed by centrifugation at 20 000 x g for 10 min to pellet debris. The PEG/NaCl precipitation was then repeated and the phage resuspended in 50 mL PBS. Solid CsCl was added to the phage solution to a concentration of 31% (w/v). The phage mixture was divided amongst four 12 mL, quick-seal, polyallomer tubes which were then filled completely with 31% CsCl in PBS. The tubes were sealed and centrifuged in a pre-chilled rotor at 57, 000 rpm for 20 h. A diffuse, bluish band containing the phage was extracted with an 18-gauge needle and a 10 mL syringe. The phage bands were transferred to fresh polyallomer tubes (one tube per band), filled with PBS and centrifuged at 50, 000 rpm for 4 h. The phage pellets were resuspended in 5-10 mL PBS, typically to a final concentration of 10^{14} phage per mL (determined by absorbance analysis) (152). The phage was checked for the correct genome size by DNA gel electrophoresis, and the sequence of the peptide insert reconfirmed by DNA sequence analysis.

2.2.4 Biotinylation of Ab and HEL

Biotinylation of IgG and Fab was performed following the protocol described by Menendez *et al* (137). Briefly, 50-100 μg Ab in 50 μL PBS was mixed with 11 μL 1M bicarbonate buffer and 50 μL of a 0.5 mg/mL solution of sulfo-NHS-LC biotin in 2 mM sodium acetate, pH 6.0. Following an incubation of 2 h at RT, 500 μL 1M Tris-HCl, pH 7.4, was added for 30 min to quench the reaction. Subsequently, 1mL TBS plus 20 μL of 50 mg/mL BSA in TBS was added to the solution. The reaction was washed three times, each with 2 mL TBS in Centricon® Centrifugal filter units (30 and 10 NMWL kDa filters for IgG and Fab, respectively). After washing, an equal volume of sterile, 100% glycerol was added, along with sodium azide to final concentration of 0.02% (w/v). Ab was stored at –20°C. For the biotinylation of HEL, 100 μg of protein underwent the same procedure as for the Abs except that the amount/volume of all of the reagents was doubled and the bio-protein was washed in a Centricon® Centrifugal filter units (3 NMWL kDa)

2.2.5 Affinity selection of RPLs and sublibraries.

Both solid-phase and in-solution screenings were conducted. Prior to all rounds of screening, the input phage were pre-adsorbed against the screening tools used, either SA-coated plate wells or SA-coated magnetic beads, to remove SA-binding and other "background-binding" phage (153). For all screenings presented in this chapter, 10^{11} phage particles were used for Round 1 and 10^{10} PEG/NaCl purified phage particles were used for all subsequent rounds.

For the in-solution procedure, various concentrations of bio-D1.3 Fab or bio-IgG were pre-incubated ON at 4°C with the RPLs (or sublibrary) prior to immobilization of the bio-Ab-phage complexes on SA-coated magnetic beads. Unbound phage particles were removed by washing the beads multiple times with TBS containing 0.5% Tw with the aid of a Dynal magnet, or using a 96-well filtration plate along with a vacuum manifold. For solid-phase screenings, bio-D1.3 IgG was captured on SA immobilized in plate wells (of 96-well high-binding plates). The libraries were incubated in the wells for 2 h at RT. The wells were then washed multiple times with TBS containing 0.5% Tw to remove unbound phage particles.

For the screening of the 15 primary RPLs with bio-D1.3 IgG, and the 55E3 and 55C4 sublibrary screenings, phage particles were acid eluted from the beads or plate wells in 50 µL acid elution buffer (0.1 M glycine/HCl, 1% w/v BSA, pH 2.2) for 10 min, rotating at RT. The acid eluted phage pools were transferred to a fresh microfuge tube containing 10 µL neutralization buffer (1M Tris/HCl, pH 9.1) for final pH 7.0 – 7.4. The acid elution and neutralization procedure was repeated so that all phage particles were released from the beads or wells. The eluted phage were then amplified ON in starved *E. coli* K91 cells and PEG/NaCl-purified for input into the next round of screening. For the NNK-doped E3 sublibrary screening, bead-captured phage particles were directly amplified ON, in starved *E. coli* K91 cells, and then PEG/NaCl-purified for input into the next round of screening.

Spot titer analysis of the pools, to calculate the percent yield (the number of phage enriched each round as a percentage of total input phage) was determined after each round. If a screening successfully enriches for phage clones, at each successive round, the proportion of input phage that bind the target molecule increases, and this should correlate with an increase in percent yield. The pooled phage clones were also assayed side-by-side for binding to D1.3 MAb (the screening Ab) in ELISA. For those rounds showing positive pool binding, individual clones were selected, amplified, tested for binding in ELISA, and then sequenced in the region of the peptide insert (144).

2.2.6 Direct enzyme-linked immunosorbent assay (ELISA)

Microwells were coated ON at 4 °C with 35 µL TBS containing $1x10^{10}$ phage particles or, 1 µg HEL, OVA or SA. To coat peptide directly onto the plate, 0.5 - 1 µg peptide in 35 µL TBS was "dried" in each microwell by incubation of the uncovered plate at 37°C for approximately 5 h; this procedure was conducted prior to the ON incubation of other Agns also included on the plate.

The following day the wells were blocked for 30 min at 37 °C with TBS containing 2% BSA (w/v) (TBS/BSA). To capture bio-peptide, those wells that had been coated overnight with SA were aspirated and 0.2 – 0.5 µg bio-peptide in 35 µL TBS incubated in each well for 30 min at RT. The plates were then washed six times with TBS/Tw, either by hand or with a plate washer (the plates were shaken for 5 seconds on the low setting and set to stand for 5 seconds between each wash).

For direct ELISA analysis, D1.3 IgG or Fab (bio or unbio, and at concentrations ranging from 1 nM to 100 nM) or diluted mouse serum was added to the microwells in 35 µL TBS containing 1% BSA and 0.1% Tw (TBS/BSA/Tw) and incubated for two h at RT. The wells were then washed six times with TBS/Tw. For the detection of unbio-Abs of murine origin, 35 µL HRP-conjugated-goat- (anti-mouse IgG-H+L)-Ab (for Fab) or HRP-conjugated-goat- (anti-mouse IgG-Fc)-Ab, or HRP-conjugated protein A, diluted 1:1500 in TBS/BSA/Tw was incubated in each well for 40 min at RT. For the detection of bio-Ab, HRP-conjugated-NA was used as the secondary reagent. All incubations were performed on a rocker.

ABTS development solution was prepared by mixing 3.07 mL 0.1M citric acid (19.2 g citric acid anhydrous in 1L distilled water, pH 2.4) and 1.93 mL 0.2M Na_2HPO_4 (17.2 g sodium phosphate, dibasic, anhydrous in 600ml distilled water, pH 9.2), with 2 mg of 2- 2'-azino-bis(3-ethylbenzthiazoline-6-sulfonic acid) and 5 µl (30%) (w/w) H_2O_2. After incubation with the secondary Ab/reagent, the plates were washed six times with TBS/Tw and 35 µL of the freshly prepared ABTS solution added to each well. The absorbance at 405 nm and 490 nm was measured and reported as (A_{405}-A_{490}) x 1000. Readings were typically after 15, 30 and 45 min incubation. Unless otherwise indicated, all ELISA data are presented at 30 min.

2.2.6.1 Titration ELISA

The direct ELISA procedure was followed for titration ELISAs, except that the primary Ab or serum was serially diluted in TBS/BSA/Tw before being added to the blocked microwells.

2.2.6.2 Reducing ELISA

ELISA plates were coated ON with Agn and blocked with TBS/BSA as described for direct ELISA. Subsequently, the plates were washed and the "+DTT" wells were treated with 35 µL TBS containing 15 mM DTT, and the "-DTT" wells were treated with TBS alone for 30 min at 4°C. The wells were washed and 35 µL of the primary Ab added, either in TBS alone or in TBS containing 5 mM DTT (for the "+DTT" wells), and incubated for 3 h at 4°C. Direct ELISA procedures were followed for the remainder of the assay.

2.2.6.3 Competition ELISA

For competition analysis with D1.3, 20 nM of D1.3 Fab was pre-incubated ON at 4°C with serial dilutions of peptide or HEL, starting at 1mM and using 1:3 dilutions, prior to incubation with plate-immobilized HEL or peptide. For competition analysis of sera from HEL and E3 phage-immunized mice, serially diluted serum samples (starting at 1:200 dilution) were incubated with 3-10 µM HEL or 10 µM peptide, ON at 4°C, prior to incubation with plate-immobilized Agn. After 2 h incubation at RT, the wells were washed and "free Ab" that bound to the immobilized Agn was detected with HRP-conjugated-goat- (anti-mouse-IgG-H+L)-Ab or HRP-conjugated-goat- (anti-mouse-IgG-Fc)-Ab and ABTS development.

2.2.7 MBP fusion construction

Transfer of peptides from the N-terminus of pVIII to the N-terminus of the maltose-binding protein (MBP) is described in detail in Zwick *et al.*, (151). Briefly, DNA encoding the *tac* promoter, the pVIII leader sequence and the E3 phage-displayed peptide was amplified from single-stranded, recombinant E3 phage DNA by PCR. The double-stranded PCR product was purified with a QIAquick PCR purification column and cut at its unique XhoI and PstI sites. The cut product was isolated by electrophoresis on a 6% agarose gel in Tris borate EDTA buffer (154). The isolated insert was ligated into the pMal-X vector which had been cut at the same restriction sites, isolated by electrophoresis on a 0.7% agarose gel run in Tris acetate EDTA (154), and extracted with a Qiaquick Gel Extraction kit. MC1061 *E. coli* cells were transformed with the ligated DNA and grown in Luria Bertani (LB) medium containing 100 µg/mL ampicillin

(Amp; the pMal-X vector encodes MBP and beta lactamase which confers Amp resistance). The transformed cells were diluted and plated on agar containing LB and 100 μg/mL Amp (LB/Amp plates). Individual colonies were selected and amplified, and plasmid DNA was extracted using a Qiaquick Plasmid Mini kit. Purified plasmids were analyzed in restriction digestion and then sequenced to verify presence of the E3 peptide insert. A plasmid encoding the E3 insert was used to transform E32507 *E. coli* cells, a strain of *E. coli* that does not produce MBP, which were then plated. The following day, a single, fresh, ampicillin-resistant colony was used to prepare a 20 mL ON culture of LB containing 100 μg/mL Amp and 0.2 % glucose. The next day, 10 mL of ON culture was transferred to 1 L of LB media (also containing 100 μg/mL Amp and 0.2 % glucose) and grown ON.

The cells were harvested by centrifugation at 4000 x g for 20 min at 4°C and the periplasmic fraction prepared by cold osmotic shock (155) following the Protein Fusion and Purification System manual (from NEB). The MBP-E3 fusion protein was affinity purified using an amylose resin column following the manufacturer's protocol. The MBP (of the E3-MBP fusion protein) bound the amylose resin while other proteins were removed by washing. The fusion protein was eluted with buffer containing 10 mM maltose. The purified E3-MBP fusion protein was concentrated with a Centriprep-30 (30,000 MWCO) concentrator. The final concentration of purified E3-MBP protein was determined using the Bio-Rad Protein Assay following the manufacturer's protocol.

2.2.8 KinExA analysis for Kd determination

The KinExA (Kinetic Exclusion Assay) method for Kd determination measures the concentration of free Ab in an Agn-Ab reaction solution at equilibrium. The amount of "free" Ab is determined by exposing the reactions to Agn that has been immobilized on polymethyl-methacrylate (PMMA) beads. The amount of free Ab that binds to the solid phase, as measured by fluorescence emission from a fluorescently labelled secondary Ab, is directly proportional to the concentration of free Ab in the equilibrium phase. The KinExA immunoassay is described in detail in Blake *et. al.*, (156) and in Craig *et al.*, (147).

Briefly, PMMA beads were coated with bio-BSA, followed by SA, and then bio-HEL. Between each coating, the PMMA beads were washed multiple times to remove any unbound material. To set up the Agn-Ab equilibrium state mixtures, serial dilutions of peptide, staring at 200 μM were incubated with 20 nM D1.3 Fab or IgG. This concentration of Ab is below the predicted μM Kd range for the peptides so the reaction is driven by Agn and not by Ab. The

mixtures were incubated ON at 4°C to allow them to reach equilibrium. The following day, the equilibrium phase mixtures were sequentially passed over a column packed with HEL-coated beads. The "free Ab" that bound to the Agn-coated PMMA beads was measured for each mixture using a 1:1000 dilution of the secondary Ab, Cy5-conjugated-goat- (anti-mouse-IgG-H+L)-Ab, which was detected with a laser and light reader. (A fresh pack of beads filled the chamber for each equilibrium phase mixture and the beads were washed after the primary and secondary Ab samples were passed over them.) All experiments were conducted in duplicate.

Data was analyzed with software provided by the manufacturer, Sapidyne Instruments, Inc. The fluorescent signals were recorded and plotted as a function of peptide concentration. The best-fit values for the Kd, and the concentration of Ab active sites were calculated, as well as the 95% confidence interval for these values. Binding was assumed to follow the equation: Kd =[Ab][Agn]/[AbAgn], in which [Ab] and [Agn] represent the concentrations of free Ab and Agn, respectively. Thus, free Ab at equilibrium, [Ab] = Kd[AbAgn]/[Agn]. Because total Ab (Abt) and the total Agn (Agnt) are the sum of their free and bound components, Abt = [Ab] + [AbAgn] and Agnt = [Agn] + [Ab Agn], these equations can be substituted into the free Ab equation to get free Ab as a function of Kd, Abt and Agnt.

The fluorescence signal measured by the KinExA instrument is linear with [Ab] and is defined by the signal in the absence of free Ab (Sig0%) and the signal when 100% of the Ab is free (Sig100%) (156). The calculation of intermediate signals, therefore, is a linear interpolation: Signal = (Sig100%-Sig0%)([Ab]/Abt) + Sig0%. The combination of this equation, with the equation for free Ab at equilibrium, provides a theory of signal as a function of Kd, Abt, Agnt, Sig100% and Sig0%. The KinExA software to determine the values of Kd, Abt, Sig100% and Sig0%, which minimized the squared error between the theory and the measured signals, used this theory. Varying the Kd parameter and re-optimizing other variables for each point determined the 95% confidence interval. The analysis, therefore, determines the range over which the Kd or Abt maintain fit to the data points.

2.2.9 Alanine replacement scan of the phage-displayed E3 peptide

Phage DNA mutagenesis is described in detail in protocol 16.4 of (137). Briefly, the 5' phosphorylated Ala-scan oligonucleotides were annealed with phenol-chloroform purified single-stranded phage DNA, using a 1:15 molar ratio of template to oligonucleotide, by heating the sample to 70°C and then cooling it slowly to RT. A reaction master mix, comprising T7 DNA polymerase buffer (provided with the enzyme), BSA, ATP, T4 DNA ligase and T7 DNA

polymerase, was prepared and added to each of the annealed solutions, then incubated for 5 min on ice, 5 min at RT, 60 min at 37°C, and 10 min at 70°C. Ligation products were concentrated and desalted using a 10K Ultrafree®-MC Centrifugal Filter Device. MC1061 cells were electroporated and plated on NZY/Tet ON at 37°C. The following day, colonies for each of the mutants were selected, amplified in NZY/Tet/IPTG and sequenced to verify the presence of Ala at each position along the peptide sequence.

2.2.10 Sublibrary construction

Single-stranded f88.4 vector DNA (157) was used to construct the 55E3 and 55C4 sublibraries and the E3 doped sublibrary as described in (144). The cloning strategy is illustrated in Figure 2.1. Briefly: (1) Single-stranded, circular f88.4 phage DNA was extracted from phage with phenol/chloroform/isoamyl alcohol. (2) A short oligonucleotide, complementary to the *HINDIII* restriction site of the phage DNA was annealed to the phage DNA so that it could be cut with *HINDIII*. (3) The sublibrary or doped-NNK sublibrary oligonucleotide (see reagents) was annealed to the cut and linearized phage vector DNA *via* a 15-base overlap. (4) Both ends were filled using VENT and Klenow Fragment DNA polymerases. (5) The two ends were cut with *PstI* and ligated to form monomeric circular DNA. (6) Vector DNA was used to transform MC1061 *E. coli* cells and the sublibrary amplified. (7) Phage were PEG/NaCl-purified from the cell supernatant.

Figure 2.1. Cloning strategy for phage-displayed RPL construction.

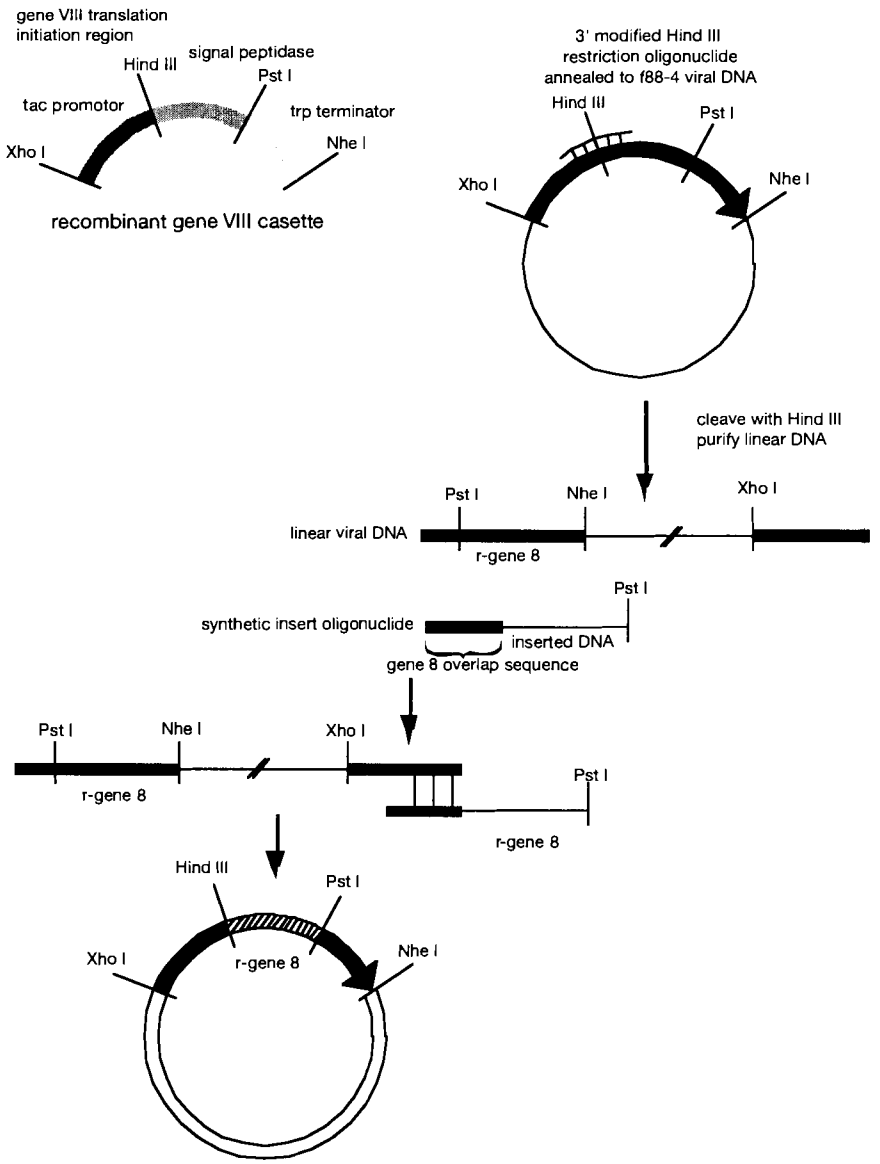

2.2.11 Glutaraldehyde cross-linking of HEL

Glutaraldehyde is a commonly used reagent for cross-linking proteins *via* primary amine groups (*i.e.*, the N-terminus of a protein or the epsilon-amino group of Lys) (158). To produce cross-linked HEL, 1mg HEL was dissolved in 250 µL PBS and 250 µl 0.2% (v/v) glutaraldehyde was added drop-wise. The solution was rotated at RT for 30 min. To quench the reaction, 125 µL 1M Tris was added and incubated for 1 h at RT. The cross-linked protein was dialyzed ON at 4°C in 3500 MWCO dialysis tubing in 2 L PBS. The following day, the buffer was replaced with 2 L fresh PBS buffer, and dialysis continued for another 5 h. The cross-linked protein was analyzed by SDS-PAGE analysis. To prepare HEL-f1-K phage conjugate, 1 mg HEL and 500 µg f1-K phage (2 x 10^{13} phage particles) were combined in 200 µL PBS and 200 µL 0.2% (v/v) glutaraldehyde was added drop-wise. The reaction was similarly quenched and dialyzed as described for the HEL conjugate.

2.2.12 Mouse immunizations

Mice were immunized every second week intraperitoneally (ip) with 50 µg of HEL or cross-linked HEL, and the Adjuvax adjuvant according to the manufacturer's recommendations (Figure 2.8). For the prime-boost immunization study (section 2.3.8), mice were immunized subcutaneously (sc) with 10 µg HEL-f1K conjugate or 100 µg recombinant phage, along with the Ribi adjuvant, according the manufacturer's suggestions. Mice were bled from the tail or from the ankle just prior to each immunization. Five days after the final boost, the mice were bled by cardiac puncture under CO_2 anaesthesia. The blood samples were left to clot ON at 4°C, and then centrifuged at 12, 000 x g for 10 min. The sera were transferred to fresh microfuge tubes and stored at –20°C.

2.2.13 Sodium dodecylsulfate polyacrylamide gel electrophoresis (SDS-PAGE) of the major coat protein pVIII

SDS-PAGE was carried out following the protocol of Zwick *et. al.*, (146), modified from Schagger and von Jagow (159). The major coat protein of f88-4 was resolved on a 16% polyacrylamide gel in a Tris-tricine buffered system using the Bio-Rad Mini-Protean®II Electrophoresis Cell (Bio-Rad Laboratories). Phage were mixed with buffer containing SDS and

glycerol, boiled for 5 min to lyse the phage particles and denature their coat proteins, before loading them into wells of the gel. The gels were silver stained (160).

2.3 Results

2.3.1 RPL screening with bio-D1.3 Ab yields two consensus sequences.

A panel of 15 RPLs (Table 2.1) was screened with bio-D1.3 IgG. To capture all of the D1.3-binding phage clones, Round 1 was conducted as a solid-phase assay in wells coated with SA-captured bio-D1.3 IgG. The final three rounds were conducted in-solution with 100 nM, 50 nM and 5 nM of bio-D1.3 IgG, respectively. For the in-solution rounds, bio-D1.3 IgG-phage complexes were captured on SA-coated magnetic beads

Several copies of two D1.3-binding phage clones were enriched from each of two RPLs, Cys4 and LX10. Direct ELISA binding data with D1.3 IgG and sequences of these clones are presented in Table 2.2. In order to optimize the D1.3-binding peptides, two sublibraries, 55E3 and 55C4 (also shown in Table 2.2) were constructed. For the 55E3 sublibrary, both Cys residues, as well as the consensus residues (underlined) were fixed and all others were fully randomized. For the 55C4 sublibrary, the Cys residues as well as Pro and Gln (underlined) were fixed. The Tyr and Ser residues were both randomized with Tyr, Ser and Ala (underlined and shown in brackets).

Table 2.2. ELISA binding data and distinct consensus sequences identified for D1.3 Ab-binding phage clones selected from a panel of RPLs.

Phage Clone	OD $_{405-490}$ [c]	Sequence
55E.2 (Cys4)[a]	0.37	RKENCAGDLCQRWI[b]
55E.3 (Cys4)	0.57	SNRNCDGHYCLRMG
55E3 Sublibrary:		X_3NCXGX$_2$CXRX$_2$
55C.1 (LX10)[a]	0.38	HCFPQTSTVPATCT[b]
55C.4 (LX10)	0.27	QCRPQTSKLPAMCS
55C4 Sublibrary:		XCXPQ(T/S/A)(T/S/A)X_5CX
HEL	0.34	
f88-4 phage	0.01	

[a] RPL from which the clones were derived.
[a] Consensus residues fixed in the sublibraries are underlined.
[c] Binding of 100 nM D1.3 IgG detected with HRP-conjugated protein A.

2.3.2 Sublibrary screening yields optimized D1.3-binding phage clones.

Three rounds of screening were conducted for the 55E3 and 55C4 sublibraries (Table 2.2). The Fab concentration used for the three rounds, as well as ELISA analysis of the phage pools, are presented in Table 2.3. Also shown is ELISA analysis of two of the parental phage clones as well as the unscreened sublibraries. The data shows that D1.3-binding phage clones were enriched for both sublibraries by the second round of screening.

Round 1 was conducted as a solid-phase screening (on 96-well plates) and Rounds 2 and 3 were carried out in-solution (with capture of bio-D1.3 Ab-phage complexes on SA-magnetic beads). To increase the stringency of the screening and select for stronger binding phage clones, the concentration of D1.3 Fab was decreased for the second and third rounds. The screening was also conducted with Fab instead of IgG (a monovalent screening agent *versus* a bivalent one) to select for higher affinity phage clones (161).

Table 2.3. ELISA analysis of the 55E3 and 55C4 sublibrary screening phage pools with D1.3 Fab.

Controls		**55C4 Sublibrary Screening**		**55E3 Sublibrary Screening**	
	$OD_{405-490}$[a]		$OD_{405-490}$		$OD_{405-490}$
f88 phage	0.03	**Round 1**[b]		**Round 1**	
		100 nM	0.04	100nM	0.17
HEL	1.04	**Round 2**[c]		**Round 2**	
		10 nM	0.10	10 nM	0.40
		1 nM	0.15	1 nM	1.07
		0.1 nM	0.07	0.1 nM	0.99
Sublibrary:		**Round 3**[d]		**Round 3**	
55E3	0.03	1nM	0.11	1 nM	0.89
55C4	0.03				
Parental clones:		(Input from R2 10 nM screening)		(Input from R2 10nM screening)	
55E.3	0.57				
55C.4	0.05				

[a]ELISA analysis of the sublibrary pools with 100 nM bio-D1.3 Fab.
[b,c,d] D1.3 Fab concentrations used for the three rounds of screening.

ELISA and sequence data for phage clones selected from Rounds 2 and 3 are presented in Table 2.4. Clones identified from the 55E3 and 55C4 sublibraries showed improved binding to bio-D1.3 Fab as compared to their respective parental clones, and clones isolated from the 55E3 sublibrary bound better to bio-D1.3 Fab than clones from the 55C4 sublibrary (Table 2.3 and Table 2.4).

Numerous independent phage clones were selected from the 55E3 sublibrary, and Asp and His (underlined in Table 2.4) were identified as additional consensus residues. Also, Ser residues were present, at different positions in the peptide sequence, for 7 of the 9 clones. Only two peptide sequences, however, were identified from 55C4 sublibrary screening. Both of the 55C4 sublibrary optimized clones bear two additional Pro residues, as well as Tyr, Thr and Asp (underlined).

Table 2.4. Summary of phage clones selected from the 55E3 and 55C4 sublibrary screenings.

Clone	Sequence	OD $_{405\text{-}490}$ [a]
55E3 Sublibrary: X_3**NC**X**G**X_2C**X**RX_2 [b]		
E3R2.4 (**"E3"**)	SQP**NC**D**G**LV**C**N**R**WH [c]	1.14
E3R2.5	GSS**NC**D**G**GS**C**V**R**RH	1.10
E3R2.15	PVS**NC**D**G**SN**C**I**R**YH	1.06
E3R2.10	RVR**NC**D**G**KY**C**V**R**SH	1.04
E3R3.8	DLK**NC**D**G**EA**C**V**R**WH	1.04
E3R2.2	GSS**NC**D**G**GS**C**V**R**RH	0.94
E3R2.7	LTT**NC**D**G**QA**C**I**R**WH	0.92
E3R2.16	PLP**NC**D**G**AS**C**V**R**RS	0.76
E3R2.18	YPP**NC**D**G**SYCF**R**IH	0.63
55C4 Sublibrary: X**C**X**PQ**(**T/S/A**) (**T/S/A**) X_5**C**X		
C4R3.14 (**"C4"**)	TC**Y**P**QTS**TTPPH**C**D	0.35
C4R3.8	R**C**Y**PQSS**TDPPY**C**D	0.27

[a] ELISA analysis of sublibrary clones with 100 nM bio-D1.3 Fab. The ELISA was repeated to confirm reproducibility of results.
[b] Fixed consensus residues are shown in bold.
[c] Additional consensus residues identified in the sublibrary screenings are underlined.

One peptide from each of the sublibraries, ASQPNCDGLVCNRWH (E3 peptide) and TCYPQTSTTPPHCD (C4 peptide), was chosen for affinity studies as well as to test for the presence of D1.3 or D1.3-like Abs in the sera of HEL-immunized mice. Synthetic peptide was prepared for both peptide sequences with Pro-Ala-Glu or Pro-Ala-Glu-Lys-bio included at the carboxy terminus (explained in Materials and Methods).

2.3.3 Competition ELISA reveals that the E3 and C4 peptides cross-react with each other and with HEL for binding D1.3 Fab.

Although the E3 and C4 peptides bear few residues in common, they compete with one another for binding D1.3 Fab. They also cross-react with the cognate Agn, HEL. Figure 2.3 presents competition ELISA data, testing the ability of both peptides (the peptide in solution was not bio) to block binding of D1.3 Fab to immobilized bio-E3 peptide, bio-C4 peptide and HEL. (Both bio-peptides were captured in the wells *via* SA). The signal against the bio-C4 peptide is low for these ELISAs because only 20 nM bio-D1.3 Fab was used for the assays (due to a limited supply of both bio-D1.3 Fab and the peptides). Also, the ELISA signal of D1.3 Fab binding to

bio-E3 peptide is always stronger than to bio-C4 peptide (this is also true for binding of D1.3 Fab to the recombinant E3 and C4 phage clones; Table 2.4).

For both ELISAs, 20 nM D1.3 Fab was incubated with decreasing concentrations of peptide, starting at 1mM. At the highest concentration of both the E3 and C4 peptides in solution, full competition occurred against the plate immobilized E3 peptide, as well as against the plate immobilized HEL. This suggests that the peptides are binding to the same, or overlapping, region of the D1.3 paratope that is buried in binding with HEL. Figure 2.2 reveals that the IC_{50} (inhibitory concentration 50%) of E3 peptide against immobilized HEL is approximately 37 μM and the IC_{50} of the E3 peptide against plate-immobilized bio-E3 peptide is about 4 μM. Thus, there is approximately a 10-fold difference between these two IC_{50} values. The IC_{50} against the C4 peptide could not be determined due to low ELISA signals. Figure 2.3 reveals an IC_{50} of approximately 110 μM for the C4 peptide against HEL and an IC_{50} of about 12 μM for the C4 peptide in competition against immobilized bio-E3 peptide. Once again there is approximately a 10-fold difference in the IC_{50} values of peptide *versus* peptide and peptide *versus* HEL.

These data demonstrate that D1.3 Fab binds more strongly to plate-captured HEL than to SA-immobilized bio-E3 or bio-C4 peptide as evidenced by higher ELISA signals against HEL than against the peptides. The ELISA signal for 20 nM D1.3 Fab is approximately 0.85 for HEL, 0.5 for bio-E3 peptide and less than 0.15 for bio-C4 peptide. The competition analysis suggests that the affinity of D1.3 Fab is higher for HEL than for either of the peptides because it takes a 10-fold higher concentration of both peptides in solution to reach IC_{50} against HEL than against the E3 peptide. Also, approximately 3-fold more C4 peptide in solution is required to reach IC_{50} against the E3 peptide than for the E3 peptide to reach IC_{50} in competition with itself (12 μM versus 4 μM). Thus the affinity of D1.3 Fab is probably higher for the E3 peptide than for the C4 peptide.

Figure 2.2. Competition ELISA of the E3 peptide against plate-captured HEL, bio-E3 peptide and bio-C4 peptide, for binding D1.3 Fab.

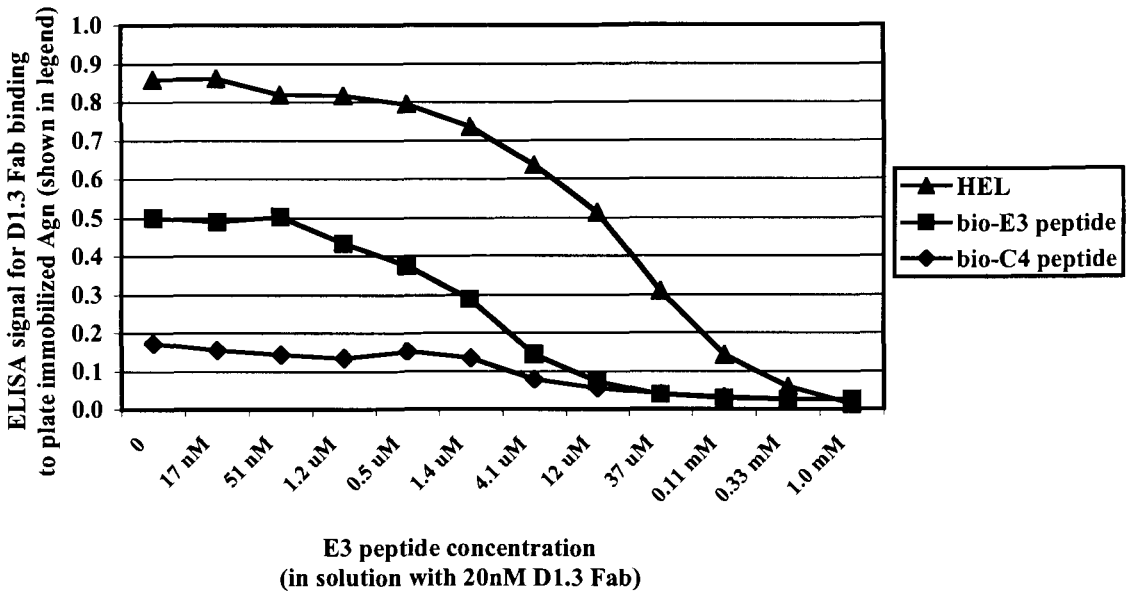

For the competition analysis, 20 nM D1.3 Fab was incubated with decreasing concentrations of E3 peptide, starting at 1 mM. The free Fab in solution was tested for binding to 1 μg plate immobilized HEL or 0.2 μg bio-E3 or bio-C4 peptide captured on immobilized SA.

Figure 2.3. Competition ELISA of the C4 peptide against plate-captured HEL, bio-E3 peptide and bio-C4 peptide, for binding D1.3 Fab.

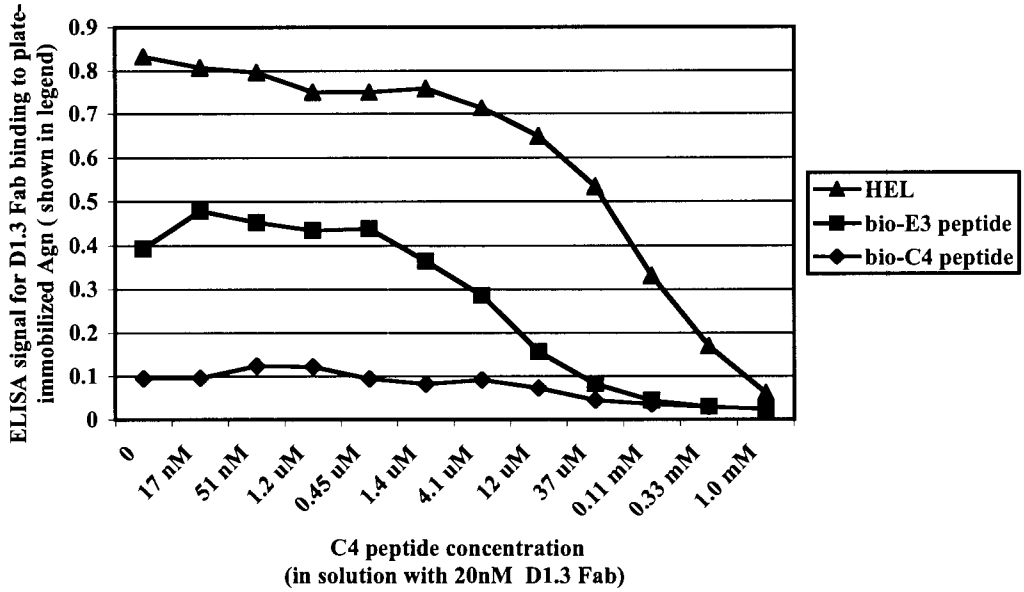

For the competition analysis, 20 nM D1.3 Fab was incubated with decreasing concentrations of C4 peptide, starting at 1 mM. The free Fab in solution was then tested for binding to 1 μg plate immobilized HEL or 0.2 μg bio-E3 or bio-C4 peptide captured on immobilized SA.

2.3.4 Kd determination for D1.3 Ab with HEL, the E3 and C4 synthetic peptides, and the E3-MBP fusion protein.

Several Kd values have been published for D1.3 Ab and HEL (described section 1.7.2 of the thesis introduction). England *et al.,* reported a Kd of 11.5+/-1.9 nM (125) and Hawkins *et al.*, reported a Kd of 3.3 nM (127). Prior to conducting Kd analysis of the E3 and C4 peptides, the Kd for D1.3 Fab and HEL was measured with the KinExA (Kinetic Exclusion Assay) instrument as a control experiment. The KinExA method for Kd determination measures the concentration of free Ab in an Agn-Ab equilibrium solution (described in methods section 2.2.8). All Kd experiments were conducted in duplicate and the data collected, including Kd value, % error, Kd high and Kd low values, summarized in Table 2.4, are averaged from the two experiments.

Table 2.5. Summary of Kd data calculated by KinExA analysis.

Binding Interaction	Kd Value	% Error	Kd high	Kd low
HEL and D1.3 Fab	3.4 nM	2.8	4.4 nM	14 nM
E3-MBP fusion protein and D1.3 Fab	31 nM	4.8	44 nM	13 nM
C4 synthetic peptide and D1.3 Fab	6.2 μM	1.6	7.5 μM	4.7 μM
C4 synthetic peptide and D1.3 IgG	4.1 μM	4.1	8 μM	1.5 μM
E3 synthetic peptide and D1.3 Fab	1.7 μM	4.4	2.4 μM	1.9 μM

The Kd high and Kd low represent a 95% confidence interval in the Kd estimate, and are a function of the best-fit error of the theoretical binding curve to the data. All values are averaged from two experiments.

The Kd for D1.3 Fab and HEL was measured as 3.4 nM, which falls within the range of published values (3.3 nM and 11.5+/-1.9 nM) (125) (127). D1.3 Fab bound the E3 and the C4 peptides with an affinity of 1.7 and 6.2 μM, respectively. Thus, as indicated from the competition ELISA data in Figure 2.2 and Figure 2.3, D1.3 Fab binds with highest affinity to HEL and with lowest affinity to the C4 peptide. The Kd for D1.3 IgG and the C4 peptide was determined to be 4.1 μM, similar to the Kd for D1.3 Fab and the C4 peptide. Because the KinExA instrument uses an in-solution assay to measure Kd values, and the Agn-Ab equilibrium mixture passes very quickly over the Agn-coated beads (the beads capture free Ab), the avidity effect from bivalent IgG molecules *versus* monovalent Fab molecules is minimized (156).

One of two Kd curves determined for D1.3 Fab and E3 peptide is shown in Figure 2.4. The 95% confidence interval for Kd high and Kd low for that curve is presented in Figure 2.5. On the y-axis in Figure 2.4 is shown the percent free D1.3 Fab, and on the x-axis is the concentration of E3 peptide in solution - as the concentration of E3 peptide increases, the percent free Ab decreases. Note that the data presented in Table 2.5 for D1.3 Fab and E3 peptide are the mean values from two experiments so the numbers in the figures are different from those in the table.

Figure 2.4. Kd determination for D1.3 Fab and the E3 peptide.

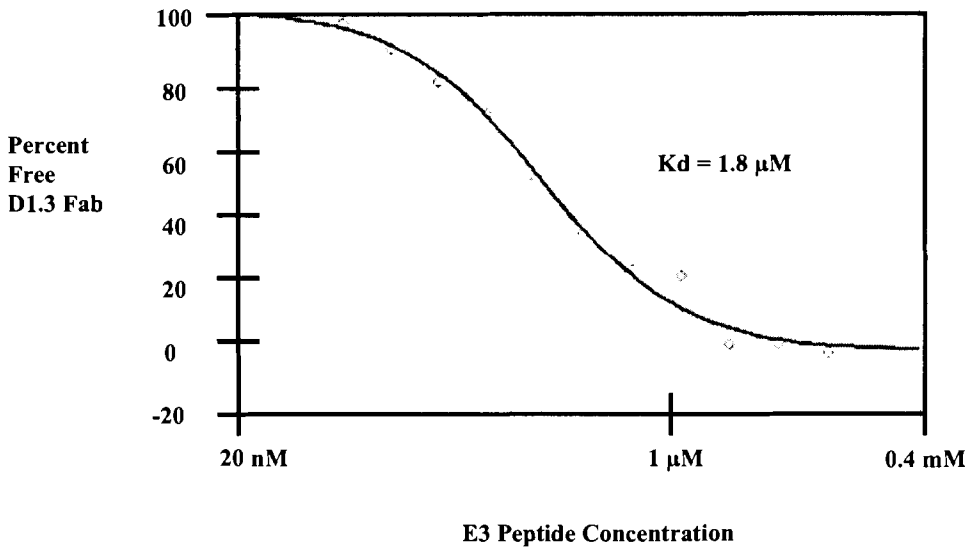

Figure 2.5. The 95% confidence interval for Kd high and the Kd low for D1.3 Fab and E3 peptide.

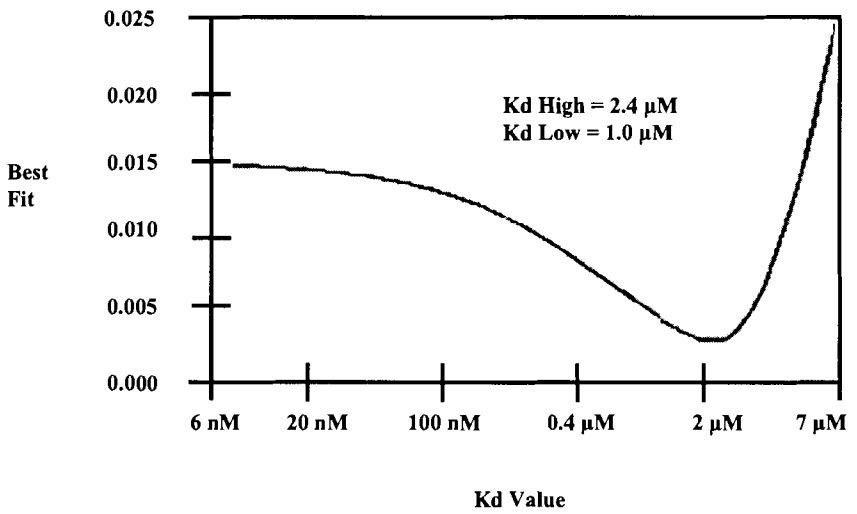

Previous work, by our lab and others, has shown that it is not uncommon to observe a drop in Ab-binding strength when recombinantly-displayed peptides are replaced by their free synthetic counterparts (19, 162, 163). In the context of a fusion protein, the peptide's structure and range of movement may be stabilized because it is "tethered" *via* a peptide bond to the carrier– this stabilization may in turn improve the apparent affinity of the Ab for the peptide. Therefore, to gauge the affinity of the phage-displayed E3 peptide (as compared to synthetic peptide), the E3 peptide was recombinantly displayed at the amino terminus of MBP (E3-MBP)

following the procedure established by (151). The Kd of D1.3 Fab and E3-MBP fusion protein is 31 nM, a two order of magnitude increase in affinity over the E3 synthetic peptide, but still ten-fold weaker than the affinity of D1.3 Fab for HEL. All Kd data for D1.3 Fab and E3-MBP is summarized in Table 2.5.

The Kd values were determined for D1.3 Fab and both free synthetic E3 peptide and E3-MBP because the Kd might influence the peptide's immunogenicity. As described in the thesis introduction, (Section 1.4, page 9) the production of TD Ab responses takes place within the GC, and the survival and ultimate amplification of a particular B cell clone is thought to be determined by competition for Agn (72). Thus, a B cell bearing a BCR with higher affinity for Agn will receive signals for survival and those bearing lower affinity BCRs will be "out competed" and hence eliminated from the pool. Thus, the immunogenicity of the peptide and/or the probability of amplifying B cells bearing D1.3 or D1.3-like Abs *might* be higher using recombinant E3 phage as immunogen rather than E3 peptide chemically cross-linked to a carrier protein.

2.3.5 Alanine replacement scan for the phage-displayed E3 peptide reveals critical binding residues in common with its cognate HEL epitope.

A series of recombinant E3 phage mutants was produced in which each amino acid of the E3 peptide was individually replaced with Ala. Phage clones bearing single Ala substitutions were then tested in direct ELISA for binding to D1.3 Fab and various concentrations of D1.3 IgG. The binding data for each of the mutants are presented as a percentage of Ab binding to the wild-type E3 phage clone. Figure 2.6 shows the percent binding of 10 nM D1.3 Fab to each of the mutants and Figure 2.7 shows the percent binding of D1.3 IgG to the mutants as compared to the wild-type E3 phage clone. These figures reveal that D1.3 Fab showed greater discrimination in binding the phage mutants than the IgG. As the IgG concentration was lowered in the assay, however, its reactivity against the Ala replacement mutants more closely resembled that of D1.3 Fab. ELISA analysis against the E3 Ala replacement clones was repeated three times with various concentrations of D1.3 Fab and IgG to ensure reproducibility of results.

Figure 2.6. Percent binding of D1.3 Fab to the E3 phage Ala replacement mutants as compared to the wild-type E3 clone.

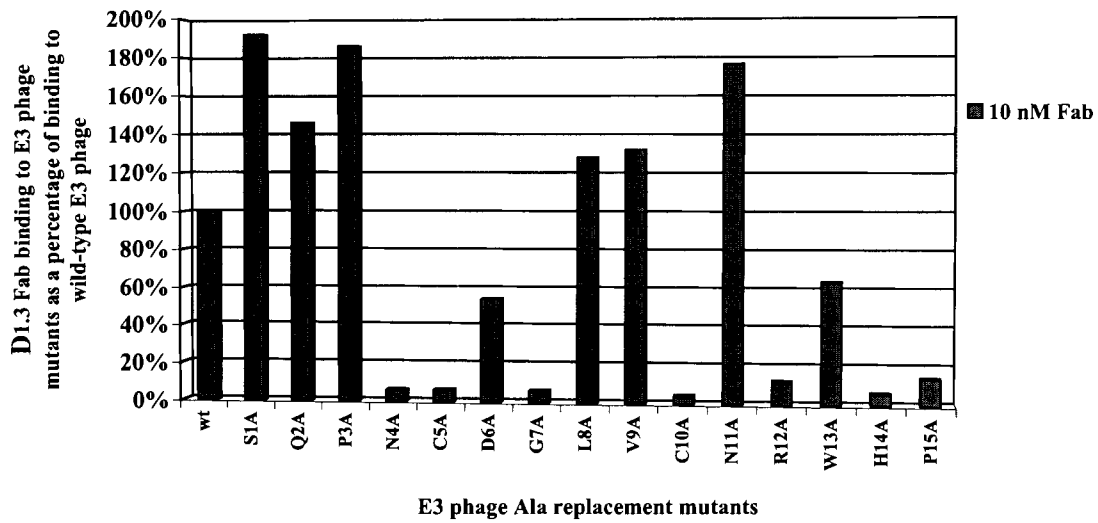

Binding of 10 nM D1.3 Fab to the plate-immobilized phage clones was measured in direct ELISA. Direct ELISA OD $_{405\text{-}490}$ for binding to the wild-type (wt) E3 phage (less background binding to f88 phage) is 0.70. HRP-conjugated-goat-(anti-mouse-IgG-H+L)-Ab was used as the secondary detection reagent.

Figure 2.7. Percent binding of D1.3 IgG to the E3 phage Ala replacement mutants as compared to the wild-type clone.

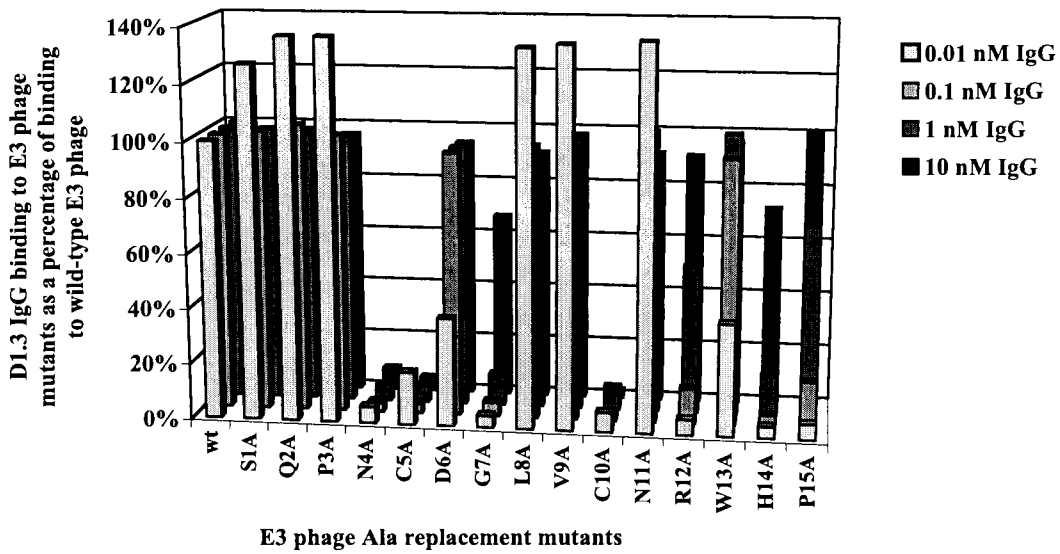

Binding of D1.3 IgG to the plate-immobilized phage clones was measured in direct ELISA. Four concentrations of D1.3 IgG (shown in the legend) were used for the assay. Direct ELISA OD 405-490 for binding to the wt E3 phage, from the highest to lowest IgG concentration tested (less background binding to f88 phage), were 1.25, 1.22, 1.12 and 0.62, respectively. HRP-conjugated-goat-(anti-mouse-IgG-H+L)-Ab was used as the secondary detection reagent.

Analysis of the data in Figure 2.6 and Figure 2.7 reveals that some of the E3 peptide's residues are critical for binding D1.3 Ab because their replacement with Ala abolishes binding by the Ab. Other Ala replacement mutants, however, improve binding by D1.3 Ab to the phage clone. In these instances, the replacement with Ala may have eliminated a side chain that was a hindrance to Ab binding. Interestingly, although Pro15 is fixed in the recombinant pVIII protein (it is not encoded as a part of the recombinant peptide), it is critical for the D1.3 Ab-E3 phage interaction. Pro residues often form "kinks" in proteins. Thus, this residue may be important for proper orientation of the side chains of other amino acids in the peptide sequence.

The importance of each residue comprising the E3 peptide for binding by D1.3 Fab and D1.3 IgG are summarized in Table 2.6. Each residue is defined as critical (C), important (I), not

important (N) or alanine is best (A) as explained in Table 2.6. Because IgG binding to the phage mutants was influenced by its concentration, the relative importance of residues is gauged at both low and high IgG concentration. From the analysis, Asn4, Cy5, Gly7, Cys10, Arg12, His14 and Pro15 were identified as CBRs for binding 10 nM D1.3 Fab. Only Asn4, Cys5 and Cys10 were characterized as CBRs for 10 nM D1.3 IgG. At 0.01 nM D1.3 IgG, however, Gly7, Arg12, His14 and Pro15 were also considered CBRs. CBRs in common between the E3 peptide and its cognate HEL epitope are presented in the discussion.

Table 2.6. Importance of E3 residues for binding D1.3 Fab and IgG.

Residue:	S1	Q2	P3	N4	C5	D6	G7	L8	V9	C10	N11	R12	W13	H14	P15
D1.3 Fab	A	A	A	**C**	**C**	I	**C**	A	A	**C**	A	**C**	I	**C**	**C**
D1.3 IgG	A-N	A-N	A-N	**C**	**C**	N-I	**N-C**	A-N	A-N	**C**	A-N	**I-C**	N-I	**I-C**	**I-C**

E3 residues were defined as: (i) critical (C) if binding to the Ala mutant was less than 25% of wt binding (shown in bold), (ii) important (I) if binding ranged from 25% to 75% of wt binding, (iii) not important (N) if percentage of wild-type binding was greater than 75% and (iv) alanine best (A) if binding to the mutants was greater than 100%.

2.3.6 Strong anti-HEL titers are found in sera of HEL-immunized mice but there is no reactivity with the E3 or C4 peptides.

Mice were immunized with HEL or HEL conjugate, and Adjuvax adjuvant. Sera collected after four immunizations with 10 μg immunogen were tested in ELISA analysis for binding to HEL and the cross-reactive peptides, E3 and C4. Serum titration ELISA against HEL, shown in Figure 2.8, reveals strong anti-HEL Ab responses were generated in the mice (half-max titers are approximately 1 in 300,000). As shown Table 2.7, there was no binding of the anti-HEL the sera with the cross-reactive E3 and C4 peptides (the bio-peptides were captured on SA) or the recombinant E3 and C4 phage clones.

Sera from numerous HEL-immunized mice, at even lower dilutions, have also been tested for reactivity with the E3 and C4 peptides but none have shown evidence of binding (data not shown). This lack of reactivity of anti-HEL sera with the peptides could be a result of: (i) low representation of D1.3 or D1.3-like Abs amongst HEL-immunized BALB/c mice, (ii) low titres of the Ab(s) within individual BALB/c mice, or, (iii) insufficient affinity of the peptides for the D1.3 or D1.3-like Abs resulting in undetectable levels of binding *via* ELISA assays. Because D1.3 Ab is so close in sequence to its germline genes, it was strongly suspected that low titers, coupled with insufficient affinity of the D1.3 or D1.3-like serum Abs for the E3 peptide or recombinant

E3 phage, may have prevented their detection in direct serum ELISA. Thus, the E3 peptide was further optimized through an NNK-doped E3 sublibrary construction and screening.

Figure 2.8. Serum titration ELISA against HEL for four BALB/c after four immunizations with HEL or HEL conjugate in Adjuvax.

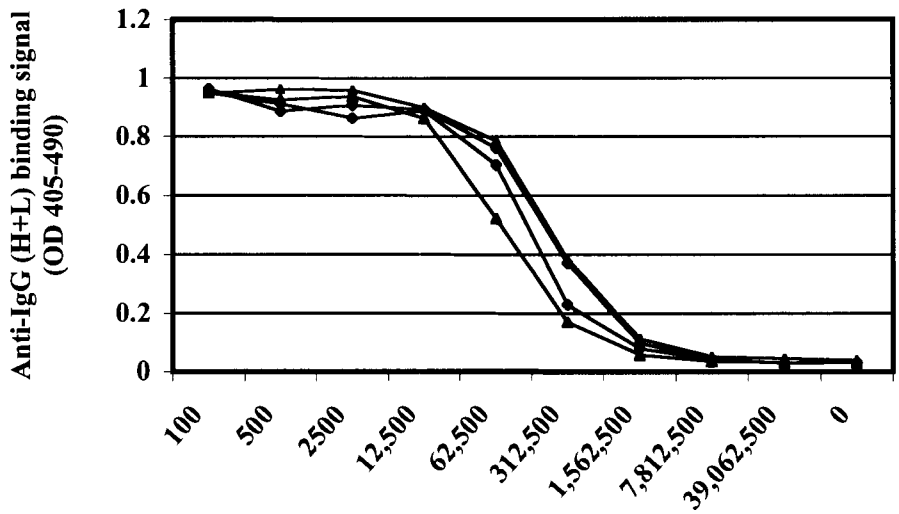

Table 2.7. Direct ELISA of sera from HEL-immunized BALB/c mice shows binding to HEL but not to the E3 or C4 peptides.

Anti-HEL Mouse Serum[a]	1	2	3	4	5	6	7	8	20 nM D1.3 Fab[b]
f88 phage (negative control)	0.07	0.04	0.07	0.05	0.10	0.05	0.05	0.07	0.04
HEL	**1.06**	**1.02**	**1.02**	**0.99**	**0.94**	**1.12**	**1.06**	**1.05**	**0.92**
bio-C4 peptide[c]	0.05	0.03	0.05	0.04	0.10	0.04	0.04	0.05	**0.24**
C4 phage	0.06	0.04	0.06	0.04	0.05	0.05	0.04	0.06	**0.38**
bio-E3 peptide	0.09	0.04	0.06	0.05	0.08	0.05	0.05	0.07	**0.69**
E3 phage	0.02	0.06	0.08	0.07	0.06	0.08	0.06	0.07	**0.96**

[a] 1:500 dilution of serum used for the assay

[b]ELISA signals showing binding of serum, or D1.3 Fab (positive control) to plate-captured Agn are in bold. HRP-conjugated-goat- (anti-mouse-IgG-H+L) was used as the secondary Ab.

[c]The bio-peptides were immobilized on the plates *via* SA.

2.3.7 Optimized clones are selected from NNK–doped E3 sublibrary screening but they do not bind to anti-HEL serum Abs.

In a final attempt to identify D1.3 or D1.3-like Abs in the sera of HEL-immunized mice, an NNK-doped E3 sublibrary was constructed and screened to select stronger D1.3 Ab-binding clones. For the doped sublibrary, each codon of the oligonucleotides encoding the recombinant peptide sequence was doped 50% wt codon and 50% NNK. Only the codons for the Cys residues were fixed because the Ala replacement (Table 2.6) showed that their presence is required for binding by D1.3 Ab to the phage-displayed E3 peptide. This was confirmed by ELISA analysis, presented in Table 2.8, of the clone under reducing conditions. The direct ELISA data in this table shows that D1.3 Ab does not bind to DTT-treated (*i.e.*, reduced) recombinant E3 phage.

Table 2.8. ELISA analysis of D1.3 IgG binding to E3 phage under reducing conditions.

	-DTT	+DTT
E3 phage	0.59	0.02
HEL	0.57	0.30
f88 phage	0.01	0.01

The E3 doped sublibrary was screened in-solution with bio-D1.3 Fab and capture of the bio-D1.3 Fab-phage complexes on SA-coated magnetic beads. ELISA binding data for D1.3 Fab and the library phage pools, as compared to the unscreened doped library, are presented in Table 2.9. Also shown is the concentration of Fab used for each round of screening. Round 1 was conducted with 100 nM bio-D1.3 Fab, and the stringency of the selection was increased in subsequent rounds by decreasing the concentration of Fab used.

Table 2.9. ELISA analysis of the enriched phage pools from the NNK-doped E3 sublibrary screening.

Round	bio-D1.3 Fab (nM) used for the screening[b]		$O.D._{405-490}$ [a]
NNK-doped E3 sublibrary	-		0.05
Round 1	R1	100	0.18
Round 2	R2A	10 [c]	0.66
	R2B	1	0.85
	R2C	0.1	0.80
Round 3	R3A	1	1.25
	R3B	0.1	1.02
	R3C	0.1	0.64
f88 phage	-		0.09

[a] ELISA signals for 10 nM D1.3 Fab and detection with HRP-conjugated goat-(anti-mouse-IgG-H+L)-Ab.
[b]Rounds 2 and 3 were conducted with three different concentrations of Fab.
[c]R2A was used as input for R3A and R2B was used as input for R3B *etc.*

Phage clones, mostly selected from the second round of screening, were tested for binding to D1.3 IgG and D1.3 Fab. The direct ELISA data in Table 2.10 shows that several phage clones were identified in the screening with enhanced binding to D1.3 Fab, as compared to the parental E3 phage clone. The apparent optimization may be due to improved direct contact(s) and/or conformational complementarity between D1.3 Fab and the recombinant peptides.

The optimized peptides identified in the sublibrary screening were all very similar in sequence to the E3 peptide (Table 2.10). Residues fixed in the original 55E3 sublibrary, Asn4, Gly7 and Arg12, as well as Asp6, a consensus residue identified in the 55E3 sublibrary screening, were maintained in all optimized phage clones (except for clone 2B.5). This indicates (but does not prove) that they represent CBRs for binding D1.3. Several bulky residues, including Pro, His and Trp, were also highly conserved amongst the clones and they may be important for structuring the peptides. At least one of the residues at positions 1, 2, 8 and 11, all of which were defined by Ala replacement analysis as "N" or "A" residues (not important for binding D1.3, or their replacement by Ala improves binding to D1.3) were replaced amongst all of the optimized sublibrary clones (except for clone 2B.5).

Table 2.10. Screening of the NNK-doped E3 sublibrary yields optimized phage clones.

	Sequence[a]	10nM D1.3 Fab	1nM D1.3 IgG[c]
4A.9	PR**PNCDG**SVCI**RWH**	1.09	1.36
4B.17	**SQPNCDGLVCIRWH**	0.91	1.31
3C.15	**SQPNCDGLVCVRWH**	0.81	1.34
4B.12	PA**PNCDGGVCVRWH**	0.80	1.33
4A.5	L**QPNCDGHKCVRWH**	0.79	1.34
3A.1	P**QPNCDGLVCVRWH**	0.78	1.37
3B.6	LP**PNCDGPVCRRHT**	0.76	1.26
2B.5	**SQPNCDGLVCNSWH**	0.75	1.29
	HEL	0.73	1.17
3B.4	P**QPNCDGLVCNRWH**	0.72	1.27
3B.7	R**QPNCDGLVCNRRH**	0.72	1.27
3B.10	R**QPNCDGLVCNRRH**	0.71	1.32
3C.18	KR**PNCDGGTCNRWH**	0.71	1.30
4A.3	SL**PNCDGLVCNRWH**	0.71	1.25
2A.15	P**QPNCDGTVCARWH**	0.70	1.26
3A.7	AT**PNCDGLVCSRWH**	0.65	1.33
4C.10	AA**PNCDGLVCNRWH**	0.61	1.24
4A.7	PL**PNCDGGVCNRWH**	0.60	1.20
E3	**SQPNCDGLVCNRWH**	**0.60**[b]	**1.18**
2A.11	VT**PNCDGTFCNRWH**	0.59	1.34
3C.13	**SIPNCDGLVCYRWH**	0.59	1.34
3A.9	LL**PNCDGLVCNRLH**	0.38	1.11
2A.1	P**QANCDGLVCERWH**	0.36	1.14
4A.2	RT**PNCDGQVCNRWH**	0.25	1.31
	f88 phage	0.23	0.03
2A.12	PD**PNCDGLVCNRAP**	0.16	0.04
3A.14	**STPHCDTLFCNRWR**	0.16	0.04
2A.9	**SAPNCDGLVCSRWS**	0.14	0.10
3B.5	HP**PNCHPQNCNTQL**	0.08	0.04
3C.4	**SQPNCDHPMCNPWH**	0.04	0.18

[a] Residues in common with the E3 peptide are in bold.
[b] ELISA binding signals for the wt E3 phage are in bold.
[c] HRP-conjugated-goat-(anti-mouse-IgG-H+L)-Ab was used as the secondary Ab for detecting D1.3 Fab and D1.3 IgG.

Findings from the Ala replacement scan and the NNK-doped E3 sublibrary screening mostly complemented one another but some residues, conserved in the optimized NNK-doped E3 sublibrary clones, were not shown by Ala scan replacement to be CBRs. For example, although Pro3 was conserved in all NNK-doped E3 sublibrary clones, suggesting that it may be an important residue for the D1.3-E3 peptide interaction, the Ala replacement analysis revealed improved binding of the Ala3 mutant to D1.3. This indicates that not only is Pro not a CBR, it in

fact hinders binding by D1.3 Ab. The conservation of Pro residues amongst the optimized clones may be a confounding effect of the RPLs on the analysis. Phage-displayed peptides have a high incidence of Pro residues, probably because they stabilize recombinant pVIII and confer a growth advantage over others that do not bear Pro residues (144). Thus, amino acids that are enriched, or conserved, in a sublibrary screening are not necessarily CBRs; an Ala replacement scan is required to characterize CBRs.

Like the parental E3 phage clone, the optimized phage clones 4A.9 and 4B.17 showed no reactivity with any of the anti-HEL sera with which they were tested in direct ELISA analysis. This indicates that D1.3 may not be a common Ab specificity in the immune response to HEL.

Table 2.11. Direct ELISA of two optimized clones from NNK-doped E3 sublibrary with anti-HEL serum.

Anti-HEL serum	#1[a]	#2	#3	#4	D1.3 IgG[b]
HEL	**1.41**	**1.31**	**1.49**	**1.42**	**1.43**
F88 phage	0.02	0.02	0.02	0.03	0.07
4A.9	0.05	0.07	0.06	0.11	**1.40**
4B.17	0.07	0.06	0.06	0.06	**1.45**

[a] Anti-HEL mouse serum (1:200) binding detected with HRP-conjugated goat-anti-(mouse-IgG-FC)-Ab.
[b] D1.3 IgG (20 nM) binding also detected with HRP-conjugated goat-anti-(mouse-IgG-FC)-Ab.

2.3.8 Immunization with the E3 phage yields anti-E3 peptide Abs.

Mice were immunized sc with recombinant E3 phage in Ribi adjuvant (164) to determine if the E3 peptide is immunogenic in mice. Prior to the immunization, however, the copy number of the recombinant pVIII protein was determined by SDS-PAGE analysis. Shown in Figure 2.9 are the pVIII band for 1 x 10^{10} f88 phage particles in column 1, and the wild-type and recombinant pVIII bands (the recombinant band is the upper one) for the E3 phage clone, serially diluted 1:3 from 1 x10^{11} phage particles in column 3. The recombinant pVIII band in column 6 approximately matches the wild-type pVIII band in column 8. Because 1:3 serial dilutions of phage were used for the gel, a comparison of these two bands reveals that there are approximately nine times more copies of wild-type pVIII than recombinant pVIII per phage clone. Thus, assuming that there are 3000 copies of pVIII per phage particle, there are approximately 333 copies of recombinant pVIII per particle (3000/9=333) - this represents a copy number of approximately 11% (333/3000x100%=11%). Had the peptide been present at a very low copy

number on the surface of the phage (*i.e.*, the immunized mice would have received a very low dosage of the E3 peptide in comparison to the phage carrier) it may have been necessary to immunize the mice with peptide conjugated at high copy number to a carrier protein.

Figure 2.9. SDS-PAGE analysis of recombinant pVIII of E3 phage.

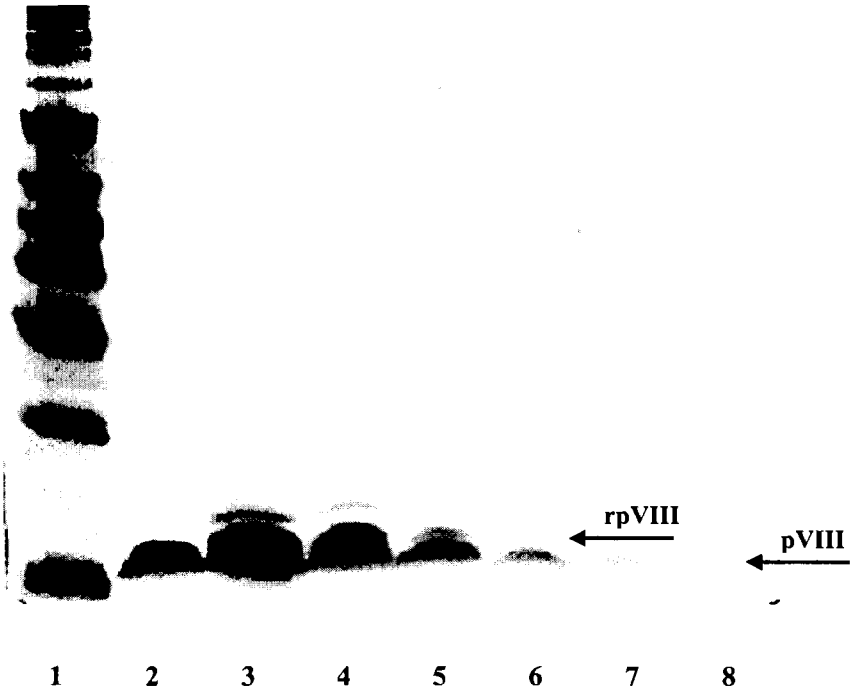

See-Blue® prestained standard protein marker was run in column 1, $1x10^{10}$ f88 phage in column 2, $1x10^{11}$ E3 phage in row 3, and 1:3 serial dilutions of E3 phage in columns 4 through 8. The upper band, visible in rows 3 to 7, is the recombinant (r) E3 pVIII band. The major coat protein pVIII comprises 50 amino acids and its molecular weight is 5,235 Da.

The serum titration analysis presented in Figure 2.10 shows that anti-E3 peptide Abs are elicited in E3-phage immunized BALB/c mice. For sera pooled from four mice, the half-max titer against the unbio-E3 peptide is approximately 1:15,000 and the half-max titer against f88 phage is approximately 1:150,000. The pooled sera were tested for binding to HEL, as well as OVA as a negative control. No binding to HEL was observed above background binding to OVA. Titration analysis for serum samples from individual mice was also conducted (data not shown); there was slight variability amongst the half-max titers against HEL and the E3 peptide but none of the samples showed evidence of HEL-binding Abs. Thus, the E3 peptide is not an immunogenic mimic of its cognate HEL epitope.

Figure 2.10. Titration ELISA for sera combined from four mice, immunized three times with recombinant E3 phage.

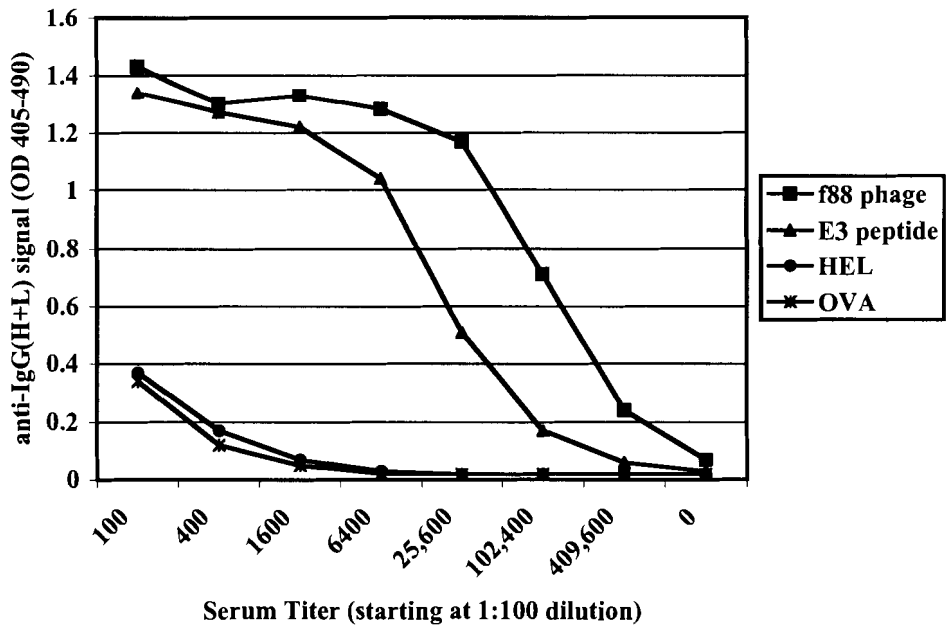

2.3.9 Prime-boost immunization of BALB/c mice with E3 phage fails to yield Abs that cross-react with HEL.

Under the assumption that D1.3 or D1.3-like Abs are commonly produced in HEL-immunized mice, albeit at low titers, a prime-boost immunization was conducted with HEL and recombinant E3 phage. For the immunization, mice were primed with HEL to elicit a pcAb responses, including D1.3 or D1.3-like Abs, and boosted with recombinant E3 phage in an attempt to amplify the D1.3 or D1.3-like Ab response, initially stimulated in the priming immunization with HEL. In order to keep T cell epitopes in common throughout the immunizations, HEL was conjugated to f1-K phage (f1 phage with a Lys residue added near the amino terminus for conjugation purposes) for the priming immunization. The mice were immunized sc, every second week with Ribi adjuvant.

As shown in Figure 2.11, both anti-HEL Ab and anti-E3 peptide Ab were elicited in the immunized mice. Competition ELISA analysis of the sera, however, showed no evidence of Ab specificities that cross-react with HEL and the E3 peptide. The data in Table 2.12 shows that E3 peptide incubated in solution with serum from the prime-boost immunization does not compete with plate-captured HEL for binding to serum Abs. Conversely, Table 2.13, reveals that HEL, similarly incubated in solution with serum, does not compete serum Abs from binding to plate

captured E3 peptide. This lack of cross-reactivity is likely not due to failure of the competition assays (both of which were repeated and also conducted for serum from an individual mouse); HEL in solution was able to compete with plate-captured HEL for binding the serum (Table 2.12) and the E3 peptide in solution competes with plate-immobilized E3 peptide for binding the serum (Table 2.13). Thus the data show that the prime-boost immunization did not produce Abs that cross-react with HEL and the E3 peptide.

Figure 2.11. Titration ELISA for sera pooled from four mice primed with HEL-f1-K conjugate and boosted two times with recombinant E3 phage.

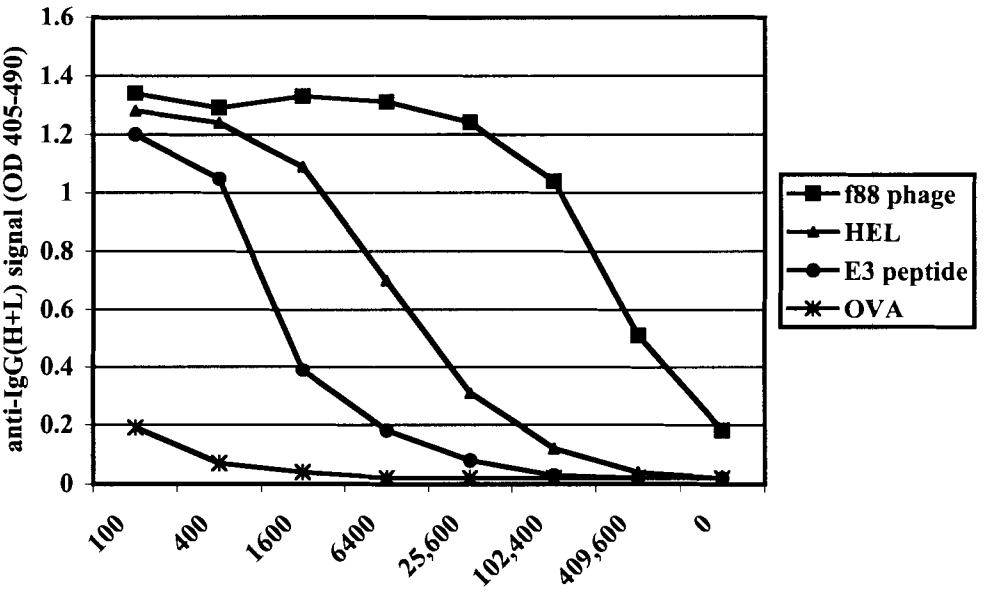

Table 2.12. Competition ELISA of prime-boost sera incubated with HEL, E3 peptide and OVA *versus* plate-immobilized HEL.

Serum Dilution	1:200	1:400	1:800	1:1600	1:3200	1:6400	1:12,800	0
Serum	1.27	1.08	0.99	0.78	0.56	0.33	0.21	0.06
Serum + 10μM HEL	0.14	0.11	0.09	0.07	0.07	0.06	0.06	0.06
Serum + 10μM E3 peptide	1.21	1.11	0.95	0.50	0.48	0.28	0.18	0.06
Serum + 10μM OVA	1.15	0.98	0.75	0.50	0.34	0.23	0.16	0.07

Sera were pooled from four mice primed with HEL-f1-K conjugate and boosted twice with recombinant E3 phage. Shown in bold, 10 μM HEL, incubated ON in solution with serum from prime-boost immunization, competes with plate-captured HEL. Any "competition" that there appears to be between the E3 peptide and HEL is probably non-specific because OVA shows similar levels of competition. The competition ELISA was repeated to ensure reproducibility of results.

Table 2.13. Competition ELISA of prime-boost sera incubated with HEL, E3 peptide and OVA *versus* plate-immobilized E3 peptide.

Serum Dilution	1:200	1:400	1:800	1:1600	1:3200	1:6400	1:12,800	0
Serum	0.60	0.42	0.25	0.15	0.12	0.08	0.07	0.07
Serum + 10μM HEL	0.64	0.41	0.27	0.18	0.14	0.09	0.07	0.06
Serum + 10μM E3 peptide	0.10	0.09	0.08	0.07	0.07	0.05	0.05	0.06
Serum + 10μM OVA	0.62	0.41	0.25	0.17	0.12	0.08	0.07	0.07

Sera were pooled from four mice primed with HEL-fl-K conjugate and boosted twice with recombinant E3 phage. Shown in bold, 10 μM E3 peptide, incubated ON in solution with serum from prime-boost immunization, competes with plate-captured E3 peptide. Neither HEL, nor OVA compete for binding to anti-E3 peptide Abs. The competition ELISA was repeated to ensure reproducibility of results.

2.4 Discussion

As previously discussed in Chapter 1 (section 1.7, page 17), the model protein HEL has been well-characterized with respect to both antigenicity and immunogenicity, and the D1.3 Ab-HEL complex represents one of the most thoroughly studied protein-protein interactions to date (101) (125) (126) (123) (165) (166) (125) (167) (127). Moreover, Goldbaum *et al* were able to establish an idiotypic network for D1.3 Ab (129); they showed that anti-anti-Id MAbs (raised in mice with rabbit pcAbs against D1.3) made several contacts with HEL in common with D1.3, and, that the gene usage of the anti-anti-Id MAbs was similar to that of D1.3. Therefore, the D1.3 epitope was considered an excellent candidate for exploring the concept of epitope-targeted vaccine design.

For this study, it was hypothesized that peptides that cross-react with the discontinuous D1.3 epitope could be selected from RPL screenings with D1.3 Ab and: (i) be used as markers for the detection of D1.3 or D1.3-like Abs in the sera from HEL-immunized mice, and (ii) in a prime-boost immunization with HEL, be used to amplify the production of D1.3 or D1.3-like Abs. These hypotheses were based on the facts that: (i) BALB/c mice are inbred (*i.e.*, all of the mice have identical Ab genes), (ii) D1.3 has only five replacement somatic mutations from its germline genes (168) and, (iii) an idiotypic network established for D1.3 Ab showed that it is possible to elicit "D1.3-like" Abs (129).

The work in this chapter describes the identification and characterization of the D1.3-binding peptide E3 (SQPNCDGLVCNRWH). The E3 peptide was isolated with D1.3 Fab from a random peptide sublibrary in which three consensus residues, Asn4, Gly7, Arg12, as well as two Cys residues that form a disulfide bridge, were fixed. Two additional consensus residues, Asp6 and His14, were identified in the sublibrary screening. ELISA analysis under reducing conditions

showed that the E3 peptide must be constrained *via* a disulfide bridge for binding by D1.3, and an Ala replacement scan of the recombinant peptide confirmed this finding. Thus, conformation of the peptide is critical for its interaction with D1.3 MAb.

An Ala replacement scan of the phage-displayed E3 peptide was used to identify its CBRs. Residues were defined as critical if binding by D1.3 Ab was decreased to less than 25% of binding by D1.3 to wt E3 phage. Epitope CBRs can play a functional role, or a structural role, or both, in their interaction with Ab. That is, they can either mediate direct contact with D1.3 or they help to structure the peptide so that the side-chains of other residues can interact with D1.3, or both. In the absence of structural data it is not possible to determine the roles played by the CBRs.

Direct ELISA analysis of the phage Ala mutants revealed that 7 of the peptides' residues, Asn4, Cys5, Gly7, Cys10, Arg12, His14 and Pro15 are CBRs for binding by D1.3 Fab. The residues Asp6 and Trp13 were identified as important for binding D1.3 Fab. Refer to Table 2.6 (page 58) for a summary for this data. In direct ELISA analysis, D1.3 IgG (which is bivalent *versus* monovalent Fab) showed less sensitivity, especially at higher concentrations, in binding to the Ala mutants. Residues identified as critical for binding by D1.3 IgG are Asn4, and the two Cys residues. Gly7 ranged from being not important to critical, and Arg12, His14 and Pro15 ranged from being important to critical at higher and lower IgG concentrations, respectively.

Residues on HEL that have been identified as playing an important role in binding by D1.3Ab are Ser24, Lys116, Gly117, Tyr118, Asp119, Val120, Gln121, Ile124 and Arg125 (127) (128) (discussed in section 1.7.2, page 23). These surface exposed residues are highlighted in the Swiss-PDB viewer analysis (169) of HEL shown in Figure 2.12. Thus, important or CBRs in common between the E3 peptide and its cognate HEL epitope are Gly, Asp, and Arg. (Note that Gly is not important (N) at high IgG concentration). It is also possible that, given their similarities, Asn4 residue of the E3 peptide is mimicking Gln121 of HEL (169). Contact made by HEL residues Gly117, Asp119, Gln121 and Arg125 with D1.3 Ab are shown in Table 2.14. Only Arg125 does not make direct contact with D1.3.

The D1.3 epitope CBRs in common with the E3 peptide (for D1.3 Fab) are shown in bold in Figure 2.13, also generated with the Swiss PDB viewer (169). Because the peptide bears an intramolecular disulfide bridge, these CBRs may orient themselves in a similar fashion as their counterparts in the D1.3 epitope. Thus, there are potentially four important or CBRs in common between the D1.3 epitope and the E3 peptide. From the NNK-doped E3 sublibrary screening, several optimized clones were identified that bore Val and Ile, both of which are CBRs of the

D1.3 epitope. These clones are presented in Table 2.10 (page 62). Ala replacement of these clones would need to be undertaken to ascertain if these residues are responsible for improved binding by D1.3 Fab.

Figure 2.12. Swiss-PDB Viewer analysis of the CBRs of the D1.3 epitope on HEL (IGXV).

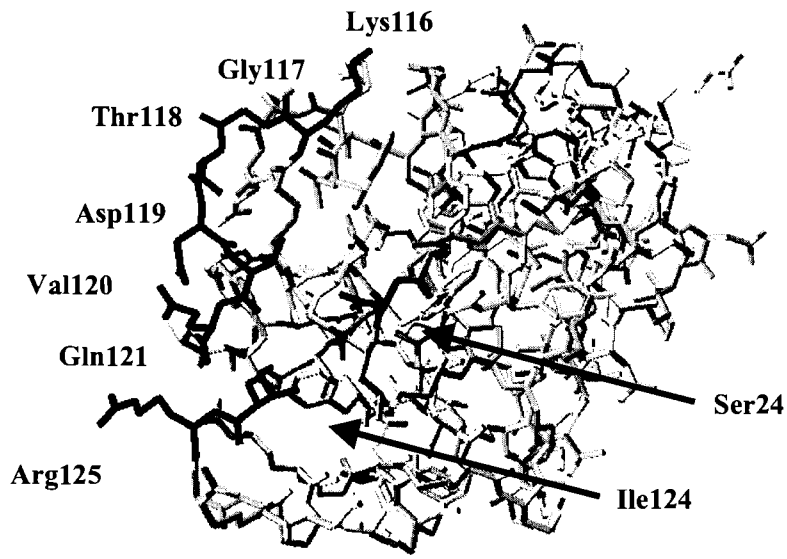

Table 2.14. Contact made by D1.3 Ab with HEL CBRs that are in common with CBRs of the E3 peptide.

	Total Ab Contacts	Light Chain			Heavy Chain		
CBR		CDR1	CDR2	CDR3	CDR1	CDR2	CDR3
Gly117	6H				✓✓✓	✓✓✓	
Asp119	2H					✓	✓
Gln121 (Asn)	4L	✓			✓✓✓		✓
Arg125	none						

Data from Amit *et al.* (122).

Figure 2.13. Swiss-PDB Viewer analysis of the crystal co-ordinates of HEL (IGXV) with the CBRs in common between the E3 peptide and HEL with D1.3 Ab highlighted.

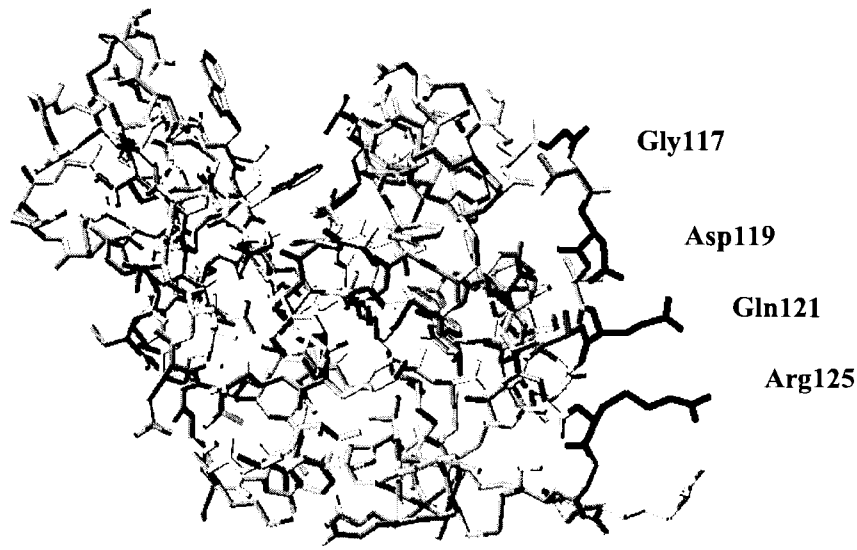

The E3 peptide (SQPNCDGLVCNRWH) bears an intramolecular disulfide bridge so the side-chains of Asp119, Gln121 and Arg125 may orient themselves in a similar manner as their counterparts in HEL.

Affinity analyses were undertaken for D1.3 Fab with the C4 peptide, the E3 peptide and the E3-MBP fusion protein. The Kd of D1.3 Fab and the E3 peptide was determined to be 1.6 μM and the Kd of D1.3 Fab and the E3-MBP fusion protein (probably a better representation of the affinity of the phage-displayed E3 peptide) was 31 nM. Through this extensive characterization, including an Ala replacement analysis, an NNK-doped E3 sublibrary screening,

and affinity studies, it was clearly shown that the phage-displayed E3 peptide is optimized for binding D1.3 Ab. However, neither the C4 peptide, nor the E3 peptide (and two of the optimized phage clones from the doped-NNK E3 sublibrary which were also tested) showed reactivity with sera from HEL-immunized mice. This suggested that either D1.3 is not commonly produced in the BALB/c immune response to HEL or D1.3 Abs are at too low a titer for detection *via* direct ELISA analysis.

The E3 phage clone was tested in direct and prime-boost immunization for its ability to elicit or amplify the production of D1.3 or D1.3-like Abs in BALB/c mice. Although the E3 peptide is itself immunogenic in BALB/c mice, direct immunization with recombinant E3 phage did not elicit Abs that cross-react with HEL. There are major differences in the binding site topographies of Abs elicited against protein *versus* peptides. The binding sites of anti-protein Abs are typically flat with small protuberances and depressions that form a complementary interface with protein, whereas, the binding sites of anti-peptide Abs tend to be groove-like and peptides frequently bury themselves as beta turns within the grooves (46) (23). These differences in paratope topology may *a priori* limit the ability of a peptide to elicit an Ab that cross-reacts with protein.

Had the E3 peptide elicited Abs that cross-react with HEL, it would have been the first example of a peptide mimic of a discontinuous epitope successfully being used as an immunogen to elict Abs against cognate protein. In the literature there are examples of linear peptide fragments (170) [Meola, 1995 #39] (171) (172) (173) (26) and peptide mimics of linear epitopes (174) (33) (175), (31) (36) (32) (176) only that are capable of eliciting Abs that cross-react with cognate linear epitopes.

It was hypothesized, however, that if D1.3 or D1.3-like Abs were generated in the priming immunization with HEL, it might be possible to use the cross-reactive E3 phage in a boosting immunization(s) to specifically amplify the production of D1.3 or D1.3-like Abs. This strategy was attempted, but competition analysis of the sera from mice primed with HEL and boosted with E3 phage showed no evidence of cross-reactive Abs (Table 2.12 and Table 2.13, page 67). It is possible, however, that the prime-boost strategy failed because D1.3 Abs were never stimulated by HEL in the priming immunization in the first place.

In summary, although the E3 peptide binds specifically to D1.3 Ab, and it shares CBRs in common with its cognate HEL epitope, it did not bind to sera from HEL-immunized mice, nor was it able in direct immunization or prime-boost immunization to elicit or amplify the production of D1.3 or D1.3-like Abs. The data suggest that D1.3 Ab is not commonly produced

in the immune response to HEL, even at low titres, and that the E3 peptide/D1.3 epitope is not a feasible model for developing a prime-boost immunization strategy. These findings led to the questions of: (i) whether or not there are any epitopes commonly targeted in the immune response to HEL amongst BALB/c mice, and, if so, (ii) could a peptide marker for a commonly targeted epitope be used in a prime-boost immunization strategy to focus Ab production against that target epitope in all or most animals? These questions are addressed in Chapter 3.

CHAPTER 3 CHARACTERIZATION OF ANTIBODY REACTIVITIES FROM INDIVIDUAL MICE IMMUNIZED WITH LYSOZYME

3.1 Introduction

Chapter 2 describes the identification and characterization of the E3 peptide with the anti-HEL MAb D1.3 as well as an attempt to target the production of D1.3 or D1.3-like Abs with the cross-reactive E3 peptide in a prime-boost immunization strategy. For the prime-boost immunization mice were primed with HEL and boosted with recombinant E3 phage. This work was conducted under the hypothesis that priming mice with HEL would elicit a pcAb response, including D1.3 or D1.3-like Abs (such as the anti-anti-Id Abs characterized by (129) in their idiotypic network with D1.3 Ab), and boosting with the cross-reactive E3 peptide would specifically amplify the subpopulation of D1.3 or D1.3-like Abs. The prime-boost immunization did not yield Abs that cross-react with HEL and the E3 peptide. It is possible, however, that this strategy failed because D1.3 is not a commonly produced Ab specificity in the immune response to HEL and D1.3 or D1.3-like Abs were not stimulated in the priming immunization with HEL in the first place.

The next logical step in testing the concept of epitope-targeted, prime-boost immunization was to identify peptide markers for Abs commonly produced (*i.e.*, immunodominant Abs) amongst BALB/c mice in the immune response to HEL. Thus, HEL would elicit a pcAb response, including the target Ab specificity, in the priming immunization, and the cross-reactive peptide could be tested for its ability to amplify the subpopulation of target Abs in the boosting immunization. The assumption that such peptide markers for common Ab specificities could be selected was based on the facts that: (i) BALB/c mice are inbred, and, (ii) such peptide markers have been identified for various Agns with IgG purified from immune human sera. Kouzmitcheva *et. al.* (177), for example, identified peptide markers from RPLs for Abs present in the sera of patients with Lyme disease; the peptides showed reactivity with multiple sera from infected patients but no reactivity with negative sera. Similarly, Dybwad *et. al.*, (178) selected peptides specific for Abs found in the synovial fluid of rheumatoid arthritis patients. Two additional examples are, Prezzi *et. al.*, (179) and Folgori *et. al.*, (180), who

identified peptides from RPLs that react exclusively with the sera from hepatitis C and B infected patients, respectively

For this chapter, 15 RPLs were screened with pcAbs from the sera of three HEL-immunized mice in an attempt to identify cross-reactive peptide markers for "immunodominant" anti-HEL IgG(s) produced amongst BALB/c mice. Although 22 HEL cross-reactive phage clones with unique recombinant peptide sequences were identified in the screenings, competition analysis amongst the clones ultimately showed that they represent only three HEL epitopes. Analysis of the cross-reactive clones with sera from different HEL-immunized showed that only one of them, phage clone 3D (peptide sequence: TCIHGLPPSECH), represents a marker for an anti-HEL IgG specificity commonly produced amongst BALB/c mice. Moreover, sequence analysis of the clones also showed that only phage clone 3D bears any sequence alignment to HEL (underlined). Direct immunization with the 3D phage clone did not yield anti-HEL Abs but results from a prime-boost immunization are pending.

The 22 HEL cross-reactive phage clones were tested for binding to anti-HEL IgGs from a rabbit. Similarly, HEL cross-reactive phage clones previously identified with anti-HEL rabbit IgG, did not show reactivity with any murine anti-HEL serum samples. Thus, rabbits and mice produce different Abs in response to HEL immunization. In order to further characterize the anti-HEL Ab response in mice, sera from HEL-immunized mice were also tested for reactivity with three HEL peptide fragments, peptides 38-54, 64-82 (described in Chapter 1, section1.7.1, page 19) and 76-100, as well as a set of 10-mer overlapping peptides covering the entire sequence of HEL. The anti-HEL mouse sera did not bind to any of the three HEL peptide fragments but they reacted with a number of the HEL 10-mer peptides. Interestingly, the different serum samples showed similar patterns of reactivity with the 10-mer peptides suggesting that several common HEL epitopes are targeted by Abs produced in different mice.

3.2 Materials and Methods

3.2.1 Reagents

Female BALB/c mice were purchased from Charles River Laboratories (Wilmington, MA). HEL and ALUM adjuvant were purchased from Sigma-Aldrich (St. Louis, MO).

HRP-conjugated protein A/G for the detection of rabbit Abs was purchased from Pierce (Rockford, IL). Protein A/G is a genetically engineered protein that combines the IgG-Fc binding

profiles of protein G and protein A, which come from *Staphylococcus* (72). All other reagents required for ELISA analyses, as well as those needed for RPL screenings, are listed in the Materials and Methods for Chapter 2 (section 2.2.1, page 32).

SA-magnetic beads were purchased from Dynal for the purification of anti-HEL mouse Abs (Dynabeads M280, Dynal, Lake Success, NY). The affinity purified anti-HEL mouse Abs were washed and concentrated in 30 NMWL kDa Centricon® Centrifugal filter unit devices (Millipore, Billerica, MA).

For phage dot blot analysis, a Bio-dot microfiltration apparatus (Bio-Rad Laboratories, Hercules, CA) containing a nitrocellulose membrane (Millipore) was used. Phage dot blot membranes were developed using the ECL Western Blotting Detection Kit (Amersham Biosciences, Piscataway, NJ).

A set of 10-mer HEL peptides, overlapping every second residue and covering the entire sequence of HEL, were synthesized on a cellulose membrane (the HEL peptide membrane) by PepMetric Technologies Inc. (Vancouver, BC). The overlapping peptides were synthesized in duplicate. Non-fat dry milk (NFDM) for blocking the membrane was purchased from Bio-Rad Laboratories. The HEL peptide membrane was developed with the Western Lightning Chemiluminescence reagent (Perkin-Elmer, Wellesley, MA).

The region of HEL called "the loop" comprises residues 64-82 (WCNDGRTPGSRNLCNIPCS). "The loop" peptide was displayed on phage *via* recombinant pVIII. Cys 74 (underlined) was replaced with Ser, so that it wound not interfere with disulfide-bridge formation between Cy65 and Cys81. The oligonucleotide encoding "the loop", for its display at the amino terminus of recombinant pVIII, has the sequence: 5'-ATC ACC TTC TGC AGG AGC ACT ACA AGG GAT ATT ACT CAA ATT ACG ACT ACC AGG GGT ACG ACC ATC ATT ACA AGC AGC GGC AAA GCT TAG CAT AGG AAC-3', and was synthesized at the NAPS Unit (UBC, Vancouver, BC). Reagents required for this cloning experiment are the same as those used for phage sublibrary construction, summarized in the Materials and Methods of Chapter 2 (section 2.2.1, page 32). Recombinant pVIII was shown to be present by DNA sequencing and SDS-PAGE analysis of the clone.

HEL peptide 38-54 with sequence FNTQATNRNTDGSTDYG-K-bio, was synthesized by Multiple Peptide Systems (San Diego, CA). The peptide included a bio-Lys residue at its amino terminus, was amidated at its carboxy terminus, and HPLC-purified to greater than 95% purity as determined by mass spectrometric analysis. The HEL peptide 76-100

(NIPCSALLSSDITASVNCAKKIVS) was a gift from Dr. Eli Sercarz and Dr. Claudia Raja Gabaglia (Laboratory of Vaccine Research, Torrey Pines Institute for Molecular Studies, San Diego, CA). Anti-HEL rabbit IgG was a gift from I. Kumagai (Tohoku University, Sendai, Japan).

3.2.2 Mouse immunizations

Two groups of 20 BALB/c mice were immunized three times, sc every two weeks, with 50 μL of 25 μg HEL and ALUM adjuvant in PBS buffer. An additional five BALB/c mice were immunized sc every two weeks with 25 μg CsCl-purified 3D phage in PBS buffer (no adjuvant used). Blood samples were collected and stored as described in Chapter 2, Materials and Methods (section 2.2.12, page 45).

3.2.3 ELISA analysis

Refer to Materials and Methods in Chapter 2, (section 2.2.6, page 39) for ELISA procedures. Unless otherwise indicated, all ELISA data is shown for $O.D._{405\text{-}490}$ taken after 30 min incubation with the ABTS development buffer. HRP-conjugated-goat- (anti-mouse-IgG-Fc)-Ab was used for the detection of Agn-binding mouse sera.

3.2.4 Purification of anti-HEL Abs on bio-HEL-coated magnetic beads

SA-coated magnetic beads were coated with bio-HEL following the manufacturer's recommendations (5 μg bio-HEL molecules were used per 300 μL beads). After rotating in a microfuge tube for 45 min at RT, the beads were washed four times with 1 mL TBS/Tw, using a magnet to immobilize the beads, to remove any unbound bio-HEL. Serum samples (50 μL) were incubated with the Agn-coated beads (300 μL bio-HEL-coated beads) in a total volume of 550 μL TBS, containing 1% (w/v) BSA, for 3 h rotating at RT. The beads were subsequently washed 4 times with 1 mL TBS/Tw to remove unbound Ab. The captured anti-HEL Abs were eluted with 300 μL 0.1M glycine-HCl, pH 2.2, containing 0.1 mg/mL BSA, and neutralized with 60 μL 1M Tris-HCl, pH 9.1, to a final pH of 7.0-7.5. The eluted Ab was washed and concentrated four times with 1 mL PBS in 30 NMWL kDa Centricon® Centrifugal filter units. The final volume for each washed Ab sample was 100 μL.

To ensure that the purified Abs retained their HEL-binding activity, they were titered against HEL in ELISA analysis. ELISA analysis was also used to determine Ab concentration by comparing the titration curves for purified anti-HEL Abs with the titration curve for a mouse

control IgG sample of known concentration. The titrated anti-HEL Ab and control IgGs were captured in wells coated with goat- (anti-mouse-IgG-H+L)-Ab and detected with HRP-conjugated-goat- (anti-mouse-IgG-Fc)-Ab.

3.2.5 Affinity selection of RPLs with anti-HEL-enriched Abs

Serum Ab from the three mice was individually purified on HEL and then combined to screen 15 RPLs. In-solution and solid-phase screenings were conducted side-by-side. The purpose of the screenings was to identify peptide ligands for Abs commonly produced amongst BALB/c mice in the immune response to HEL. All three anti-HEL Ab samples were combined for the screenings under the assumption that there would be an additive effect for Abs in common between the mice; if all three mice produce Ab "X", for example, then by combining the three samples there would be a greater representation of Ab "X" as compared to Ab"Y" that is not commonly produced.

Before each round of screening, the RPLs were pre-adsorbed with SA-magnetic beads coated with bio-goat- (anti-mouse-IgG-Fc)-Ab for 2 h at RT to remove "background binders". After completing the screenings, the library pools were tested for the presence of goat Ab-binding phage clones that could have been inadvertently enriched in the screening. ELISA analysis revealed no binding of goat Abs to the library pools (data not shown).

For the solid-phase screening, the HEL-enriched screening Abs were captured on 20 μL (200 μg) SA-magnetic beads that had been coated with bio-goat- (anti-mouse-IgG-Fc)-Ab. The pre-adsorbed libraries were then incubated with the solid-phase anti-HEL Abs for 2 h at RT. For the in-solution screening, the pre-adsorbed libraries were incubated ON at 4°C with the screening Abs prior to their capture on the bio-goat- (anti-mouse-IgG-Fc)-Ab coated SA-magnetic beads. Screenings were conducted in TBS in a final volume of 100 μL. The phage-anti-HEL Ab complexes were captured on the beads during 2 h incubation at RT. The beads were pulsed with 100 μL 1 mM biotin to release any SA-binding phage, and washed three times in TBS/Tw to remove unbound phage particles.

Phage particles were acid eluted from the beads in 50 μL acid elution buffer (0.1 M glycine/HCl, 1% w/v BSA, pH 2.2) for 10 min, rotating at RT. The acid eluted phage pools were transferred to a fresh microfuge tube containing 10 μL neutralization buffer (1M Tris/HCl, pH 9.1) for final pH 7.0 - 7.4. The acid elution and neutralization procedure was repeated to ensure all phage particles were released from the beads. Starved cells (30 μL) were added to the eluted

phage, Tet resistance induced, and the infected cells grown ON in 2 mL NZY/Tet/IPTG as previously described (section 2.2.2, page 36). A10 μL sample from each of the pool infections, as well as a control infection of 10^6 f88 phage particles, was diluted 10^{-1}, 10^{-2} and 10^{-3} and plated on NZY/Tet to calculate percent yield of phage after each round of screening. Percent yield is explained in Chapter 2, section 2.2.5 (page 38).

Round 1 screening was conducted with 50 nM anti-HEL IgG (the three HEL-enriched Ab samples were combined) and approximately 10^{11} input phage (the amount of individual RPLs used varied according to library size such that each clone per library was represented by approximately 50 – 80 copies). The RPLs used in the screening are described in Table 2.1 (page 33). Rounds 2 and 3 were conducted with 50 nM and 20 nM screening Ab, respectively, along with 10^{10} input phage from the ON culture supernatant (the phage were not PEG/NaCl precipitated) of the preceding round of screening.

A fairly high concentration of the pcAbs was used in Rounds 1 and 2 to ensure the highest yield per Ab-binding clone possible. The stringency was increased in Round 3 to select for tighter-binding phage clones, as well as for clones recognized by more highly represented Ab (*i.e.*, immunodominant) specificities.

3.2.6 Dot blot analysis of phage clones

Individual phage clones were isolated by infecting 30 μL K91 starved cells with 10^6 phage particles from the Round 2 and 3 screening pools, Tet resistance induced and the cells plated ON at 37°C on NZY/Tet as previously described (Section 2.2.2, page 36). Well- isolated colonies were selected and used to inoculate wells of 96-deep-well plates, containing 1 mL NZY/Tet/IPTG media. The deep-well plates were shaken at 250 rpm ON at 37°C. The following day the deep-well plates were centrifuged at 3500 rpm for 25 min to pellet the cells and the supernatant transferred to a new deep-well plate. Ab-binding clones identified by probing the dot blots were eventually purified by PEG/NaCl precipitation.

From each well of the plate, 50 μL culture supernatant was transferred to the well of a Bio-dot micro-filtration apparatus containing a nitrocellulose membrane. The supernatants were filtered through the membrane by gravity for 30 min and the wells washed once with 100 μl TBS using the vacuum. The membrane was removed from the apparatus and blocked in a solution of TBS containing 5% NFDM for 40 min at 37°C. The blocking solution was decanted, and the membrane incubated at RT for 2 h with a 1:1000 dilution of the three screening serum Abs (using

a volume sufficient to cover the membrane, about 12 mL) in TBS/Tw containing 5% NFDM. The membrane was subsequently washed three times in TBS/Tw (5 min per wash). The membrane was incubated with a 1: 2500 dilution of the secondary Ab, HRP-conjugated-goat-(anti-mouse-IgG-Fc)-Ab, for 1 h at RT. The membrane was then rinsed in TBS/Tw, washed once for 15 min in a solution of TBS containing 5% NFDM, and then washed four times (5 min each) with TBS/Tw. The membrane was developed using the ECL Western Blotting Detection Kit according to the manufacturer's instructions and exposed to X-ray film.

3.2.7 Development of the overlapping HEL 10-mer peptide membrane

The dry HEL overlapping peptide membrane was placed in 20 mL 100% ethanol and rehydrated by the addition of 50 mL PBS every 10 min at RT. The membrane was then blocked in PBS containing 5% NFDM and 0.2% Tw (PBS/NFDM/Tw) ON at 4°C. The following day, the membrane was washed once for 15 min in PBS containing 0.2% (v/v) Tw (PBS/Tw) and then incubated for 2 h at RT with a 1:100 dilution of anti-HEL mouse serum in PBS/NFDM/Tw. All anti-HEL mouse sera were titered against HEL *via* ELISA analysis prior to being used to probe the HEL peptide membrane. Also, control sera (serum from an unimmunized mouse and serum from a mouse immunized three times with 25 μg OVA) were shown by serum titration ELISA to have similar total IgG content as the serum from HEL-immunized mice (data not shown). The cellulose membrane was then washed three times for 5 min each in PBS/Tw before adding the secondary Ab, HRP-conjugated-goat- (anti-mouse-IgG-Fc)-Ab, diluted 1:2500 in PBS/NFDM/Tw. The membrane was incubated with the secondary Ab for 2 h at RT and then washed three times for 5 min each with PBS/Tw, and three times with PBS only. (All washes and Ab incubations were conducted at RT on a rocker.) Excess buffer was removed from the membrane by blotting it on Kim Wipes. The membrane was developed with the Western Lightning Chemiluminescence Kit according to the manufacturer's instructions, and exposed to fast Fuji X-ray film. Films were typically developed after 1-2 sec, 10 sec, and 1 min exposure times in a metal folder.

3.2.8 Cloning of "the loop" peptide 64-82 onto pVIII of phage

A hybrid recombinant f88.4 phage bearing 64-82 of HEL (amino acid sequence: CNDGRTPGSRNLSNIPCSA, with Cys76 mutated to Ser) fused to the N-terminus of pVIII was constructed. The cloning procedure used was the same as the phage library construction protocol described in the Materials and Methods of Chapter 2 (section 2.2.10, page 43).

3.3 Results

3.3.1 RPL screenings with anti-HEL mouse Abs yields phage clones that cross-react with HEL.

To identify peptide markers for Abs commonly produced amongst BALB/c mice in the immune response to HEL, 15 RPLs (described in Table 2.1, page 33) were screened with Abs from three HEL-immunized mice (the mice were immunized three times with 25 μg HEL and ALUM adjuvant). Serum samples from the mice were individually affinity purified on bio-HEL coated SA-magnetic beads to enrich for anti-HEL IgG (anti-HEL Ab responses in BALB/c mice are mostly IgG1 isotype (115)), and eliminate non-specific/polyreactive Abs (181) that may interfere with the screening. A total of 50 μL serum was purified from each of three mice (AH3, AH6 and AH8), and each of the final Ab samples were suspended in 100 μL final volume (*i.e.*, a 1:2 dilution from the original serum sample). Prior to the serum purification on bio-HEL, the half-max ELISA titration signals for the serum samples against HEL were approximately 1:10,000, 1:9000 and 1:6500 for AH3, AH6 and AH8, respectively (data not shown).

The HEL-binding activity of the affinity purified Ab samples was tested by titration ELISA prior to the screening. Titration ELISA of the Abs was also used to determine IgG concentration: the enriched Ab samples were titrated on goat- (anti-mouse-IgG-H+L)-Ab, side-by-side with a mouse IgG sample of known concentration. Figure 3.1 shows the titration curve for the control IgG sample, starting at 100 nM, against goat- (anti-mouse-IgG-H+L)-Ab. For this IgG curve, the half-max signal of approximately 0.4 corresponds with an IgG concentration of 0.04 nM.

The titration curves for the three purified Ab samples against HEL, as well as against goat- (anti-mouse-IgG-H+L)-Ab, are shown in Figure 3.4. The titration curves reveal that the Ab samples comprise similar concentrations of anti-HEL IgG but the total IgG content is greater for AH6 than the other two samples. So that an equal representation of anti-HEL Ab specificities was used from each of the three mice, the "anti-HEL IgG" concentration (rather than total IgG) was estimated for the purified Ab samples; to estimate this concentration, the dilution of Ab captured on HEL for an ELISA reading of 0.4 (this O.D. fell within the linear range of all three curves) was multiplied by a factor of 0.04. Figure 3.2 shows that the half-max titration titers for each of the three Ab samples purified on bio-HEL falls at an O.D. of approximately 0.4. Therefore, the serum half-max titers are approximately 1:5500, 1:3500 and 1:4000 for AH3, AH6

and AH8, respectively. Thus, the concentrations of "anti-HEL IgG" in samples AH3, AH6 and AH8 are approximately 220 nM, 140 nM and 160 nM, respectively.

By multiplying the half-max titration signals for the purified Ab samples against HEL by two, one can compare them with the half-max values against HEL for the original serum samples (recall that 50 μL serum was purified and resuspended in a final volume of 100 μL). Doing so reveals that the half-max titers of the samples are very similar before and after the purification. This indicates that most of the anti-HEL IgG present in the original anti-HEL serum samples were enriched on the bio-HEL-coated beads (*i.e.*, there was an excess of available HEL binding sites to the total number of anti-HEL IgG molecules in the sample).

Figure 3.1. Titration ELISA curve for mouse IgGs of known concentration against goat-(anti-mouse-IgG-H+L)-Ab.

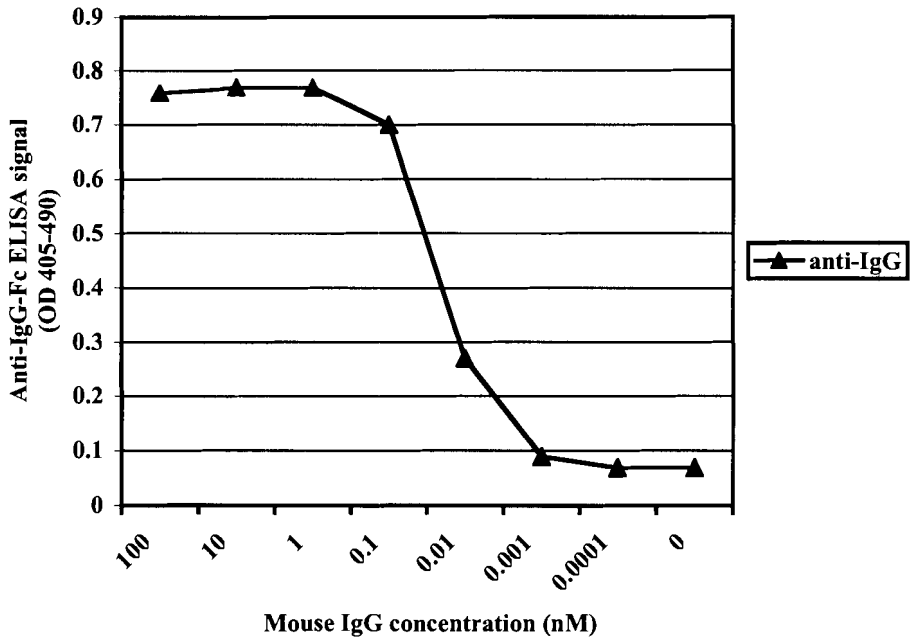

Figure 3.2. Titration ELISA curves for the three HEL-enriched Ab samples against HEL and goat-(anti-mouse-IgG-H+L)-Ab.

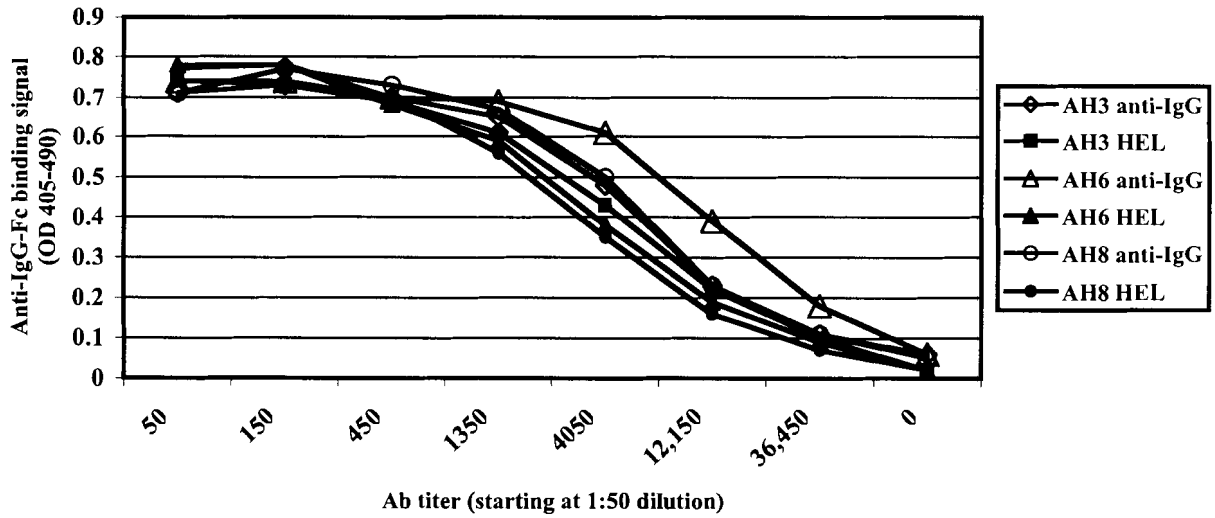

Solid-phase and in-solution phase RPL screenings were conducted side-by-side with the bio-HEL-purified Ab samples. Details of the screening are provided in Materials and Methods (section 3.2.5, page 77). Table 3.1 presents the ELISA analysis of the phage pools from the three rounds of screening. For the ELISA, serum samples AH3, AH6 and AH8 (not the bio-HEL-purified Abs) were combined in equal volumes and then used to analyze the screening pools. Interestingly, the Round 2 in-solution pool showed higher binding to the screening Abs than the Round 2 solid-phase pool. This may be due to the mobility of the Abs in the solution-phase, allowing for multiple Abs of the same specificity to bind to the same phage particle. For the solid-phase screening, the pcAbs are immobilized so there is less opportunity for an avidity effect to occur - Abs adjacent to one another in the solid-phase may be of different specificity. Also, there was a longer incubation period between screening Abs and the phage libraries for the in-solution screening than the solid-phase screening (ON at 4°C *versus* 2 h at RT). The data presented in Table 3.1 suggest that both the in-solution and the solid-phase screenings enriched for Ab-binding phage clones and that a lower concentration of screening Ab could have been used for the second round.

Table 3.1. ELISA analysis of RPL screening pools with the anti-HEL screening serum.

Round	Solid Phase	In-Solution Phase
R1	0.21[a]	0.18
R2	0.99	1.47
R3	1.61	1.80
Plate Controls		
f88 phage	0.11	
HEL	2.10	

[a] ELISA signals for 1:400 dilution of combined screening serum samples AH3, AH6 and AH8.

Prior to the isolation of phage clones, the screening pools were tested in competition ELISA with HEL. The data presented in Table 3.2 demonstrate that HEL competes with the pools for binding to the anti-HEL screening Ab AH6. This indicates that the enriched pools comprise phage clones that bind specifically to anti-HEL Abs.

Table 3.2. Competition ELISA analysis with HEL of Rounds 2 and 3 enriched phage.

		O.D. $_{405-490}$	
Round Pool	**In-Solution for ELISA**	**Solid Phase Screening**	**In-Solution Screening**
R2	Ab[a]	**0.16**	**0.33**
R2	Ab + HEL[b]	0.09	0.02
R3	Ab	**0.48**	**0.48**
R3	Ab + HEL	0.02	0.02
Plate Controls			
HEL	Ab	1.05	
HEL	Ab + HEL	0.24	
f88 phage	Ab	0.02	
f88 phage	Ab + HEL	0.02	

[a] Anti-IgG-Fc signal for 0.5 nM AH6 screening Ab bound to screening pool.

[b] Anti-IgG-Fc signal for free AH6 screening Ab bound to screening pool after incubation with 3 μM HEL for 3 h at RT.

As shown in Table 3.3, ELISA analysis of the screening pools with the individual screening serum samples, AH3, AH6 and AH8, revealed that the pools were enriched for only AH6. Eight other anti-HEL serum samples, as well as serum from a non-immune mouse, were tested for binding to the pools (Table 3.3). Of the additional serum samples tested, only one showed reactivity against the second and third rounds of solid-phase and in-solution phase screenings, while two others showed reactivity against the third round of in-solution screening. This suggests that there are phage clones amongst the pools that bind to Abs in common between these particular serum samples.

Table 3.3. ELISA analysis of Rounds 2 and 3 RPL screenings with sera from eleven HEL-immunized mice.

Mouse Serum Sample[a]	Screening Sera			Eight anti-HEL serum samples								Non-immune sera
	AH3	AH6	AH8	A	B	C	D	E	F	G	H	
R2 in-solution	0.06	**0.89**[b]	0.07	0.09	0.16	**0.88**	0.13	0.08	0.05	0.09	0.14	0.03
R2 solid-phase	0.10	**1.32**	0.11	0.11	0.18	**1.01**	0.19	0.07	0.09	0.11	0.14	0.04
R3 in-solution	0.14	**1.31**	0.12	0.11	0.18	**1.05**	0.16	**0.48**	0.08	0.13	**0.33**	0.04
R3 solid-phase	0.06	**1.36**	0.12	0.10	0.15	**0.73**	0.15	0.08	0.06	0.12	0.13	0.05
HEL	1.23	1.34	1.44	1.39	1.36	1.42	1.42	1.47	0.69	1.42	1.34	0.04
f88 phage	0.14	0.32	0.14	0.11	0.20	0.25	0.14	0.06	0.10	0.14	0.12	0.03

[a] Anti-IgG-Fc signals for sera at 1:200 dilutions.
[b] Phage binding signals that are > two-fold above background binding to f88 phage are in bold.

A total of 80 phage clones were isolated and PEG/NaCl purified from the second and third rounds of screening. Phage clones showing reactivity with the combined screening sera are listed in Table 3.4

Table 3.4. Competition ELISA analysis of HEL and the phage clones selected from in-solution and solid-phase screenings with anti-HEL sera.

Phage clone/ Plate control	Peptide sequence	Sera [a]	Sera + 3μM HEL[b]
HEL	-	1.06	0.60
f88 phage	-	0.03	0.03
2N.18	GCEPSWDLDRCR	1.10	0.04
3N.3 (2x)[c]	QCARDMPPWLCR	1.05	0.05
3N.6	HCEGGPNKCRGG	1.02	0.05
3N.13	QSARNTPQWLRR	1.10	0.04
3D.15	TCIHGLPPSECH	1.10	0.33
3D.20	TCTGDPSKCR	1.10	0.10
3D.25	TCWESGTQAACR	0.67	0.46

[a] Anti-IgG-Fc signals for sera combined from AH3, AH6 and AH8 at 1:200 dilution.
[b] Anti-IgG-Fc signal for 1:200 dilution of combined sera after incubation with 3 μM HEL for 3 h at RT.
[c] Clone was selected twice.

Of the 40 clones selected from Round 2, only one phage clone (clone 2N.18: the 18th clone selected from the Round 2 of in-solution (N) screening) bound the anti-HEL sera. Of the 40 clones selected from the third round of screening, seven clones (three from the solid-phase (D) and four from the in-solution screening) bound to the screening sera. All of the phage clones that showed reactivity with the anti-HEL sera were also cross-reactive with HEL (Table 3.4).

Table 3.5 presents the peptide sequences for eight of the 72 non-binding phage clones selected in the screenings. All eight sequences include stop (B) codons. Thus, these clones may have "survived" the screening process due to a relative growth advantage conferred on clones that do not express the recombinant pVIII protein.

Table 3.5. Peptide sequences of eight non-binding phage clones selected from the RPL screenings.

Clone	Peptide sequence
2N.19	BKALTD*
2D.1	BCKSRTIMREMPEGDSP
2D.10	BCTPHBTTTWPLLSEHH
2D.11	HCSPLHSGWQIHQTCD
3N.18	BCERCPESPRPPPNCQ
3N.26	GCNPRBTLRPDRLSCQ
3D.10	PWARGTKNLPPCBRCA
3D.26	PCNBVHBRPPPPKYCG

* stop codons (B) are underlined

3.3.2 Reactivity of cross-reactive phage clones with a panel of anti-HEL sera.

Even though multiple anti-HEL sera did not bind any of the enriched phage pools (Table 3.3), single clones isolated from these pools may do so. ELISA analysis of the six positive clones (Table 3.4) with four additional anti-HEL sera, as well as serum from a non-immune mouse, is shown in Table 3.6. Although all of the phage clones bound screening serum AH6, only phage clone 3D.15, selected from the third round of the solid-phase screening, reacted with all of the immune sera tested. The other phage clones reacted exclusively with serum AH6. Although anti-HEL serum sample C showed reactivity with the Rounds 2 and 3 screening pools (Table 3.3), it did not bind to any of the isolated phage clones (Table 3.6). Thus, of the 80 clones selected from the second and third rounds of screening, eight clones (representing seven unique sequences) were cross-reactive with HEL, and one of those eight was broadly reactive.

Table 3.6. ELISA analysis of cross-reactive phage clones with a panel of anti-HEL sera.

Phage Clone	AH3	AH6	AH8[b]	C	I	J	K	Non-immune serum
2N.18	0.03[a]	**1.16**	0.06	0.04	0.03	0.19	0.04	0.03
3N.3	0.05	**1.16**	0.03	0.03	0.03	0.12	0.04	0.05
3N.6	0.03	**1.18**	0.03	0.04	0.03	0.10	0.04	0.03
3N.13	0.03	**1.19**	0.05	0.03	0.03	0.10	0.04	0.05
3D.15	**1.13**	**1.14**	**1.34**	**0.90**	**0.48**	**1.04**	**1.17**	0.04
3D.20	0.03	**1.18**	0.06	0.04	0.03	0.18	0.04	0.03
3D.25	0.03	**1.21**	0.06	0.04	0.03	0.16	0.05	0.03
f88 phage	0.04	0.05	0.07	0.05	0.04	0.07	0.05	0.04
HEL	**1.22**	**1.23**	**1.33**	**1.16**	**1.16**	**1.14**	**1.19**	0.08

[a] Anti-IgG-Fc signals for 1:200 dilutions of sera.
[b] Anti-IgG-Fc signals for AH8 are from an independent ELISA conducted under same conditions.

3.3.3 Dot blot identification of HEL cross-reactive phage clones.

In the first phage selection from the RPL screening pools, one of eight HEL cross-reactive phage clones was broadly reactive with anti-HEL sera. It was suspected, therefore, that additional broadly reactive phage clones might have been enriched in the screening. Thus, an additional 564 phage clones were selected and analyzed using the dot blot assay. The dot blot procedure is described in the Materials and Methods (section 3.2.6, page 78). Briefly, K91 starved cells were infected with the Round 3 phage pools and plated ON on NZY/Tet. Only the Round 3 pools were used because six of the seven previously selected positive clones (Table 3.6), including the broadly reactive phage clone 3D.15, were from that round. The following day, 564 colonies from the two pools were selected and amplified in deep-well plates containing NZY/Tet/IPTG medium. Aliquots of supernatants from ON cultures were individually transferred and adsorbed onto a nitrocellulose membrane placed in a dot-blot apparatus; a total of six membranes were used. HEL and supernatant from an ON f88 phage culture were adsorbed to each membrane as positive and negative controls, respectively.

The membrane blots were tested for reactivity with the screening serum AH6. The films developed for two of the phage dot blot membranes probed with serum AH6 are shown in Figure 3.3. Forty of the 564 selected clones (7%) showed reactivity with serum Ab AH6 (represented by dark spots on the film exposed to the developed membrane). The culture supernatants for the positive dot blot clones, as well as two negative clones, were PEG/NaCl purified and tested by ELISA analysis.

Figure 3.3. Films developed for two of the phage dot blot membranes probed with serum AH6.

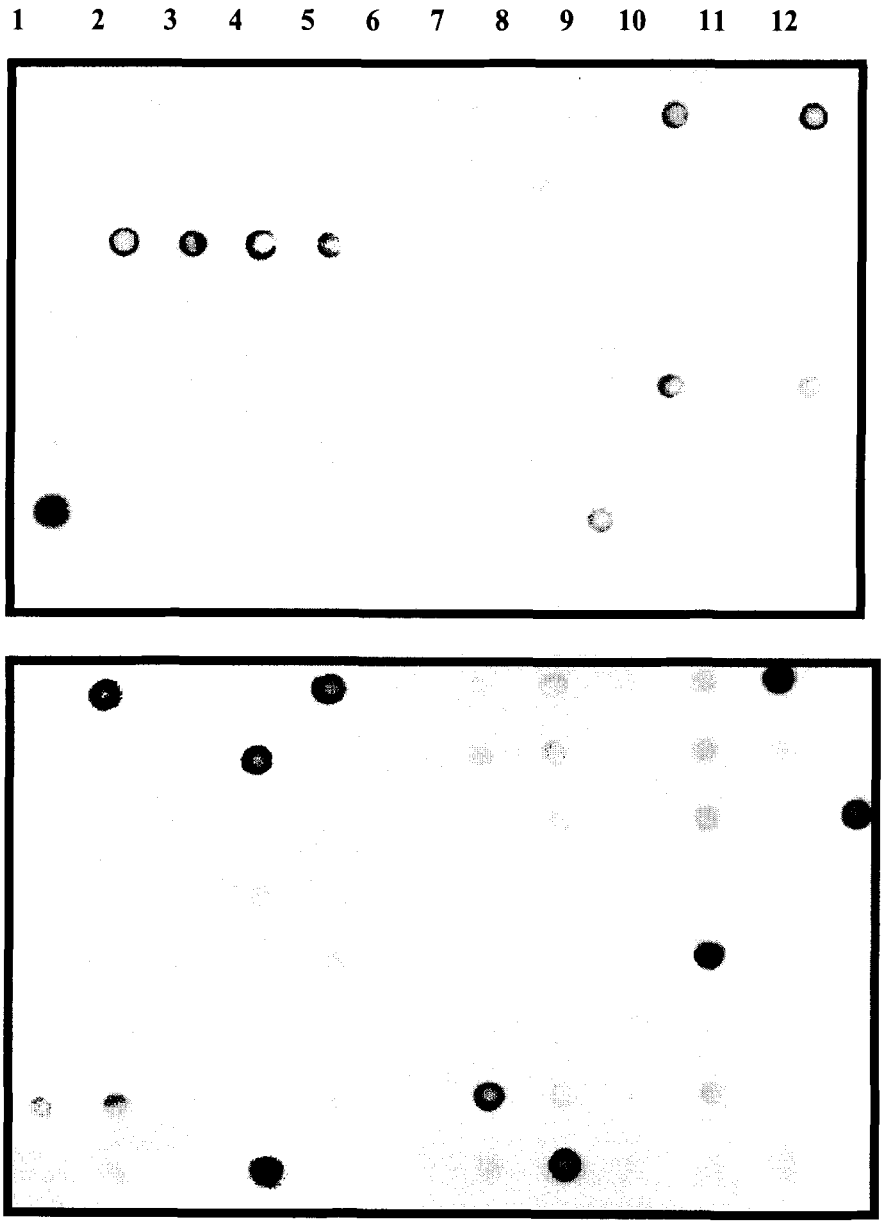

The films are images of two nitrocellulose membranes "blotted" with phage culture supernatants in 96 wells (12 columns by 8 rows), probed with serum AH6 and developed with the secondary reagent, HRP-conjugated-goat-(anti-mouse-IgG-Fc)-Ab plus an ECL detection kit. For each film, the dot in column 1, row 7 is the HEL protein positive control and the dot in column 1, row 8 is the f88 phage culture supernatant negative control. Nine spots were considered positive for each of the upper and the lower blot.

Competition ELISA analysis, summarized in Table 3.7, showed that all 40 positive dot blot clones also cross-react with HEL in binding screening serum AH6. The 40 clones were

tested by direct ELISA for binding to three additional anti-HEL serum samples (data not shown) but the clones only showed reactivity with screening serum AH6. Thus, no additional peptide markers for immunodominant anti-HEL Abs were identified in the dot blot selection.

Table 3.7. Competition ELISA of dot blot phage clones with HEL.

Phage Clone/ Plate Control	Serum AH6[a]	Serum AH6 + 5 μM HEL
HEL	1.14	0.48
F88	0.12	0.11
D3.A3 [c]	0.10	0.19
N1.A3 [c]	0.10	0.20
D1.H3	1.08	0.23
D1.F11	1.12	0.26
D1.E10	1.07	0.28
D2.H6	0.82	0.25
D2.B12	0.85	0.27
D2.G3	0.80	0.27
D2.D4	0.68	0.27
D2.G10	0.89	0.22
D2.E1	0.98	0.17
D2.F8	1.09	0.14
D2.F6	1.11	0.15
D3.B7	0.96	0.10
D3.H9	1.09	0.18
D3.D8	0.90	0.19
D3.G8	0.82	0.17
N1.C12	1.04	0.17
N1.H8	1.09	0.19
N1.H4	1.09	0.19

Phage Clone	Serum AH6	Serum AH6 + 5 μM HEL
N1.B4	1.09	0.17
N1.E10	1.01	0.12
N1.A5	1.09	0.14
N1.G7	1.09	0.14
N1.A2	1.14	0.13
N1.A11	1.12	0.17
N2.F3	0.93	0.16
N2.D11	1.16	0.10
N2.B5	0.96	0.16
N2.C9	1.10	0.14
N2.G5	0.55	0.16
N3.A12	1.08	0.12
N3.A10	1.11	0.13
N3.C5	1.05	0.12
N3.G9	1.06	0.12
N3.C3	1.01	0.11
N3.C2	1.12	0.14
N3.C4	1.18	0.10
N2.G12	1.10	0.13
N2.F4	1.13	0.15
N2.G8	1.11	0.12
N2.H7	1.03	0.13

[a] Anti-IgG-Fc signals for serum AH6 at 1:400 dilution.
[b] Anti-IgG-Fc signal for 1:400 dilution serum AH6 after incubation with 5 μM HEL for 3 h at RT.
[c] These clones were non-binders in the dot blot analysis and are also non-binders in the ELISA analysis.

3.3.4 Competition amongst cross-reactive phage clones.

From both phage selections (80 in the initial PEG/NaCl purification and 564 in the dot blot analysis), a total of 22 unique peptide sequences for HEL cross-reactive phage clones were identified. Peptide sequences, as well as their alignment into consensus groups, are presented in Table 3.8. A comparison of the nucleotide sequences indicates that the clones are independent and not mutants of one another (data not shown). Only one of the 22 phage clones, 3D.15

(abbreviated to "3D"), aligns with the linear sequence of HEL (residues HGL; underlined in Table 3.8) and shows broad reactivity with anti-HEL sera (Table 3.6). 3D may mimic a linear HEL epitope or it may cross-react with one contiguous segment of a conformational epitope.

To determine if the 22 cross-reactive phage clones bind to the same or different anti-HEL Ab specificities in serum AH6, the clones were tested in competition ELISA with one another. The results of the competition ELISA are presented in Table 3.8. For the assay, five of the cross-reactive phage clones, D2.G10, N3.G9, D3.D8, 3N.13 and 3N.3, as well as HEL and f88 phage were coated in the plate wells. All of the cross-reactive phage clones, as well as HEL and f88 phage were independently incubated with serum AH6. Comparison of the full signal (no competition) for the plate-captured clone *versus* the competition signals, determined whether the immobilized and solution-phase phage clones bind to common or different Abs. Competition amongst clones indicates that that clones represent the same HEL epitope and no competition indicates that the clones represent independent HEL epitopes.

The data in Table 3.8 show that, as previously observed (Table 3.4 and Table 3.7), HEL competes with the cross-reactive phage clones for binding to serum AH6. There is also a drop in signal with the negative control, f88 phage, presumably due to steric hindrance of the Abs by the in-solution f88 phage particles, or non-specific adsorption of Abs to them. The competition revealed that, of the 22 unique phage clones selected in the screening, only three HEL epitopes are represented. The broadly reactive phage clone 3D did not compete in solution against any of the five plate-immobilized clones. Phage clones 3N.13 and 3N.3 competed with one another only, and the remaining 19 clones competed against plate immobilized phage D2.G10, N3.G9 and D3.D8, indicating that all 19 clones represent the same epitope. The phage competition ELISA was conducted three times to confirm reproducibility of results.

The Ab specificity that targeted the HEL epitope represented by the 19 phage clones dominated the screening, suggesting that the Ab is either: (i) multispecific and therefore able to bind to a range of related consensus sequences, (ii) immunodominant in terms of titer within serum AH6, or, (iii) able to cross-react particularly well with peptide ligands in comparison to other anti-HEL Abs. It is also possible that the 19 clones represent a series of two or more highly overlapping HEL epitopes that were immunodominantly targeted during the immune response in mouse AH6.

Table 3.8. Sequence alignment and competition ELISA of HEL cross-reactive phage clones with serum AH6.

Competitor in solution[a]	Peptide sequence and consensus residues	Plate-immobilized phage clones				
		D2.G10	**N3.G9**	**D3.D8**	**3N.13**	**3N.3**
None	-	0.47[c]	0.28	0.34	1.07	0.33
HEL	-	**0.06**[e]	**0.06**	**0.05**	**0.05**	**0.05**
f88 phage	-	0.35	0.28	0.30	0.97	0.23
	G...D...KCR					
N3.C2	TCTGDPSKCR[b]	**0.04**	**0.04**	**0.03**	0.65	0.20
D2.D4,	RCFGDGTKCR	**0.06**	**0.04**	**0.04**	0.59	0.20
D2.F8	KCLGDNTKCRGG	**0.04**	**0.04**	**0.03**	0.76	0.25
D2.G10[f]	YCTGDPTKCR	**0.05**	**0.06**	**0.04**	0.72	0.25
D3.G8	SCIGDVMKCR	**0.13**	**0.05**	**0.08**	0.69	0.23
N3.A10	SCGPLTDLLKCR	**0.05**	**0.04**	**0.04**	0.61	0.22
N3.G9	QCTAQTGHNDGSLKCR	**0.09**	**0.04**	**0.06**	0.58	0.20
D2.H6	ACVGAEDKCR	**0.04**	**0.04**	**0.04**	0.69	0.25
D2.G3	NCQGMTDKCR	**0.04**	**0.05**	**0.04**	0.81	0.21
D3.B12	MCEMGPPKCR	**0.06**	**0.04**	**0.05**	0.67	0.25
D3.H9	QCLGGAPKCR	**0.05**	**0.04**	**0.05**	0.68	0.24
N1.C12	HCEGGPNKCRGG	**0.26**	**0.15**	**0.20**	0.78	0.24
	S/T...CR					
D1.F11	NCRLTGTPAACR	**0.03**	**0.04**	**0.03**	0.64	0.22
N2.B5	NCRSTDPNGPCR	**0.09**	**0.04**	**0.06**	0.61	0.20
D2.F6	TCWESGTQAACR	**0.03**	**0.03**	**0.03**	0.57	0.17
2N.18	GCEPSWDLDRCR	**0.13**	**0.05**	**0.08**	0.75	0.25
	CDXSKYRC					
N2.G5	QCDTSKYRCL	**0.19**	**0.07**	**0.13**	0.66	0.24
D3.D8	ECDVSKYRCA	**0.07**	**0.04**	**0.05**	0.68	0.24
N2.H7	QCDESKYRCA	**0.15**	**0.06**	**0.10**	0.85	0.25
	QXARXXPXWLXR					
3N.13	QSARNTPQWLRR	0.36	0.27	0.32	**0.19**	**0.04**
3N.3	QCARDMPPWLCR	0.36	0.24	0.29	**0.28**	**0.05**
3D	TCI**HGL**PPSECH[d]	0.37	0.27	0.32	0.69	0.23
HEL[g]	KVFGRCELAAAMKR**HGL**DNYRGYSLGNWVCAAKFESNFNTQATNRNTDGSTDYG ILQINSR**WW**CNDGRTPGSRNLCNIPCSALLSSDITASVNCAKKIVSDGNGMNAW VAWRNRCKGTDVQAWIRGCRL					

[a] 1:1200 dilution AH6 serum incubated ON at 4°C with 4 x 10^{10} phage particles or 3 μM HEL.

[b] Consensus sequences are underlined.

[c] Anti-IgG-Fc signal for binding by AH6 sera to plate-immobilized phage clones.

[d] Sequence alignment with HEL in bold.

[e] ELISA signals indicating competition between plate-immobilized and in-solution phage clones in bold.

[f] In-solution phage clones in competition with plate-immobilized self.

[g] Sequence of HEL. Residues that are greater than 30% exposed on the surface of HEL are shaded (determined with the Swiss PDB viewer software).

3.3.5 There is no reactivity of the 22 HEL cross-reactive phage clones with rabbit anti-HEL IgG

The 22 HEL cross-reactive phage clones presented in Table 3.8 were tested for reactivity with rabbit anti-HEL IgG to determine if there are epitopes targeted in common amongst the two species. Shown in Table 3.9 is direct ELISA analysis of the 22 HEL cross-reactive phage clones with mouse anti-HEL serum AH6 and rabbit anti-HEL IgG. The data shows that the rabbit anti-HEL IgG does not bind to any of the phage clones enriched with anti-HEL mouse Abs. Therefore, the rabbit IgG response did not target these same HEL epitopes as the mouse serum AH6.

Table 3.9. Direct ELISA analysis of HEL cross-reactive phage clones with anti-HEL rabbit IgG.

Cross-reactive phage clone	Murine anti-HEL serum AH6 (1:1200 dilution)[a]	Anti-HEL rabbit IgG (20 nM)[b]
HEL	**1.07**	**1.10**
f88 phage	0.21	0.07
N3.C2	**0.95**	0.05
D2.D4	**0.93**	0.05
D2.F8	**0.94**	0.05
D2.G10	**0.93**	0.04
D3.G8	**0.74**	0.07
N3.A10	**0.95**	0.05
N3.G9	**0.92**	0.04
D2.H6	**0.94**	0.06
D2.G3	**0.94**	0.05
D3.B12	**0.79**	0.05
D3.H9	**0.93**	0.06
N1.C12	**0.34**	0.06
D1.F11	**0.80**	0.05
N2.B5	**0.63**	0.05
D2.F6	**0.81**	0.04
2N.18	**0.75**	0.04
N2.G5	**0.52**	0.06
D3.D8	**0.84**	0.06
N2.H7	**0.53**	0.05
3N.13	**1.25**	0.04
3N. 3	**0.79**	0.04
3D.15	**1.03**	0.05

[a] Binding of murine anti-HEL serum AH6 (1:1200 dilution) detected with HRP-conjugated-goat-(anti-mouse-IgG-Fc)-Ab.
[b] Binding of rabbit anti-HEL IgG detected with HRP-conjugated-Protein A/G.

3.3.6 There is no reactivity of murine anti-HEL serum with HEL cross-reactive phage clones selected rabbit anti-HEL IgG

Previous RPL screenings in our lab conducted with anti-HEL rabbit IgG selected for peptides that fell into five consensus groups all of which aligned to linear regions of HEL (147). The strongest anti-HEL rabbit IgG-binding clones for each of the five groups were tested for reactivity with four different murine anti-HEL serum samples. As shown in Table 3.10, there was no reactivity of the murine anti-HEL serum samples with HEL cross-reactive phage clones selected with rabbit anti-HEL IgG. This indicates that the humoral immune response of these four mice produced different Ab specificities against HEL (*i.e.*, they targeted different HEL epitopes) than the rabbit.

Table 3.10. Direct ELISA analysis of HEL cross-reactive phage clones enriched with rabbit anti-HEL IgG.

Phage clone sequence and alignment with HEL	Anti-HEL rabbit IgG[a]	Murine anti-HEL serum #1[b]	Murine anti-HEL serum #2	Murine anti-HEL serum #3	Murine anti-HEL serum #4
HEL	**1.13**[c]	**1.08**	**1.07**	**0.98**	**0.94**
f88 phage	0.04	0.06	0.05	0.05	0.04
HEL 38-50 **FN**TQATNR**N**TDGS**					
MATNRVYGCQHSMYARS[d]	**0.23**	0.07	0.07	0.07	0.04
SCVTQASNRGCL	**0.32**	0.07	0.06	0.07	0.04
HEL 66-74 **NDGRTPGSRN**					
SKTPGA	**0.25**	0.09	0.07	0.08	0.04
HEL 83-95 **LLSDITASVNC**					
NQPSCQDITACLTPQ	**0.57**	0.08	0.09	0.09	0.05
QCHADITKCL	**0.20**	0.09	0.09	0.08	0.05
HEL 104-111 **GMNAWVAW**					
NAWA(Z_{13})HAPGSFF(Z_6)	**1.06**	0.07	0.06	0.07	0.05
HEL 113-127 **NRCKGTDVQAWIRGC**					
VNIACNPTDIQCLIRL	**0.90**	0.08	0.06	0.06	0.03
HDVQRELIQLQRYMP	**0.88**	0.11	0.12	0.14	0.04

[a] Rabbit anti-HEL IgG (20nM) binding was detected with HRP-conjugated protein-A/G.
[b] Murine anti-HEL Ab (1:100) binding was detected with HRP-conjugated goat-(anti-mouse-IgG-H+L)-Ab.
[c] ELISA signals greater than 0.2 are in bold.
[d] The enrichment of cross-reactive phage clones with rabbit anti-HEL IgG is described in (147)

3.3.7 Titration analysis of pre-immune and immune HEL sera against HEL and 3D phage.

Figure 3.4 presents titration ELISA analysis of pre-immune and immune sera (serum A in Table 3.3), following three immunizations with HEL and ALUM adjuvant, against HEL and the broadly reactive phage clone 3D. The half-max titer against HEL increases from approximately 1:150 after the first immunization, to 1:8000 after the second immunization to 1:73,000 after the third immunization. After the first HEL immunization there is no detectable Ab reactivity against 3D phage but after the second HEL immunization there is a half-max titer of approximately 1:150 and after the third immunization the half-max titer against 3D phage doubles to 1:300. There is no reactivity of pre-immune sera against either of the Agns. Therefore, the strength of the Ab response against HEL is related to the strength of the Ab response against the cross-reactive peptide 3D.

Figure 3.4. Titration ELISA of pre-immune and immune HEL sera against HEL and 3D phage.

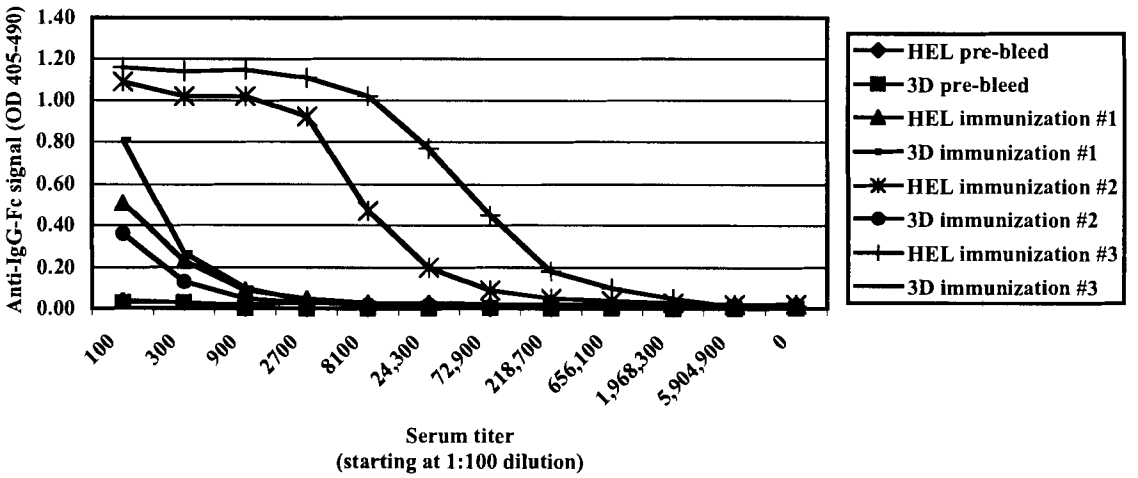

Serum titration ELISA, for pre-immune and HEL immune mouse sera against plate immobilized HEL and 3D phage, starting at 1:100 dilution of serum and using 1:3 serial dilutions. Background binding to f88 phage was subtracted from the binding signal against 3D phage.

3.3.8 Serum from HEL-immunized mice binds 3D phage after one or two immunizations.

Serum samples from three HEL-immunized mice were tested for reactivity (at 1:100 dilutions) with the 3D phage clone. Shown in Table 3.11 is direct ELISA data for pre-immune and immune mouse sera (after one, two and three immunizations with HEL) binding to HEL, 3D phage and the negative plate controls f88 phage and NFDM. The data show that for one of the three serum samples there was reactivity against the 3D phage clone after just one immunization but for the other two samples anti-3D Abs were only detected after the second immunization with HEL. An additional 17 anti-HEL serum samples from mice immunized once with 25 μg HEL were tested for reactivity with 3D phage in direct ELISA analysis. Of those 17 samples, ten showed reactivity with the 3D phage clone (data not shown). Therefore, more than half of the mice had produced Abs against the "3D epitope" after just one immunization with HEL. For a prime-boost immunization study it may be necessary to immunize the mice twice with HEL before they are boosted with the cross-reactive 3D phage clone.

Table 3.11. Direct ELISA analysis of anti-HEL sera from three mice against 3D phage.

	HEL[a]	3D phage	f88 phage	NFDM
Pre-bleed				
Mouse 1	0.05	0.02	0.01	0.02
Mouse 2	0.01	0.01	0.02	0.01
Mouse 3	0.02	0.03	0.03	0.02
HEL Immunization #1				
Mouse 1	1.21	**1.21**[b]	0.01	0.02
Mouse 2	0.85	0.02	0.02	0.04
Mouse 3	0.84	0.05	0.02	0.02
HEL Immunization #2				
Mouse 1	1.29	**1.27**	0.01	0.02
Mouse 2	1.24	**0.67**	0.02	0.02
Mouse 3	1.15	**1.15**	0.02	0.02
HEL Immunization #3				
Mouse 1	1.27	**1.12**	0.01	0.02
Mouse 2	1.23	**0.73**	0.02	0.021
Mouse 3	1.30	**0.93**	0.03	0.02

[a] Agn coated in ELISA plate wells.
[b] Anti-IgG-Fc binding signals for 1:100 dilution of serum Abs.
Positive binding signals for 3D phage are in bold.

3.3.9 Immunization with 3D phage does not elicit Abs that cross-react with HEL.

A preliminary immunization has been conducted with the 3D phage clone. Five mice immunized twice with 25 μg 3D phage (no adjuvant) have all produced anti-3D peptide and anti-f88 phage Ab responses. Serum titration analysis for one of the five mice shown in Figure 3.5 reveals that cross-reactive Abs against HEL have not been elicited with the peptide. Although there is a low level binding of the immune serum against HEL (at 1:100 dilution) it is not significantly higher than background binding by pre-immune serum with HEL. For this serum sample the half-max titer against the 3D peptide is approximately 1:2000 and the half-max titer against f88 phage is approximately 1:50,000. Sera from all five mice showed similar binding patterns and all ELISA analyses were repeated (data not shown). Therefore, the 3D peptide does not appear to be an immunogenic mimic of its cognate HEL epitope.

Figure 3.5. Titration ELISA analysis for serum from a mouse immunized twice with 3D phage against 3D peptide, f88 phage, HEL and OVA.

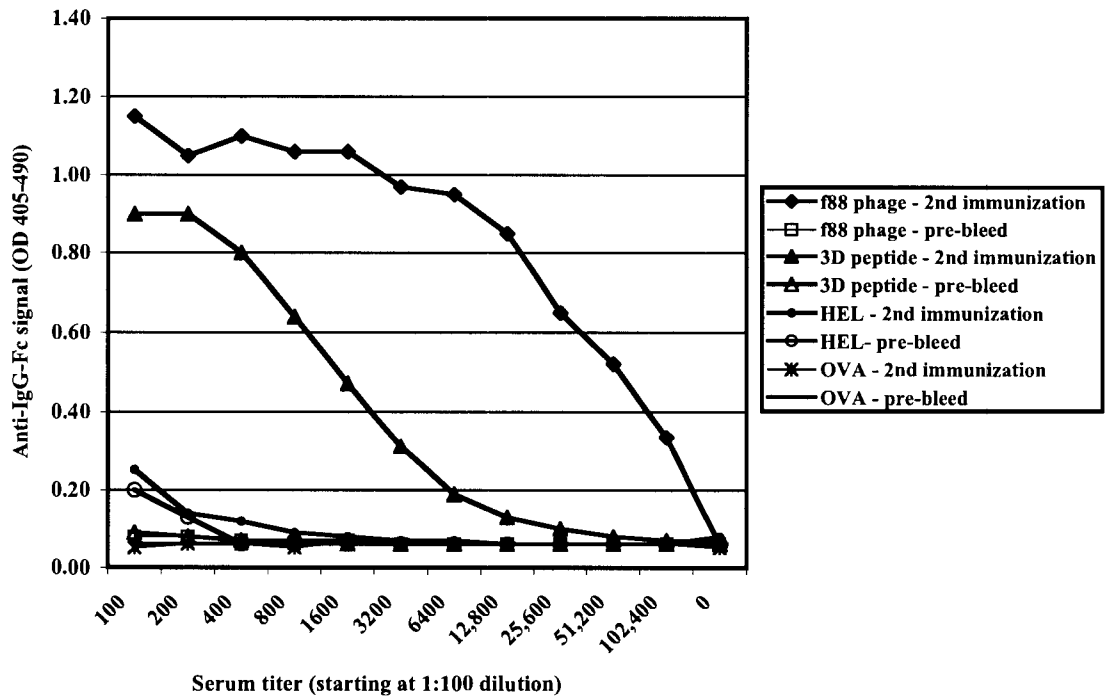

3.3.10 Murine anti-HEL sera do not bind HEL peptide fragments but react with a variety of 10-mer overlapping HEL peptides.

To further characterize Ab specificities elicited in HEL-immunized BALB/c mice, anti-HEL sera were tested for binding to three HEL peptide fragments, bio-38-54 (FNTQATNRNTDGSTDYG), 64-82 (WCNDGRTPGSRNLCNIPCS; expressed at the amino terminus of recombinant pVIII with Cys replaced by Ser) and 76-100 (NIPCSALLSSDITASVNCAKKIVS), as well as a set of 10-mer overlapping HEL peptides. As described in Chapter 1 (Section 1.7.1, page 19) previous studies have shown antigenic and immunogenic cross-reactivity of some HEL peptide fragments with native HEL for sera from certain strains of mice and rabbits (101) (108) (112, 182).

Presented in Table 3.12 is direct ELISA binding data for pre-immune and HEL immune mouse sera, as well as anti-HEL rabbit IgG, with the three HEL peptide fragments. The anti-HEL mouse serum (three additional anti-HEL mouse serum samples were later tested as well; data not shown) did not react with any of the HEL fragments. The anti-HEL rabbit IgG, however, bound strongly to all three HEL peptides.

Table 3.12. ELISA analysis of HEL peptide fragments 38-54, 64-82 and 76-100 with murine anti-HEL sera and rabbit anti-HEL IgG.

Ab sample	HEL	bio-Peptide 38-54[c]	Phage-displayed peptide 64-82	Peptide 76-100	f88 phage[e]	OVA[f]
Anti-HEL mouse serum[a]	**1.1**[d]	0.02	0.02	0.02	0.03	0.03
Pre-immune mouse serum	**0.07**	0.02	0.02	0.02	0.02	0.02
Anti-HEL rabbit IgG[b]	**1.20**	**0.97**	**1.1**	**0.98**	0.07	0.19

[a] Mouse sera were tested for reactivity at 1:200 dilutions. Assuming the IgG concentration for mouse sera is 10 mg/mL, a 1:200 dilution is approximately 500 nM IgG.
[b] Rabbit IgG was used at 100 nM.
[c] Bio-peptide 38-54 was immobilized directly in the plate well (not *via* SA). SA-immobilized bio-38-54 does not bind to murine anti-HEL sera either (data not shown).
[d] Positive ELISA binding data are in bold.
[e,f] f88 phage and OVA were used as negative controls for the ELISA analysis.

Murine anti-HEL sera were also tested for reactivity with a set of 10-mer overlapping HEL peptides synthesized on a cellulose membrane and prepared in duplicate; the peptides overlap every second residue and cover the entire HEL sequence (section 3.2.7, page 79). The

films showing reactivity of two representative anti-HEL serum samples against the peptide membrane are presented in Figure 3.6. Based on the fact that murine anti-HEL sera did not bind to the three HEL peptide fragments, as well as the extensive evidence in the literature that most murine anti-HEL Abs are directed against conformational epitopes (reviewed in (101)) reactivity of anti-HEL Abs against the 10-mer peptides was expected to be limited. The anti-HEL mouse sera, however, reacted with a variety of the overlapping peptides. Interestingly, binding patterns against the HEL peptides were very similar for all five anti-HEL sera that were tested. Pre-immune mouse serum, serum from an OVA-immunized mouse, as well as the secondary Ab alone (HRP-conjugated-goat- (anti-mouse-IgG-Fc)-Ab), did not bind to any of the 10-mer peptides. The binding pattern for one of the serum samples (Figure 3.6, B) is summarized in Table 3.13.

Figure 3.6. Films of the HEL overlapping peptide blot developed with two different anti-HEL serum samples.

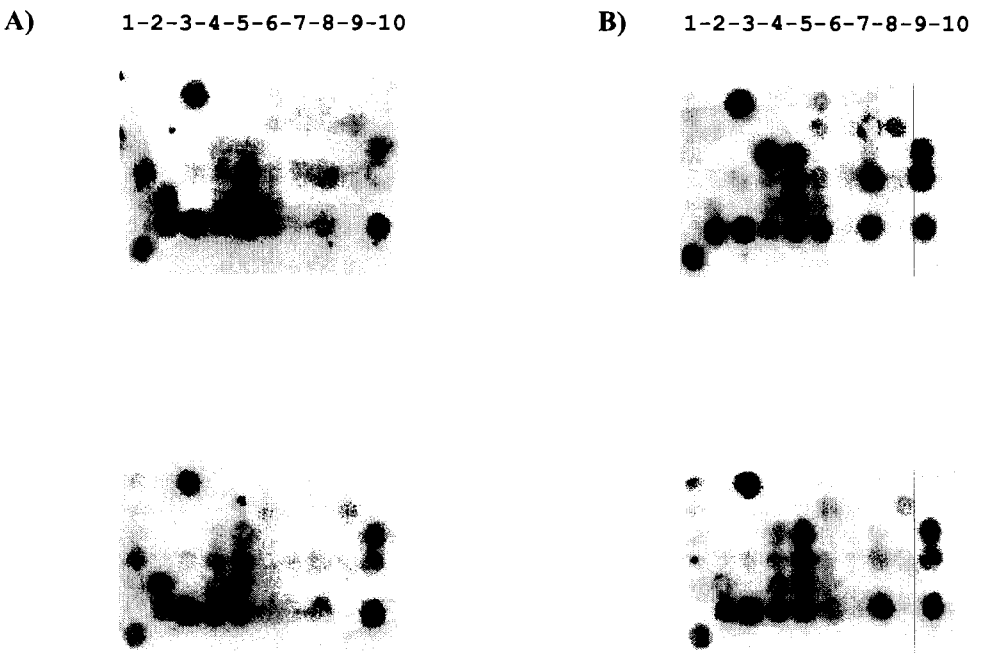

Images of films exposed to HEL overlapping peptide blots (top and bottom are duplicates of the overlapping peptides) probed with two different anti-HEL serum samples (A and B) and developed with HRP-goat- (anti-mouse-IgG-Fc)-Ab plus a chemiluminescence kit.

Interestingly, the 10-mer peptides recognized by the anti-HEL sera overlapped with regions of the three HEL peptide fragments, 38-54, 64-82 and 76-100 (Table 3.13) that were not recognized by anti-HEL serum samples. The reason for this is unclear. If the reactivity against

the 10-mer peptides was non-specific (due to stickiness), pre-immune and anti-OVA sera should have also reacted with some of the peptides. Perhaps CBRs required for binding by the anti-HEL Abs are not sufficiently exposed in the context of the HEL peptide fragments immobilized in ELISA plate wells as compared to the 10-mer peptides synthesized on the cellulose membrane. The binding data for the 10-mer peptides suggests that Abs produced in different mice target common HEL epitopes.

Table 3.13. Epitope mapping of HEL with anti-HEL mouse serum.

a.a. #[a]		HEL peptides[f]	serum[g]	a.a.#		HEL peptides	serum
1-10		KVFGR**S**ELAA		61-70		RWW**S**NDGRTP	
3-12		FGR**S**ELAAAM		63-72	**Peptide 64-82**	W**S**NDGRTPGS	
5-14		R**S**ELAAAMKR		65-74		NDGRTPGSRN	
7-16		ELAAAMKRHG		67-76	**64-82 and 76-100 overlap**	GRTPGSRNL**S**	
9-18	**HGL of 3D peptide[b]**	AAAMKRHGLD		69-78		TPGSRNL**S**NI	
11-20		AMKRHGLDNY		71-80		GSRNL**S**NIPS	
13-22		KRHGLDNYRG		73-82		RNL**S**NIPSSA	
15-24		HGLDNYRGYS		75-84		L**S**NIP**S**SALL	
17-26		LDNYRGYSLG		77-86	**Peptide 76-100[e]**	NIP**S**SALLSS	
19-28		NYRGYSLGNW		79-88		P**S**SALLSSDI	
21-30		RGYSLGNWV**S**		81-90		SALLSSDITA	
23-32		YSLGNWV**S**AK		83-92		LLSSDITASV	
25-34		LGNWV**S**AAKF		85-94		SSDITASVN**S**	
27-36		NWV**S**AAKFE		87-96		DITASVN**S**AK	
29-38		V**S**AAKFESNF		89-98		TASVN**S**AKKI	
31-40	**Peptide 38-54[c]**	AAKFESNFNT		91-100		SVN**S**AKKIVS	
33-42		KFESNFNTQA		93-102		N**S**AKKIVSDG	
35-44		ESNFNTQATN		95-104		AKKIVSDGNG	
37-46		NFNTQATNRN		97-106		KIVSDGNGMN	
39-48		NTQATNRNTD		99-108		VSDGNGMNAW	
41-50		QATNRNTDGS		101-110		DGNGMNAWVA	
43-52		TNRNTDGSTD		103-112		NGMNAWVAWR	
45-54		RNTDGSTDYG		105-114		MNAWVAWRNR	
47-56		TDGSTDYGIL		107-116		AWVAWRNR**S**K	
49-58		GSTDYGILQI		109-118		VAWRNR**S**KGT	
51-60		TDYGILQINS		111-120		WRNR**S**KGTDV	
53-62		YGILQINSRW		113-122		NR**S**KGTDVQA	
55-64		ILQINSRWW**S**		115-124		**S**KGTDVQAWI	
57-66	**Peptide 64-82[d]**	QINSRWW**S**ND		117-126		GTDVQAWIRG	
59-68		NSRWW**S**NDGR		119-127		DVQAWIRG**S**R	
				120-129		VQAWIRG**S**RL	

Legend:

No binding	
Weak binding	
Medium binding	
Strong binding	

[a] HEL amino acid number (a.a.#).

[b] Residues HGL of the commonly reactive 3D peptide that align with HEL.

[c,d&e] Residues of HEL that overlap with HEL peptide fragments 38-54, 64-82 and 76-100

[f] HEL Cys resides replaced by Ser in the overlapping peptides are in bold.

[g] Anti-HEL sera were diluted 1:100 to probe the HEL peptide membrane. Sera from an unimmunized mouse as well as from an OVA-immunized mouse (also diluted 1:100) did not bind to any of the HEL peptides. The secondary Ab alone, HRP-conjugated-goat- (anti-mouse-IgG-Fc)-Ab, diluted 1:2500, did not bind to any of the peptides either.

3.4 Discussion

The goals of this chapter were to identify a peptide marker for a commonly produced Ab specificity in the BALB/c mouse immune response to HEL, and to characterize the anti-HEL Ab response in individual mice with peptide ligands. Serum samples from three HEL-immunized mice were affinity-purified on HEL and used to screen 15 RPLs. Although 22 unique cross-reactive phage clones were selected, direct ELISA analysis revealed that only one of the phage clones, 3D, was broadly recognized by serum Abs from different HEL-immunized mice (Table 3.8, page 91). In fact, all of the remaining clones reacted exclusively with one of the three Ab samples (AH6) used in the screening. Competition ELISA analysis of the clones revealed that they cross-react with only three HEL epitopes as 19 of the 22 clones competed with another for binding to the screening serum AH6. Thus, these 19 peptides may be markers for an immunodominant anti-HEL Ab specificity (or overlapping specificities) in the screening serum sample AH6, or they may have been selected by an Ab specificity that is polyreactive and/or cross-reacts well with peptide ligands and thus dominated the screening.

Of all 22 cross-reactive phage clones selected in the screening, only 3D (TCIHGLPPSECH) showed any alignment to the linear sequence of HEL (underlined residues). In Figure 3.7, a Swiss PDB viewer analysis of HEL with these residues high-lighted, shows that they have some exposure on the protein's surface. Because the residues are not completely "buried" in the protein, they could feasibly constitute a linear epitope (or a part of one), or a contiguous segment of a discontinuous epitope. Without conducting an Ala replacement scan of the 3D peptide, however, one cannot assume that any of these three residues are responsible for the peptide's cross-reactivity with HEL. Moreover, if replacement of these residues with Ala were to abolish the antigenicity of the peptide, it still would not prove that the peptide cross-reacts with His15, Gly16 and Leu16 of HEL. To do so would require the enrichment of anti-HEL Abs on a short peptide spanning residues of HGL of HEL (reactivity of peptide 11-20 of the overlapping 10-mer HEL peptides suggests that it may be possible to do this; Table 3.13) and then testing the Abs for reactivity with the 3D peptide. The 3D peptide could also be optimized through NNK-doped 3D sublibrary construction and screening to try and select for additional residues that align with HEL.

Figure 3.7. Swiss-PDB Viewer analysis HEL (IGXV) with residues His15, Gly16 and Leu17 highlighted.

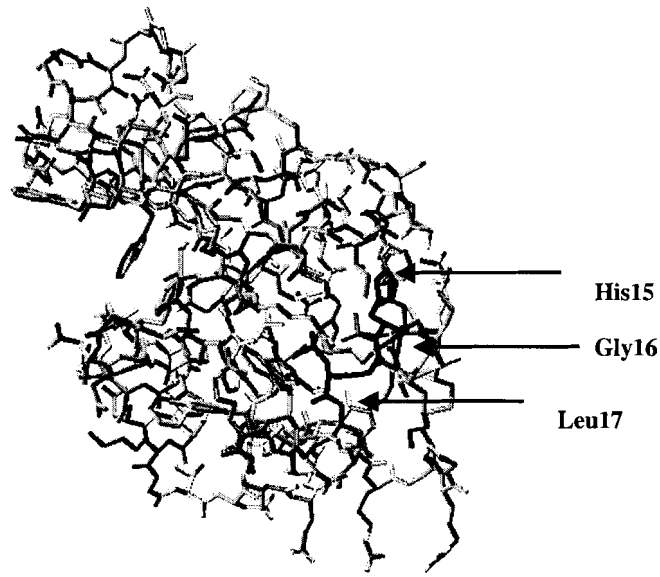

Similar to the peptides enriched in this study, the RPL screening of Matthews *et. al.*, (26) with murine anti-T4 bacteriophage Abs enriched mostly for peptides that aligned to consensus groups but did not match the linear sequence of any of the T4 proteins. Of the 35 unique anti-T4 binding phage clones identified in their screening, four motifs could be assigned to about 70% of the clones (most of the clones aligned to two of the four motifs), while the remaining 30% showed no sequence similarity to one another. Also, amongst all 35 clones, only two aligned to linear regions (five contiguous residues each) of two different T4 proteins.

This is in contrast to previous screenings in our lab by Craig *et. al.*, with rabbit anti-HEL IgGs – in these screenings peptides were selected that fell into five obvious consensus groups, all of which aligned to linear regions of HEL (147). There is no straightforward explanation for the differences in peptide ligands enriched with mouse *versus* rabbit anti-HEL Ab. Perhaps rabbit Ab preferentially targets linear epitopes whereas murine Ab is more often produced against discontinuous epitopes. It is also possible, however, that the rabbit Ab enriched for peptides that cross-react with contiguous segments of discontinuous HEL epitopes. There was no reactivity of the rabbit anti-HEL IgG to any of the cross-reactive phage clones enriched with mouse Ab (Table 3.9). Similarly, there was no reactivity of murine anti-HEL serum with cross-reactive phage clones identified by (147) with rabbit IgG (Table 3.10). This finding has obvious implications for developing epitope-targeted vaccines in animal models – even if it is possible to target the

production of Ab against a particular epitope in an animal model, given genetic differences in Ab repertoires for humans *versus* an animal model, the vaccine candidate may fail when tested in humans.

Based on the fact that BALB/c mice are inbred, and HEL is a fairly small protein, it was assumed that the immunized mice would share several anti-HEL Abs in common. By combining the three screening Abs, it was hypothesized that the representation of Abs in common between the three mice would increase and thereby give them a competitive advantage in the screening process. Should this screening have failed, the alternative plan was to screen with one individual Ab sample after another for two to three rounds. In this way, phage clones would be enriched for the first Ab sample in Round 1 and then a subpopulation of that pool of phage clones, recognized by second Ab sample, would be enriched in the next round. This screening format has been used in the identification of peptide markers for commonly produced IgG specificities in humans against various Agns (177-180). On the other hand, if the screening had been conducted in this fashion, a polyreactive but not commonly produced Ab specificity, such as the one in sample AH6 that enriched for the 19 cross-reactive phage clones, could have dominated the first round of screening and prevented the enrichment of any phage clones at all in the next round with a second Ab sample.

To further characterize the anti-HEL Ab response in individual BALB/c mice, anti-HEL serum samples were tested for reactivity against three HEL peptide fragments, 38-54, 64-82 and 76-100. Early work by Palmer and Sercarz (182), analyzing the relationship between T and B cells specific for HEL, showed humoral cross-reaction of peptide 74-96 with HEL for sera from H-$2^{b,d\&\ k}$ strains of mice immunized with peptide 76-100 (BALB/c mice are H-2^{d}). Similarly, Fujio *et al.*, showed that peptide 38-54 could induce HEL-reactive Ab populations in H-$2^{a\&d}$ strains of mice and that serum from HEL-immunized H-2^{d} mice reacted weakly with peptide 38-54. The serum from BALB/c mice immunized with HEL and ALUM for this work, however, did not bind to either of the peptides. This may be due to differences in the immunizations, such as type of adjuvant (Complete Freund' adjuvant *versus* ALUM used for this work), route of administration, and dosage *etc.* The other possibility is that the Ab specificities do exist, but at too low a titer for detection *via* ELISA analysis. The lack of reactivity of anti-HEL BALB/c mouse sera with peptide 64-82 corroborated findings of Mozes *et. al.*, that H-2^{d} haplotype mice do not produce Abs against this region of HEL (112). The reactivity of peptides 38-54 and 64-82 with anti-HEL rabbit IgG (the same anti-HEL rabbit IgG used by (147)) was expected because these peptides have been well characterized in the rabbit model for their strong antigenic and

immunogenic cross-reactivity with HEL (183) (108). Also, cross-reactive phage clones identified by (147) aligned to all three of these regions. The reactivity of the anti-HEL rabbit IgG indicates that the peptides have probably, at least in part, maintained the integrity of the native epitopes present in the context of the whole protein.

Anti-HEL serum samples from individual mice were also used to probe a set of 10-mer, overlapping HEL peptides. Because early studies with HEL have shown that the majority of B cell determinants on HEL are conformational (101), reactivity against the 10-mer peptides was expected to be quite limited. The anti-HEL sera, however, bound to a variety of the peptides and serum samples from different mice showed almost identical patterns of reactivity against the peptides. Also, although not all of the peptides were antigenic, together the sera reacted with peptides encompassing all 129 residues of HEL. Similarly, Geysen *et. al.*, mapped 6-mer overlapping peptides for the model protein myohemerythrin (MHr) with Abs raised in seven outbred rabbits against native MHr protein (24). Their analyses showed that not all peptides were antigenic but together the sera from all seven rabbits reacted with hexapeptides encompassing all 118 residues of MHr. Interestingly, although similar regions of the protein were identified as being immunodominant amongst the seven serum samples, no Ab specificity was common to the sera from all seven rabbits; four peptides were recognized by six of the seven sera, 31 reacted with only one serum sample and 35 showed no reactivity with any of the sera. This difference in binding activity of the murine anti-HEL sera (almost identical patterns of reactivity against the HEL 10-mer peptides) *versus* the rabbit anti-MHr sera (no MHr 6-mer peptides were recognized in common amongst all seven rabbits) may be due to the fact that the mice are inbred and the rabbits are outbred.

The work in this chapter was primarily driven by the goal of identifying a cross-reactive peptide, broadly recognized by anti-HEL serum Abs that could be used in a prime-boost immunization strategy with HEL. For the immunization the mice would be primed with HEL to elicit a pcAb response, including a subpopulation of anti-3D peptide Abs, and then boosted with the 3D phage to specifically amplify the production of anti-3D Abs that cross-react with HEL. A preliminary immunization of five BALB/c mice with 25 μg 3D phage, in the absence of adjuvant, has shown that the peptide itself is immunogenic but after two immunizations no cross-reactivity with HEL was observed (Figure 3.5). A prime-boost immunization study with the 3D peptide is currently being conducted and results are pending. For the study, different concentrations of both HEL and the 3D phage clone are being tested and a "universal T cell epitope" derived from OVA has been conjugated to HEL and the 3D phage clone so as to keep T cell epitopes in common

between the priming and boosting immunizations. Serum titration and competition ELISA analyses will be used to characterize the serum Ab response to immunization. Should this prime-boost immunization succeed, it is also of interest to track the production of B cells producing Abs that cross-react with HEL and the 3D peptide. Aside from hapten model work (184) (79), such molecular characterization of immune responses to immunization is lacking in the literature. For most immunization studies only the serum is analyzed. Therefore, the final objective of this thesis is to develop B cell assays that can be used to track the production of 3D-peptide reactive B cells.

CHAPTER 4 IDENTIFICATION OF EPITOPE-SPECIFIC B CELLS AMONGST SPLEEN CELLS FROM LYSOZYME-IMMUNIZED MICE

4.1 Introduction

Thus far, the work presented in this thesis has focused on the characterization of anti-HEL serum Ab responses with peptide markers; the peptides were derived either from the linear sequence of HEL or from RPLs screened with anti-HEL Abs. In Chapter 3, a peptide, that cross-reacts with HEL, and is broadly recognized by serum Abs from HEL-immunized BALB/c mice, was identified in a RPL screening anti-HEL pcAbs. The broadly reactive peptide, 3D, has the sequence TCIHGLPPSECH and three of its residues align with the linear sequence of HEL (underlined). The 3D peptide will be used in a prime-boost immunization strategy with HEL, under the assumption that priming the mice with HEL will elicit a pc anti-HEL Ab response, including a subpopulation against the cognate epitope of HEL, and boosting with the 3D peptide will specifically amplify this subpopulation of Abs. The presence of cross-reactive Abs in the mouse sera will be tested *via* competition ELISA.

The work in this chapter describes the development of assays to identify 3D peptide-reactive B cells amongst pools of spleen cells extracted from HEL-immunized mice. The 3D peptide is assumed to represent a single, "immunodominant" epitope on HEL (*i.e.*, broadly recognized by serum Abs) that *might* include residues His15, Gly16 and Leu17 of HEL. Thus, B cells identified with the peptide represent clones against a discrete epitope on HEL. Ultimately the frequency of 3D-reactive and HEL-reactive B cells will be analyzed after the primary and secondary immune responses to HEL and following a prime-boost immunization. The frequencies of the cells will then be compared with serum titers against HEL and 3D peptide. It is assumed that as the serum titers increase so too will the frequencies of Agn-specific B cells. In this way, the effectiveness of a prime-boost immunization strategy with HEL and the 3D peptide can be assessed at both the serum Ab and cellular level.

Several methods have been developed for identifying Agn-specific B cells. In the early 1960s, the plaque-forming cell (PFC) assay was established to determine the frequencies of IgG and IgM, Agn-reactive B cells amongst a pool of cells (185) (186). For the PFC assay, Ab-

forming cells are measured by mixing the test population of cells with Agn-sensitized red cells. Following an incubation period, the red cells surrounding the Ab-secreting B cells become coated with Ab and so may be lysed by the addition of complement. Two types of plaques can be identified with this technique, direct plaques and indirect plaques. Direct plaques are the result of Agn-specific IgM that directly induces complement-mediated lysis (IgM fixes complement well). To develop indirect plaques, anti-IgG Abs are added to enhance the ability of the Agn-specific IgG to lyse the red cells (187).

In the early eighties, the ELISPOT assay (Enzyme-Linked Immunospot, also known as the ELISA plaque assay), for quantifying Agn-specific B cells was developed (188) (189). For this assay, the test cells are plated onto an Agn-sensitized plate, secreted Ab binds to Agn in the vicinity of cells secreting Agn-specific Ab, and "spots" of bound Ab (representing an individual Agn-specific, Ab-secreting B cell) are detected chromatographically using an enzyme coupled to anti-Ig Ab and a chromogen substrate. Thus, similar to the individual plaques in the PFC assay, the "spots" in the ELISPOT each represent a single Agn-specific B cell.

Another method for identifying Agn-specific B cells amongst a pool of test cells is to culture the cells under conditions that stimulate them to secrete Ab and then test the supernatant *via* ELISA analysis for the presence of Agn-binding Abs. Various combinations of immunostimulants can used to drive the differentiation of B cells into Ab-secreting plasma cells. In the late 1980s, Snapper and Paul (190) (191) showed that IL-4 promotes isotype switching to IgG1 and IgE, and Purkerson *et. al.*, (192) showed that IL-2 and IL-5 have a cooperative effect on IL-4-induced IgG1 secretion from anti-Ig-treated B cell blasts. Loughnan and Nossal (193) then demonstrated a connection between ILs 2, 4 and 5 on B cell proliferation; they showed that IL-4 and IL-5 could independently upregulate the IL-2 receptor on B cells, leading to IL-2 dependent B cell proliferation in the absence of Agn or mitogen. This lead to a study by McHeyzer-Williams, on Ab production by single hapten-specific B cells stimulated with lipopolysaccharide (LPS) and various combinations of ILs 2, 4 and 5 (73). (LPS is a TI Agn and stimulates polyclonal activation of B cells.) He found that different concentrations as well as different combinations of the immunostimulants influenced the amount and isotype of Ab secreted by the single B cells. Since then, others such as Takahashi *et al.*, (194) have used LPS and ILs 2, 4 and 5 to stimulate single B cells so that the secreted Ab could be tested for Agn-binding *via* ELISA and the Ig VH genes could be cloned from the amplified cells.

In more recent years, investigators have developed methods to track Agn-specific B cells using flow cytometry (78) (90) (89). Fluorescently labelled Abs against various cell surface markers can be used to phenotypically characterize a pool of test cells, and fluorescently labelled Agn can be used to label Agn-specific B cells that bear surface Ig. With respect to lymphocytes of murine origin, B220 is considered a "pan B cell marker" because it is present on all B cells except for terminally differentiated plasma cells, and CD138 (also known as syndecan) is a marker for terminally differentiated plasma cells (83, 84) (85) (86). Markers against T cells (CD3) and macrophages (CD11b), for example, can also be used during an analysis to "gate-out" non-B cells in an attempt to reduce background binding levels (72). Recently, investigators have also used a combination of technologies to more effectively analyze Agn-specific B cell populations. Weitkamp *et. al.*, for example, used fluorescent virus-like particles to identify and sort single rotavirus specific B cells into cultures containing ILs 2 and 4. The culture supernatants were then tested for rotavirus-specific Ab secretion and the VH and VL genes were cloned from the amplified B cells.

For this chapter, flow cytometry, the *in vitro* culture of cells and subsequent ELISA analysis of secreted Abs, as well as the ELISPOT assay, were set up and optimized in an attempt to identify 3D-peptide reactive B cells amongst pools of spleen cells extracted from HEL-immunized mice. Although significant efforts were made to identify and sort HEL and peptide-reactive B cells *via* flow cytometry, the frequency of Agn-labelled cells (less than 0.1% of live gated lymphocytes) fell at, or below, background levels of binding by the cells to the SA-conjugated fluorophores only (*i.e.* no Agn). Moreover, similar frequencies of Agn-reactive B cells were observed amongst spleen cells from unimmunized mice. Therefore, the flow cytometry data will not be presented.

For the *in vitro* culture analysis, different numbers of spleen cells or splenic B cells (10^5, 10^4, 10^3) were cultured over several days with the immunostimulant LPS and/or various combinations of ILs 2, 4 and 5, anti-Ig Ab and HEL Agn. The purpose of the stimulation was to drive the B cells present within the wells to divide and differentiate into Ab-secreting plasma cells. The Ab secreted into the culture supernatant by the stimulated cells was analyzed *via* ELISA analysis for the presence of IgG specificities, anti-HEL IgG, anti-3D phage IgG and anti-"background" IgG (IgG against f88 phage and NFDM). From the ELISA analysis of supernatant from the pools of 10^5 spleen cells, for example, there was evidence of HEL-specific IgG after just one day of culture. Although anti-3D phage Ab was present in the supernatants by day 4 of culture, there were similar levels of reactivity against the non-specific Agns, f88 phage and

NFDM. The same held true of the enriched B cells - reactivity against 3D phage was not above background binding to f88 phage.

The third approach for identifying peptide-reactive B cells, ELISPOT analysis enabled the quantification of total IgG+ secreting B cells *versus* HEL+ secreting B cells amongst a pool of spleen cells from HEL-immunized mice. The frequency of 3D-peptide reactive B cells was just under 1% of total IgG+ secreting B cells. Unlike the *in vitro* culture analysis, there was no reactivity with the negative controls f88 phage and NFDM. Thus, the ELISPOT showed that 3D peptide-reactive B cells can be found in the spleens of HEL-immunized mice.

4.2 Materials and Methods

4.2.1 Reagents.

Female BALB/c mice were purchased from Charles River Laboratories (Wilmington, MA). HEL and ALUM adjuvant were acquired from Sigma-Aldrich (Saint Louis, MO).

All tissue culture plastic and glassware, such as disposable pipettes, sterile flasks and multi-well culture plates were BD Falcon brand (VWR, West Chester, PA). Dissociated spleen cells were filtered through a sterile 40-μm mesh (BD Biosciences Pharmingen, San Jose, CA). Trypan blue for staining and for counting viable cells was purchased from Life Technologies (Rockville, MD). Cells were cultured in RPMI-1640 medium, supplemented with 2 mM L-glutamine (L-Gln), 2-mercaptoethanol (2-ME), fetal bovine serum (FBS), penicillin (Pen) and streptomycin (Strep) (all from Sigma-Aldrich). For the stimulation of cells, LPS from *E. coli* 011:B4 (Sigma-Aldrich), and/or recombinant murine IL-2 (Roche, Mannheim, Germany), IL-5 (BD Biosciences Pharmingen) and IL-4 (Sigma-Aldrich), or goat-(anti-mouse-IgA, IgG, IgM-H+L)-Ab (Pierce, Rockford IL) or HEL (Sigma) was used.

B cells were enriched from dissociated spleen cells with a negative depletion, mouse B cell recovery column kit (Cedarlane Laboratories Inc, Hornby, ON). Prior to purification on the column, lymphocytes were isolated from total spleen cells *via* density gradient centrifugation with Lympholyte®-M cell separation medium (Cedarlane Laboratories Inc.).

ELISPOT reagents included 96-well flat-bottom, high binding plates (Corning Costar plates from VWR), SA-conjugated-alkaline phosphatase (Pierce, Rockford, IL), bio-goat- (anti-mouse-IgG-H+L)-Ab (Southern Biotech, Birmingham, AL), goat- (anti-mouse-IgG-H+L)-Ab

(Pierce), as well as X-phosphate p-toluidine salt, triton-X405 and 2-amino-2-methyl-propanol (Sigma-Aldrich). All reagents for ELISA analysis are described in Materials and Methods for Chapter 2 (section 2.2.1, page 32).

4.2.2 Spleen cell preparation.

Spleens were harvested from female BALB/c mice immunized 3 times, sc with 25 μg HEL and ALUM. The priming immunization was administered on day 1, the first boost on day 14, and the final boost was given on day 28 or beyond, 5 days prior to sacrifice. Single-cell suspensions were prepared in RPMI-1640 medium supplemented with 2 mM L-Gln, 100 U/mL Pen, 100 μg/mL Strep, 100 μM 2-ME and 5% v/v FBS, by squeezing the spleens between two frosted slides. Erythrocytes were lysed in Tris-Ammonium Chloride buffer (90 mL 0.16M NH_4OH plus 10 mL 0.17M Tris, pH 7.6; adjusted to final pH 7.2). The cells were washed in medium, filtered through a sterile 40-μm mesh, and resuspended in 1-2 mL medium or PBS.

4.2.3 *In vitro* culture of B cells.

The *in vitro* culture procedure was adapted from Michael G. McHeyzer-Williams (73) and Takahashi, Y. *et al.*, (194). Various numbers of spleen cells (10^6, 10^5, 10^4) were cultured in 200 μL supplemented RPMI-1640 medium in 96-well, round-bottom tissue culture plates. Supplemented RPMI-1640 culture medium comprised 2mM L-Gln, 100 U/mL Pen, 100 μg/mL Strep, 100 μM 2-ME, 5% v/v FBS, and various combinations of 25 μg/mL LPS, 20 U/mL IL 2, 10 U/mL IL 4,1 ng/mL IL 5, 5 μg/mL HEL or 20 μg/mL anti-Ig Ab. Cells were cultured at 37°C in 10% CO_2 and air.

4.2.4 Enrichment of splenic B cells.

Spleen cell suspensions were prepared as described above, except that they were resuspended in PBS and enriched using a mouse B cell recovery column kit following the manufacturer's protocol. Briefly, lymphocytes were prepared from the whole spleen cells by gradient separation using Cedarlane Lympholyte®-M cell separation medium. The enriched lymphocytes were incubated on ice with a cocktail of Abs that bind to non-B mononuclear cells (CD4 and CD8 lymphocytes and monocytes/macrophages) prior to being passed over a column that removes these cells, leaving the B cells in the column eluant. A sample of these B cells was stained with trypan blue stain and nonviable and viable cells counted with a haemocytometer.

4.2.5 ELISA analysis of *in vitro* culture supernatants.

The direct ELISA procedure described in Chapter 2 Materials and Methods (section 2.2.6, page 39) was used. Briefly, ELISA plate wells were coated ON at 4°C with 1 μg HEL, $1x10^{10}$ PEG/NaCl purified f88 or 3D phage, 1 μg/mL anti-IgG or 5% (w/v) NFDM, in a total volume of 35 μL TBS per well. The wells were aspirated, blocked with TBS/BSA for 30 min at 37°C, and washed 6 times with TBS/Tw. From each *in vitro* culture supernatant well (200 μL total volume per well), 35 μL was tested for binding to HEL, as well as the Agns, f88 phage, 3D phage, anti-IgG and NFDM. Care was taken not to disturb the cells at the bottom of each *in vitro* culture well when transferring the supernatant. After 2 h incubation at RT, the ELISA plate wells were washed, probed for 45 min with a 1:1500 dilution of HRP- conjugated-goat- (anti-mouse-IgG-Fc)-Ab, washed again and developed with ABTS solution. Unless otherwise indicated, ELISA $O.D._{405\text{-}490}$ readings are shown after 30 min incubations. An internal plate control of mouse IgG, titrated on immobilized goat- (anti-mouse-IgG-H+L)-Ab, was included on each ELISA plate so that data comparisons could be made between plates. Each Agn was also tested for non-specific binding to the secondary Ab. Background binding signals were subtracted from readings with the primary Ab against that Agn.

4.2.6 ELISPOT analysis of B cells.

For the ELISPOT assay, high-binding microwells were coated ON at 4°C with 1μg HEL, 1 μg/mL anti-IgG Ab or $1x10^{10}$ phage in 50 μL 0.1M $NaHCO_3$, pH8.6. The following day, the wells were aspirated and blocked with 3% FBS in PBS for 30 min at 37°C. The wells were aspirated and cells were serially diluted in the wells (starting at $1x10^5$ cells). The cells were added in 50 μL RPMI-1640 medium supplemented with 2 mM L-Gln, 100 U/mL Pen, 100 μg/mL Strep, 100 μM 2-ME and 5% v/v FBS, with or without, 25 μg/mL LPS. The plates were centrifuged for 5 min at 500 x g and care was taken not to disturb the cells afterwards. Plates were incubated for 2 h at 37°C in 10% CO_2 and the primary Ab, bio-goat- (anti-mouse-IgG-H+L)-Ab, diluted 1:500 (for a final concentration of 1 μg/mL) was added directly to the wells in 50 μL medium. The plates were incubated with the primary Ab ON at 37°C in a humidified incubator with 10% CO_2. The plates were washed four times with PBS, 0.1% Tw and 50 μL of SA-alkaline phosphatase, diluted 1:1500 (final concentration of 1 μg/mL) in PBS containing 3% (v/v) FBS, was added to the wells for 1 h at RT. The plates were washed and developed with a 1:10 ratio (v/v) of 1 mg/mL 5-bromo-4-chloro-3-indoyl phosphate, p-toluidine salt solution (dissolved at 10 mg/mL in dimethyl formamide and stored at -20°C) and AMP buffer (9.58% 2-

amino-2-methyl-1-propanol, 1mM $MgCl_2$, 0.01% Triton-X-405, pH 9.8). The developer was prepared and filtered through a 0.2 μM filter just prior to use. The plates were incubated at RT in the developer until bluish "spots" became visible. To stop the reaction, the plates were washed with water. Spots were counted by eye, with each spot representing a single, Agn-specific plasma cell.

4.3 Results

4.3.1 A comparison of *in vitro* culture conditions for stimulating the division and differentiation of splenic B cells into Ab-secreting plasma cells.

The purpose of the work in this chapter is to identify 3D peptide-reactive B cells amongst spleen cells extracted from HEL-immunized mice whose sera bind the 3D peptide. As mentioned in the introduction, the first strategy attempted, fluorescent-based, cytometric analysis of spleen cells, could not be used identify peptide-reactive B cells due to high background binding issues. Background binding resulted from the SA-fluorophore (without bio-Agn) sticking to spleen cells, as well as from Agn-labelled fluorophore binding to cells from unimmunized mice.

Instead of directly labelling B cells with Agn *via* their surface Ab, an alternative approach to proving the existence of peptide-reactive B cells is to isolate pools of spleen cells, stimulate them to secrete Ab, and then test the Ab for binding to the peptide and other Agns. In order to optimize the stimulation of splenic B cells from HEL-immunized mice into Ab-secreting plasma cells, spleen cells and enriched splenic B cells were cultured under different conditions, and the Ab secreted into the culture supernatant was tested by ELISA analysis. Two *in vitro* culture analyses were conducted. Prior to analyzing splenic B cells, sera from the HEL-immunized mice, were tested in titration ELISA for binding HEL and 3D phage. The half-max titers against HEL were approximately 1:10,000 or greater after the second immunization and the mice were sacrificed after the third immunization (data not shown). Half-max titers against 3D phage were greater than 1:200 (data not shown).

For the first *in vitro* culture assay, cell suspensions from the spleens of three HEL-immunized BALB/c mice were prepared and 10^5 live spleen cells (from each individual mouse) were added per round-bottom microwell containing medium and various combinations of the immunostimulants LPS, ILs-2, 4 and 5, HEL and anti-Ig Ab (described in Materials and Methods, page 110). The plates were incubated for one, two, five or nine days at 37°C in a humidified incubator with 10% CO_2.

After one day of culture, the supernatants from plate 1 (including cell samples for each of the three mice, cultured under all conditions) were tested in ELISA analysis. After two days of incubation, the culture supernatants for plate 2 were tested, *etc.* Thus, the culture supernatants for cells incubated with LPS, for example, is from different plates/wells (*i.e.*, produced from independent pools of spleen cells) for the ELISA analyses conducted on each day of culture. The ELISA analyses of the negative control, medium only (*i.e.*, containing no cells), against each of the Agns is not shown because background binding was consistently 0.01 for O.D. $_{405\text{-}490}$.

Presented in Table 4.1 is the mean and standard deviation of the ELISA signals for the culture supernatants of 10^5 spleen cells. For each of the three mice, supernatants from two independent culture wells (for each culture condition) were tested for reactivity against anti-IgG Ab, HEL, 3D phage, f88 phage and NFDM. Thus, each mean value is calculated from six independent ELISA readings. ELISA data were collected after one, two, five and nine days of culture.

As shown in Table 4.1, after only one day of culture of 10^5 spleen cells, there was sufficient total IgG and anti-HEL IgG present in the culture supernatants for their detection *via* ELISA analysis. This was even true for cells cultured in the absence of any external immunostimulant (cells cultured in RPMI medium only). This Ab may have resulted from plasma cells that were present amongst the pool of 10^5 spleen cells originally added to the well. It may also have been the product of B cells that were stimulated to divide and differentiate into plasma cells by cell-cell contact with Agn-specific T cells, or by cytokines secreted by T cells or APCs, also present amongst the original pools of 10^5spleen cells.

A comparison of the mean ELISA data in Table 4.1, for supernatants from medium-only treated cells, as compared to LPS stimulation, for example, reveals that for the first two days of culture the stimulation with LPS aids in the production of IgG, but by day 5 there is not such a marked advantage of any of the stimulatory conditions over the plain medium. From the data, it is also evident that anti-Ig Ab and HEL were ineffective conditions for assessing Ab production by the cells. Most likely the anti-Ig Ab and HEL stimulated the B cells but the secreted Ab was sequestered by the HEL and the anti-Ig Ab in the supernatant, thereby preventing its detection in ELISA analysis.

The data in Table 4.1 also reveals that for the first two days of culture there was no binding of the supernatant to the 3D phage clone or to the negative controls f88 phage and NFDM. For the first two days of stimulation, binding was limited to anti-IgG Ab and HEL but by day five there was background/non-specific binding to both f88 phage and NFDM, along with

reactivity against the 3D phage. The direct ELISA data suggest that, over time, B cells that produce polyreactive Abs became stimulated. In the absence of competition analysis, of the 3D peptide in solution with the culture supernatant, against the plate-immobilized 3D phage, it is not possible to determine if there is any "real" binding of the supernatant to the 3D peptide or if the ELISA signals represent background binding to the phage.

Table 4.1. Mean and standard deviation of ELISA data for *in vitro* culture supernatant analysis of spleen cells from 3 HEL-immunized mice cultured over 9 days.

ELISA plate Agn	→	HEL[a]		Anti-IgG Ab		3D phage		f88 phage		NFDM	
10^5 cells[b]	Day[d]	MEAN[e]	SD[f]	MEAN	SD	MEAN	SD	MEAN	SD	MEAN	SD
RPMI[c]	1	**0.35**[g]	0.03	**0.30**	0.06	0.01	0.00	0.01	0.00	0.01	0.01
	2	**0.33**	0.07	**0.32**	0.09	0.01	0.00	0.01	0.00	0.01	0.00
	5	**0.80**	0.18	**0.79**	0.22	**0.21**	0.10	**0.25**	0.15	**0.24**	0.15
	9	**1.12**	0.12	**1.12**	0.16	**0.50**	0.39	**0.56**	0.42	**0.76**	0.38
LPS	1	**0.60**	0.09	**0.59**	0.15	0.01	0.01	0.01	0.00	0.01	0.00
	2	**0.79**	0.10	**0.87**	0.07	0.01	0.00	0.01	0.00	0.01	0.00
	5	**1.06**	0.07	**1.10**	0.07	**0.39**	0.30	**0.41**	0.31	**0.34**	0.40
	9	**1.20**	0.01	**1.22**	0.02	**0.45**	0.17	**0.51**	0.18	**0.78**	0.34
LPS +ILs 2, 4 & 5	1	**0.58**	0.12	**0.55**	0.13	0.01	0.01	0.01	0.00	0.01	0.00
	2	**0.87**	0.04	**0.91**	0.05	0.01	0.00	0.01	0.00	0.01	0.00
	5	**1.17**	0.06	**1.14**	0.04	**0.34**	0.27	**0.35**	0.28	**0.28**	0.31
	9	**1.12**	0.26	**1.14**	0.21	**0.26**	0.22	**0.23**	0.15	**0.62**	0.32
LPS +IL2	1	**0.55**	0.17	**0.53**	0.21	0.01	0.00	0.01	0.00	0.01	0.00
	2	**0.69**	0.10	**0.76**	0.11	0.01	0.00	0.01	0.00	0.01	0.00
	5	**0.96**	0.11	**1.05**	0.05	**0.33**	0.07	**0.29**	0.06	**0.19**	0.03
	9	**1.02**	0.26	**1.14**	0.10	**0.37**	0.21	**0.41**	0.24	**0.73**	0.35
LPS +IL4	1	**0.57**	0.11	**0.62**	0.12	0.01	0.00	0.01	0.00	0.01	0.00
	2	**0.81**	0.14	**0.89**	0.06	0.01	0.00	0.01	0.00	0.01	0.00
	5	**1.00**	0.13	**1.05**	0.10	**0.28**	0.08	**0.27**	0.05	**0.19**	0.05
	9	**1.21**	0.03	**1.24**	0.04	**0.46**	0.23	**0.52**	0.30	**0.86**	0.20
LPS +IL5	1	**0.39**	0.16	**0.45**	0.19	0.01	0.00	0.01	0.00	0.01	0.00
	2	**0.69**	0.26	**0.80**	0.13	0.01	0.00	0.01	0.00	0.01	0.00
	5	**0.94**	0.28	**0.99**	0.20	**0.27**	0.08	**0.29**	0.09	**0.17**	0.04
	9	**1.07**	0.14	**1.12**	0.12	**0.29**	0.25	**0.34**	0.26	**0.58**	0.46
ILs 2, 4 & 5	1	**0.29**	0.11	**0.30**	0.06	0.01	0.00	0.01	0.00	0.01	0.00
	2	**0.44**	0.13	**0.48**	0.14	0.01	0.00	0.01	0.00	0.01	0.00
	5	**0.80**	0.34	**0.78**	0.24	**0.17**	0.07	**0.19**	0.06	**0.19**	0.10
	9	**1.12**	0.10	**1.12**	0.11	**0.28**	0.33	**0.58**	0.37	**0.79**	0.40
Anti-Ig Ab	1	0.01	0.00	0.02	0.01	0.01	0.00	0.01	0.00	0.01	0.00
	2	0.01	0.00	0.01	0.01	0.01	0.00	0.01	0.00	0.01	0.00
	5	**0.23**	0.38	**0.29**	0.39	**0.25**	0.34	**0.27**	0.37	**0.26**	0.44
	9	**0.51**	0.41	**0.42**	0.36	**0.30**	0.24	**0.35**	0.30	**0.54**	0.48
Anti-Ig Ab + LPS	1	0.01	0.00	0.01	0.00	0.01	0.00	0.01	0.00	0.01	0.00
	2	0.02	0.01	0.01	0.01	0.01	0.00	0.01	0.00	0.01	0.00
	5	**0.15**	0.10	**0.20**	0.11	**0.27**	0.20	0.07	0.04	0.21	0.19
	9	**0.75**	0.32	**0.83**	0.34	**0.42**	0.23	**0.20**	0.14	**0.76**	0.30
HEL + LPS	1	0.03	0.01	**0.43**	0.15	0.01	0.00	0.01	0.00	0.01	0.00
	2	0.03	0.00	**0.82**	0.09	0.01	0.00	0.01	0.00	0.01	0.00
	5	**0.22**	0.03	**0.98**	0.07	**0.21**	0.03	**0.23**	0.06	**0.24**	0.07
	9	**0.53**	0.31	**1.04**	0.26	**0.25**	0.19	**0.35**	0.30	**0.56**	0.40

[a] Agn immobilized in ELISA plate wells.
[b] Number of spleen cells cultured per well.
[c] Culture conditions for the spleen cells.

[d] Number of days the cells were cultured.
[e] Mean ELISA signal value (OD 405-490 after 30 min incubation).
[f] Standard deviation (SD) for the ELISA signal values.
[g] Mean ELISA signal values greater than 0.1 are in bold.

A t-test was performed on the differences between the mean ELISA data collected after two days of culture (*i.e.*, before polyreactive Abs were produced) to determine if there was any statistically significant difference between the culture conditions tested (except for those including HEL Agn or anti-Ig Ab) for stimulating the production of IgG or anti-HEL IgG from the pooled spleen cells (Table 4.1, data are shaded). The percentage values presented in Table 4.2 and Table 4.3 represent the level of confidence with which the hypothesis, that the means are the same, can be rejected.

The values in Table 4.2 and Table 4.3 reveal that, with greater than 95% confidence (data shown in bold), there is a statistically significant difference between mean values of the ELISA data for the RPMI medium-only culture condition, *versus* all conditions that include LPS stimulation (*i.e.*, LPS stimulation is better than medium only in stimulating Ab production at day two). This is not true for medium-only *versus* cells cultured with ILs 2, 4 and 5. This suggests that, on their own, ILs 2, 4 and 5 are not effective at stimulating the cells to secrete IgG or anti-HEL IgG. The mean ELISA data, combined with the t-tests for those data (Table 4.1, Table 4.2 and Table 4.3), reveal that there is no advantage of culturing spleen cells with anything more than LPS. The data also show that there is not an additive effect for the ILs - there is not a statistically significant difference in Ab production by cells cultured with LPS + IL5, for example, *versus* cells cultured with LPS + ILs 2, 4 and 5.

Table 4.2. Results of the t-test comparing the mean ELISA data of anti-HEL IgG production under different culture conditions at day two.

	RPMI	LPS	LPS + ILs 2, 4 & 5	LPS + IL2	LPS + IL4	LPS + IL5	ILs 2, 4 & 5
RPMI		**99.98***	**100.00**	**99.91**	**99.93**	**97.67**	89.04
LPS			87.02	86.75	24.65	59.26	**99.69**
LPS + ILs2, 4 & 5				**98.94**	59.14	84.41	**99.94**
LPS + IL2					86.18	0.00	**98.52**
LPS + IL4						65.28	**99.49**
LPS + IL5							90.33
ILs 2, 4 & 5							

* Values are the level of confidence in percentage with which the null hypothesis, that the means are the same, can be rejected. Confidence levels greater than 95% are in bold.

Table 4.3. Results of the t-test comparing the mean ELISA data of IgG production under different culture conditions at day two.

	RPMI	LPS	LPS + ILs 2, 4 & 5	LPS + IL2	LPS + IL4	LPS + IL5	ILs 2, 4 & 5
RPMI		**99.99***	**100.00**	**99.94**	**99.99**	**99.94**	92.59
LPS			64.00	91.46	31.59	69.85	**99.83**
LPS + ILs 2, 4 & 5				**97.13**	40.11	87.76	**99.91**
LPS + IL2					94.67	45.97	**98.79**
LPS + IL4						79.64	**99.98**
LPS + IL5							**99.14**
ILs 2, 4 & 5							

* Values are the level of confidence in percentage with which the null hypothesis, that the means are the same, can be rejected. Confidence levels greater than 95% are in bold.

Pellet sizes in individual wells, as well as cell death (*via* trypan blue staining and microscopic analysis), were followed over the course of the *in vitro* culture experiment. In general, pellet sizes increased over time and pellets were larger for cells that received immunostimulation than those that were cultured in medium only. All cells were viable after the second day of culture, some cell death had occurred by the fifth day, and by the ninth day all of the cells were dead (by day 9 the wells contained mostly cellular debris). Thus, it is not necessary to culture spleen cells as long as 9 days under these conditions.

In summary, it was not possible to confirm the presence of 3D-peptide reactive B cells amongst the pools of cultured spleen cells in this *in vitro* culture analysis and there was no

apparent advantage of stimulating the cells with any of the ILs 2, 4 or 5 along with LPS. These findings, however, may have been influenced by the actions of accessory immune cells present amongst the pools of 10^5 spleen cells. Thus, for the subsequent *in vitro* culture analysis, pools of spleen cells and enriched splenic B cells were cultured side-by-side. The cells were cultured with medium only, with LPS, or with LPS + ILs 2, 4 and 5. Cells were cultured at 10^5, 10^4 and 10^3 cells per well to determine, if at lower cell numbers (*i.e.*, including fewer pre-existing plasma cells) there was greater difference in Ab production for different culture conditions. Because all cells were dead by the ninth day of culture in the first assay, the cells were cultured up to 7 days.

Table 4.4 and Table 4.5 present the mean and standard deviation of ELISA data collected for various numbers of spleen cells and enriched splenic B cells, respectively. Similar to the first assay, pools of 10^5 spleen cells, produced detectable levels of Ab after one day on culture, but Ab was only detectable by day 4 for the smaller pools of 10^4 and 10^3 spleen cells (Table 4.4). In contrast, there was only evidence of Ab production by all pools of the enriched B cells after 4 days of culture (Table 4.5). Over the course of the *in vitro* culture, as total IgG and anti-HEL IgG produced by spleen cells increased, so did the amount of non-specific Abs that bound f88 phage. There was very little binding to either 3D phage or f88 phage by supernatants from cultured B cells. Any reactivity of culture supernatant Abs with 3D phage was at or below background binding to f88 phage. Thus, similar to the first *in vitro* culture analysis, it was not possible to verify the presence of 3D peptide-reactive Abs in the assay.

Table 4.4. Mean and standard deviation of ELISA data for *in vitro* culture supernatant analysis for various numbers of spleen cells, from two HEL-immunized mice.

ELISA plate Agn[a]		HEL		Anti-IgG Ab		3D phage		f88 phage	
Culture conditions[b]	DAY[d]	MEAN[e]	SD[f]	MEAN	SD	MEAN	SD	MEAN	SD
RPMI 10^5 spleen cells[c]	1	**0.16**[g]	0.09	**0.23**	0.20	0.01	0.00	0.01	0.00
	2	**0.42**	0.31	**0.42**	0.29	0.01	0.00	0.01	0.00
	4	**0.66**	0.16	**0.61**	0.19	**0.13**	0.13	**0.16**	0.17
	7	**0.88**	0.18	**0.87**	0.13	**0.62**	0.04	**0.73**	0.12
LPS 10^5 spleen cells	1	**0.34**	0.05	**0.46**	0.18	0.01	0.00	0.01	0.00
	2	**0.90**	0.08	**0.85**	0.14	0.01	0.00	0.01	0.00
	4	**0.86**	0.17	**0.94**	0.08	**0.16**	0.21	0.09	0.10
	7	**0.98**	0.10	**1.03**	0.07	**0.66**	0.18	**0.82**	0.15
LPS + ILs 2, 4 & 5 10^5 spleen cells	1	**0.34**	0.19	**0.51**	0.34	0.01	0.00	0.01	0.00
	2	**0.79**	0.24	**0.81**	0.08	0.01	0.00	0.01	0.00
	4	**1.07**	0.02	**1.05**	0.05	**0.19**	0.23	**0.18**	0.25
	7	**1.07**	0.05	**1.08**	0.04	**0.49**	0.24	**0.71**	0.06
RPMI 10^4 spleen cells	1	0.03	0.01	0.03	0.01	0.01	0.00	0.01	0.00
	2	0.03	0.01	0.04	0.01	0.01	0.00	0.01	0.00
	4	**0.26**	0.05	**0.20**	0.14	**0.18**	0.13	**0.31**	0.14
	7	0.06	0.02	**0.04**	0.00	0.02	0.01	0.02	0.01
LPS 10^4 spleen cells	1	0.03	0.00	0.03	0.01	0.01	0.00	0.01	0.00
	2	0.02	0.01	0.03	0.02	0.01	0.00	0.01	0.00
	4	**0.42**	0.29	**0.28**	0.23	**0.22**	0.14	**0.23**	0.26
	7	**0.21**	0.32	**0.21**	0.22	**0.12**	0.21	**0.15**	0.26
LPS + ILs 2, 4 & 5 10^4 spleen cells	1	0.05	0.02	0.04	0.02	0.01	0.00	0.01	0.00
	2	0.06	0.04	0.06	0.04	0.01	0.00	0.01	0.00
	4	**0.58**	0.09	**0.38**	0.10	**0.25**	0.17	**0.30**	0.16
	7	**0.50**	0.26	**0.85**	0.14	**0.21**	0.23	**0.24**	0.25
RPMI 10^3 spleen cells	1	0.02	0.00	0.02	0.00	0.01	0.00	0.01	0.00
	2	0.02	0.01	0.03	0.02	0.01	0.00	0.01	0.00
	4	**0.44**	0.26	**0.17**	0.09	**0.14**	0.07	**0.19**	0.06
	7	**0.20**	0.32	**0.19**	0.29	**0.16**	0.26	**0.19**	0.32
LPS 10^3 spleen cells	1	0.02	0.00	0.02	0.00	0.01	0.00	0.01	0.00
	2	0.02	0.01	0.03	0.01	0.01	0.00	0.01	0.00
	4	**0.31**	0.28	**0.18**	0.11	**0.21**	0.10	**0.13**	0.09
	7	**0.22**	0.35	**0.24**	0.42	**0.19**	0.33	**0.24**	0.41
LPS + ILs 2, 4 & 5 10^3 spleen cells	1	0.02	0.00	0.02	0.00	0.01	0.00	0.01	0.00
	2	0.02	0.01	0.02	0.01	0.01	0.00	0.01	0.00
	4	**0.41**	0.33	**0.18**	0.11	**0.20**	0.11	**0.23**	0.14
	7	**0.05**	0.02	0.06	0.04	0.03	0.01	0.03	0.02

[a] Agn immobilized in ELISA plate wells.
[b] Culture conditions for the spleen cells.
[c] Number of spleen cells cultured per well.
[d] Number of days the cells were cultured.
[e] Mean ELISA signal value (OD 405-490 after 30 min incubation).
[f] Standard deviation (SD) for the ELISA signal values.
[g] Mean ELISA signal values greater than 0.1 are in bold.
[g] Mean ELISA signal values greater than 0.1 are in bold.

Table 4.5. Mean and standard deviation of ELISA data for *in vitro* culture supernatant analysis for various numbers of enriched splenic B cells, from two HEL-immunized mice.

ELISA plate Agn[a]		HEL		Anti-IgG Ab		3D phage		f88 phage	
Culture conditions[b]	DAY[d]	MEAN[e]	SD[f]	MEAN	SD	MEAN	SD	MEAN	SD
RPMI 10^5 B cells[c]	1	0.02	0.01	0.03	0.01	0.01	0.00	0.01	0.00
	2	0.02	0.01	0.03	0.01	0.01	0.00	0.01	0.00
	4	**0.23**[g]	0.16	**0.13**	0.08	**0.12**	0.14	**0.11**	0.10
	7	0.04	0.01	0.03	0.01	0.02	0.00	0.02	0.00
LPS 10^5 B cells	1	0.04	0.03	0.03	0.02	0.01	0.00	0.01	0.00
	2	0.03	0.03	0.04	0.02	0.01	0.00	0.01	0.00
	4	**0.21**	0.21	**0.30**	0.11	**0.13**	0.14	0.10	0.10
	7	**0.53**	0.31	**0.69**	0.12	**0.14**	0.24	**0.18**	0.31
LPS + ILs 2, 4 & 5 10^5 B cells	1	0.04	0.02	0.03	0.01	0.01	0.00	0.01	0.00
	2	0.07	0.04	0.07	0.04	0.01	0.00	0.01	0.00
	4	**0.67**	0.25	**0.71**	0.14	**0.12**	0.13	**0.11**	0.11
	7	**0.78**	0.23	**1.00**	0.03	**0.17**	0.29	**0.20**	0.35
RPMI 10^4 B cells	1	0.02	0.01	0.02	0.00	0.01	0.00	0.01	0.00
	2	0.01	0.00	0.01	0.01	0.01	0.00	0.01	0.00
	4	**0.26**	0.07	**0.14**	0.03	**0.15**	0.08	**0.14**	0.10
	7	0.03	0.01	0.02	0.00	0.02	0.01	0.02	0.01
LPS 10^4 B cells	1	0.02	0.01	0.02	0.00	0.01	0.00	0.01	0.00
	2	0.01	0.01	0.02	0.01	0.01	0.00	0.01	0.00
	4	**0.21**	0.05	**0.19**	0.09	**0.15**	0.07	**0.14**	0.04
	7	0.04	0.01	**0.15**	0.04	0.02	0.01	0.02	0.01
LPS + ILs 2, 4 & 5 10^4 B cells	1	0.02	0.01	0.02	0.00	0.01	0.00	0.01	0.00
	2	0.01	0.01	0.02	0.01	0.01	0.00	0.01	0.00
	4	**0.38**	0.16	**0.20**	0.10	**0.13**	0.05	**0.20**	0.10
	7	**0.14**	0.15	**0.51**	0.42	0.02	0.01	0.02	0.01
RPMI 10^3 B cells	1	0.02	0.00	0.02	0.00	0.01	0.00	0.01	0.00
	2	0.01	0.01	0.01	0.01	0.01	0.00	0.01	0.00
	4	**0.41**	0.23	**0.14**	0.08	**0.13**	0.10	**0.14**	0.07
	7	0.04	0.01	0.03	0.01	0.03	0.01	0.03	0.01
LPS 10^3 B cells	1	0.02	0.00	0.02	0.00	0.01	0.00	0.01	0.00
	2	0.01	0.00	0.01	0.01	0.01	0.00	0.01	0.00
	4	**0.48**	0.20	**0.20**	0.07	**0.15**	0.11	**0.17**	0.06
	7	0.04	0.02	0.04	0.02	0.03	0.02	0.03	0.01
LPS + ILs 2, 4 & 5 10^3 B cells	1	0.02	0.00	0.02	0.00	0.01	0.00	0.01	0.00
	2	0.01	0.00	0.01	0.01	0.01	0.00	0.01	0.00
	4	**0.49**	0.22	**0.17**	0.05	**0.18**	0.08	**0.17**	0.06
	7	0.04	0.01	0.03	0.01	0.02	0.00	0.03	0.01

[a] Agn immobilized in ELISA plate wells.
[b] Culture conditions for the B cells.
[c] Number of B cells cultured per well.
[d] Number of days the cells were cultured.
[e] Mean ELISA signal value (OD 405-490 after 30 min incubation).
[f] Standard deviation (SD) for the ELISA signal values.
[g] Mean ELISA signal values greater than 0.1 are in bold.

For the cultured B cells (Table 4.5), anti-HEL IgG production as well as total IgG production varied quite a lot from well to well and there were not clear patterns. On the fourth day of culture of 10^5 B cells there was no difference in anti-HEL IgG production for cells cultured in medium-only *versus* those stimulated with LPS. On day 7 of culture of 10^5 B cells, however, the mean ELISA data reveal an obvious increase in anti-HEL IgG production for cells stimulated with LPS and LPS + ILs 2, 4 and 5 *versus* cells cultured in medium-only. On the seventh day of culture of 10^3 enriched B cells, there was no anti-HEL IgG production for any of the culture conditions. On fourth day of culture, however, similar levels of anti-HEL IgG were observed for 10^3 enriched B cells cultured in medium-only or in the presence of LPS or LPS + lLs 2, 4 and5. These inconsistencies may be a function of the types and specificities of cells "randomly" comprising the pools of cells in a given well.

The mean ELISA data for 10^5 spleen cells and 10^5 enriched B cells on the fourth day of culture, summarized in Table 4.6, were analyzed to determine if there is any difference in stimulating 10^5 spleen cells or 10^5 splenic B cells in medium only *versus* LPS *versus* LPS + ILs 2, 4 and 5. T-test results are shown in Table 4.7 and Table 4.8. These data show that there is a statistically significant difference in the mean ELISA data for IgG production and anti-HEL IgG production for both the spleen cells and the B cells cultured with medium-only *versus* LPS + ILs 2, 4 and 5 (shown in bold in Table 4.7). Moreover, for the B cells there was also a statistically significant difference in the mean ELISA data for IgG production and anti-HEL IgG production for cells cultured with LPS *versus* LPS + ILs 2, 4 and 5. Therefore, there was an advantage in stimulating the B cells with the ILs 2, 4 and 5 along with LPS but there was no advantage in using the ILs when culturing the spleen cells.

Table 4.6 A comparison of mean and standard deviation of ELISA data for IgG and anti-HEL IgG production for 10^5 spleen cells and 10^5 B cells after four days of culture.

10^5 cells	Culture	HEL		IgG	
		MEAN	SD	MEAN	SD
spleen cells	RPMI	0.66	0.16	0.61	0.19
	LPS	0.86	0.17	0.94	0.08
	LPS + ILs2, 4 & 5	1.07	0.02	1.05	0.050
B cells	RPMI	0.23	0.16	0.13	0.08
	LPS	0.21	0.30	0.30	0.11
	LPS + ILs2, 4 & 5	0.67	0.25	0.71	0.14

Data summarized from Table 4.4 and Table 4.5.

Table 4.7. T-test for the difference in mean ELISA data of anti-HEL IgG production for pools of 10^5 spleen cells and 10^5 enriched splenic B cells cultured under different conditions at day four.

Spleen Cells			
	RPMI	LPS	LPS + ILs 2, 4 & 5
RPMI		87.06*	**99.54**
LPS			92.18
LPS + ILs2, 4 & 5			
B Cells			
	RPMI	LPS	LPS + ILs 2, 4 & 5
RPMI		11.39	**97.09**
LPS			**96.51**
LPS + ILs2, 4 & 5			

* Values are the level of confidence in percentage with which the null hypothesis, that the means are the same, can be rejected.

Table 4.8. T-test for the difference in mean ELISA data of IgG production for pools of 10^5 spleen cells and 10^5 enriched splenic B cells cultured under different conditions at day four.

Spleen Cells			
	RPMI	LPS	LPS + ILs 2, 4 & 5
RPMI		**97.65**	**99.39**
LPS			94.14
LPS + ILs2, 4 & 5			
B Cells			
	RPMI	LPS	LPS + ILs 2, 4 & 5
RPMI		94.42	**99.92**
LPS			**99.49**
LPS + ILs2, 4 & 5			

* Values are the level of confidence in percentage with which the null hypothesis, that the means are the same, can be rejected.

4.3.2 ELISPOT analysis of splenic B cells from HEL-immunized mice.

In a final attempt to identify the presence of 3D peptide-reactive B cells, spleen cells were analysed *via* ELISPOT. For this assay, cells are cultured in wells coated with Agn, and Abs

secreted by individual, Agn-specific B cells, are ultimately detected as "spots" on the bottoms of the wells. The ELISPOT assay is described in Materials and Methods (section 4.2.6, page 111). Briefly, microtiter plate wells were coated with HEL, anti-IgG Ab, 3D phage, f88 phage and NFDM or OVA. After blocking the plates, spleen cells were titered into the wells and cultured ON in medium, with or without LPS. Because the cells settle to the bottom of the wells, any Agn-specific Ab secreted by B cells will bind to the Agn-coated wells. After developing the microtiter plates the following day, individual "spots" can be counted by eye that correlate to the location that an individual, Agn-specific plasma cell had been cultured ON. Thus, ELISPOT analysis quantifies Agn-specific B cells.

ELISPOT data for the spleen cells extracted from three HEL-immunized BALB/c mice whose sera showed reactivity with the 3D phage (as well as HEL) are shown in Table 4.9. The number of "spots" counted for each well in which various numbers of spleen cells were cultured is presented in the table. The ELISPOT assay was repeated other spleen samples from HEL-immunized BALB/c mice. In all instances the number of 3D spots was very low but above background. This assay suggests that B cells producing anti-3D Ab are indeed present in the spleens of some HEL-immunized. The ELISpot analysis was also conducted with spleen cells from an unimmunized mouse. As shown in Table 4.10, no HEL+ spots or 3D phage+ spots were observed in the wells.

Table 4.9. ELISPOT analysis of spleen cells from three HEL-immunized mice.

# Cells	Anti-IgG			HEL			3D phage		f88 phage		NFDM	
RPMI	**Mouse #1**											
1 x 10^5	37	37	38	18	11	9	0	0	0	0	0	0
5 x 10^4	28	22	23	3	3	3	0	0	0	0	0	0
1 x 10^4	13	14	11	1	1	3	0	0	0	0	0	0
LPS												
1 x 10^5	*tmtc	tmtc	tmtc	29	33	39	0	0	0	0	0	0
5 x 10^4	67	60	65	20	16	32	0	**1**	0	0	0	0
1 x 10^4	29	27	28	17	12	10	0	0	0	0	0	0
RPMI	**Mouse # 2**											
1 x 10^5	tmtc	tmtc	tmtc	40	41	60	0	0	0	0	0	0
5 x 10^4	76	65	74	25	21	21	**1**	0	0	0	0	0
1 x 10^4	32	41	44	13	17	15	0	0	0	0	0	0
LPS												
1 x 10^5	tmtc	tmtc	tmtc	35	40	30	0	0	0	0	0	0
5 x 10^4	66	67	72	21	25	22	0	0	0	0	0	0
1 x 10^4	30	17	19	5	8	7	0	0	0	0	0	0
RPMI	**Mouse # 3**											
1 x 10^5	58	39	36	15	21	19	0	0	0	0	0	0
5 x 10^4	12	8	19	15	8	10	0	0	0	0	0	0
1 x 10^4	6	9	11	5	4	4	0	**1**	0	0	0	0
LPS												
1 x 10^5	50	48	47	16	18	18	0	0	0	0	0	0
5 x 10^4	19	18	21	17	13	12	0	**1**	0	0	0	0
1 x 10^4	10	14	19	5	5	4	0	0	0	0	0	0

*tmtc = too many to count (greater than 100)

Table 4.10 ELISPOT analysis of spleen cells from an unimmunized mouse.

LPS	Anti-IgG	Anti-IgG	HEL	HEL	3D phage	3D phage	f88 phage	OVA
1 x 10^5	18	17	0	0	0	0	0	0
5 x 10^4	6	1	0	0	0	0	0	0
1 x 10^4	1	0	0	0	0	0	0	0

In Table 4.11, a comparison is made of the average number of total IgG^+ plasma cells *versus* HEL^+ plasma cells per 5 x 10^4 total spleen cells cultured in medium only, or in medium supplemented with LPS. For mouse #1 and mouse #2, the percentage of HEL^+ B cells of total IgG^+ B cells ranged from only 31-37%, in the presence or absence of LPS. Whereas, for the third mouse, the HEL^+ B cells represented greater than 70% of the total IgG^+ B cells but fewer total IgG^+ plasma cells were counted in either the presence or absence of LPS. For mouse #1, there

was an obvious advantage to stimulating the cells with LPS as almost three times more IgG^+ and HEL^+ B cells were counted in the presence of LPS. For mouse #2 and mouse #3, however, total B cell numbers counted were similar with or without LPS stimulation.

Table 4.11. Percentage of HEL-reactive B cells of total IgG+ B cells amongst 5 x 10^4 spleen cells.

	Anti-IgG^+ [a]	HEL^+ [a]	$3D^+$ [a]	% HEL^+ [b]	%$3D^+$ [b]
RPMI[c] mouse #1	24.3	9	0	37	0
LPS mouse #1	64	22.7	0.5	35	0.78
RPMI mouse #2	71.6	22.3	0.5	31	0.70
LPS mouse #2	68.3	22.6	0	33	0
RPMI mouse #3	13	11	0	85	0
LPS mouse #3	19.3	14	0.5	73	2.6

[a] Average number of spots.
[b] Percentage of IgG-secreting B cells that are HEL+ or 3D+.
[c] Culture condition in ELISPOT well.

4.4 Discussion

The purpose of this chapter was to develop assays to identify 3D peptide-reactive B cells amongst spleen cells from HEL-immunized mice whose sera bind the 3D peptide. The 3D peptide (TCIHGLPPSECH), which cross-reacts with HEL, was derived from a RPL screening with Abs from HEL-immunized mice. Three of the peptide's residues (underlined) align to the linear sequence of HEL and the peptide is broadly recognized by serum Abs from HEL-immunized mice. Thus, the 3D peptide is thought to mimic an immunodominant epitope on HEL that might include residues His15, Gly16 and Leu17.

Three different assays were undertaken in an attempt to identify 3D peptide-reactive B cells. The first one, for which data was not presented in this chapter, was cytometric analysis of spleen cells. This assay involved the labelling of spleen cells with fluorescenated HEL and/or peptide (both bio-3D peptide and bio-E3 peptide from Chapter 2 were used), as well as various cell surface markers. As described in the introduction, however, background binding by the SA-

fluorophores to cell samples, as well as the binding of Agn-labelled fluorophores to cells from unimmunized mice, were problematic. All efforts to reduce background binding, such as: (i) using different SA-conjugated fluorophores that may be less "sticky", (ii) "double-staining" the cells with both HEL and the cross-reactive peptide to reduce the frequency of "false-positive" cells (a technique called SEMS: single-epitope multiple staining) (90), (iii) enriching for B cells on a negative depletion column prior to cell staining, and, (iv) labelling the spleen cells with phenotypic markers to "gate in" B cells and "gate out" all non B cells, were unsuccessful. Markers tested included IgG-APC, B220-PE-Cy5 and CD-138-PE for staining various B cell populations and, IgM-PerCP-CY5.5, CD3-APC-Cy7 and Cd11b-PECy7 for gating out non-isotype switched B cells, T cells and monocytes/macrophages, respectively (87-89) (90). (83, 84) (85) (86).

The next assay undertaken for the identification of 3D peptide-reactive B cells was the *in vitro* culture analysis of spleen cells and enriched splenic B cells from HEL-immunized mice. For this assay, pools of cells were cultured in 96-well plates in the presence or absence of immunostimulants. Various combinations of LPS and ILs-2, 4 and 5 were tested for their ability to drive the production of Agn-specific IgG. LPS and these ILs have been well characterized for their ability to stimulate B cells. Briefly, LPS, a polymeric molecule from the endotoxin of gram-negative bacteria, is a thymus-independent (TI) Agn and has the ability to activate B cell clones that are specific for other Agns (*i.e.*, polyclonal B cell activation) (195). IL-2 is produced by activated T cells and acts on T cells to promote proliferation and differentiation as well as activate Tc cells and macrophages. It also acts on IL-2 receptors of B cells and promotes their proliferation in the absence of Agn or mitogen (193). IL-4 and IL-5 are both produced by T cells and mast cells. IL-4 is a B cell growth factor involved in early B cell activation and proliferation, and it promotes isotype switching to IgG and IgE (and inhibits IgG2a production). IL-5 is a powerful B cell activator (in mouse but not in humans) and it acts on B cells to promote B cell growth and differentiation as well as isotype switching to IgA (73) (196) (72).

From these assays it was observed that for a pool of 10^5 unstimulated spleen cells from HEL-immunized mice, IgG and anti-HEL IgG are detectable in culture supernatant after just one day of culture. This IgG may have been produced by activated plasma cells present amongst the pools of spleen cells originally added to the wells. Moreover, T cells and/or APCs also present in the wells could have stimulated the B cells. For the first few days of culture, however, there was typically higher IgG and anti-HEL IgG production for cells that received LPS stimulation *versus* no stimulation. For smaller pools of cells (10^4 or 10^3 per well), IgG and anti-HEL IgG were only

detectable by day 4. In general, there was an increase in total IgG and anti-HEL IgG production over time, even in the absence of external immunostimulation. Along with Agn-specific IgG, however, non-specific IgG that bound f88 phage and/or NFDM were also produced over time. There was no reactivity of the *in vitro* culture IgG against the 3D phage that was above background binding to f88 phage and NFDM. The non-specific Ab may have resulted from the stimulation of polyreactive B cells present amongst the pools cells (197).

Based on these findings, an ELISpot was designed in which spleen cells were titered into Agn-coated wells containing media and LPS. Agn-specific Ab secreted by the B cells bound the plate-immobilized Agn was ultimately detected as a visible "spots", with each spot representing an individual Agn-specific, Ab-secreting B cell. The ELISPOT was the only assay that showed the presence of 3D-peptide reactive B cells, representing less than 1% of total Ab-secreting B cells, amongst pools of spleen cells from HEL-immunized mice. Now that there is evidence that 3D peptide-reactive B cells are found within the spleens of HEL-immunized mice, strategies can be undertaken to isolate these cells. For example, as done by Newman *et. al.*, (89) peptide-reactive B cells could potentially be enriched from the spleens of HEL-immunized mice by incubating cell suspensions with bio-peptide and then capturing the cell-peptide complex on anti-biotin magnetic beads. The isolated B cells can then be stimulated in culture prior to being stained with various cell surface markers and being sorted *via* flow cytometry. Alternatively, the cells can be sorted and then stimulated in culture with LPS as has been done by [Weitkamp, 2003 #596]. Another option is to set up the PFC as to isolate Agn-reactive B cells (198).

Ultimately, Ab genes for 3D peptide-reactive B cells from different mice will be cloned, sequenced and expressed. It is predicted that the gene usage of anti-peptide Abs that cross-react with HEL will be restricted but this can only by proven by cloning and sequencing the Ab genes from several different mice. After expressing 3D-peptide reactive Ab(s), binding and affinity studies for the peptide and the Ab(s), as well as HEL and the Ab(s), can be conducted and the findings compared. Finally, crystallographic analysis of the 3D peptide in complex with the Ab fragment(s), coupled with an Ala replacement scan of the 3D peptide, will enable characterization of functional and structural CBRs.

CHAPTER 5 THESIS DISCUSSION

Effective anti-viral vaccines mediate protection through their specific activation of both cellular and humoral components of the immune system (72). In general, vaccines have been most successful against viruses in which natural infection is self-limited and leads to long-lasting protective immunity if the patient survives the initial infection. In these cases, the best vaccine is usually the one that most closely mimics natural infection such as live attenuated virus (199). Many viruses, however, have evolved elaborate mechanisms of evading immune clearance by Abs. The failure of many vaccine candidates against such viruses has, at least in part, been attributed to their inability to elicit adequate Nt Ab responses (8) (200) (6, 7). Thus, in the last 5-10 years researchers have focused on the development of vaccine strategies that are better at specifically inducing Abs that can prevent infection at the time of exposure (199).

In the case of the rapidly evolving retrovirus HIV-1, antigenic variation of the viral coat proteins gp120 and gp41, coupled with the masking of conserved epitopes, has made it difficult to produce a vaccine that provides adequate humoral immunity against a broad range of viral isolates (11-13, 200). In fact, as described in the thesis Introduction (section 1.1, page 1), to date only five broadly-Nt, anti-HIV-1 Abs have been identified (15). Nt Abs are known to play an important role in protection against HIV-1; it has been demonstrated that passive transfer of Nt anti-HIV-1 IgG1 MAbs can provide protection in macaques against intravenous challenge and against mucosal transmission (201, 202). Thus, if it were possible to specifically target the production of sufficient titers of these five broadly-Nt anti-HIV Abs, or others like them, that bind the same or similar conserved coat protein epitopes, scientists may be well on their way towards producing a sterilizing vaccine against HIV-1. This concept, of targeting the production of Abs against conserved epitopes, is called epitope-targeted vaccine design (200).

In the early eighties it was proposed that peptides might provide a means of directing the production of Abs against specific epitopes that are not be immunodominant in the context of the whole protein or an Agn fragment (21) (22). Indeed, linear peptides derived from proteins (203) (204) (205) (170) (171) (206) (207) (26), as well as cross-reactive peptides of continuous epitopes (208) (176) (33) (32) have been used to elicit Abs that cross-react with cognate protein. It is generally accepted, however, that most Abs bind complex discontinuous epitopes rather than continuous ones (101) (57) (209). Therein lies the challenge: to date there are no examples of

Abs being elicited against a discontinuous epitope by immunization with a cross-reactive peptide ligand.

For this thesis, epitope-targeted vaccine design was explored with the well-characterized model protein HEL, and peptide ligands. The goals of the research were to develop and optimize peptides that could be used both as markers to analyze anti-HEL Ab specificities and B cells from individual BALB/c mice, and as immunogen in a prime-boost strategy to focus Ab production against a target HEL epitope. Three types of peptides were used for this research: (i) a peptide that cross-reacts with a discontinuous HEL epitope and was identified from RPL screenings with D1.3 MAb (ii) peptides selected from RPLs with anti-HEL pcAbs, and, (iii) peptides, both long and short, derived from the linear sequence of HEL. All of the peptides were used as markers to analyze anti-HEL Ab specificities in serum from individual mice, and one of the peptides, the D1.3-binding peptide "E3" was tested in both direct, and prime-boost, immunization, for its ability to elicit or amplify the production of D1.3 or D1.3-like Abs in mice. The cross-reactive peptide, "3D", commonly recognized by sera from different HEL-immunized mice, was also used as a marker to identify "epitope-specific", splenic B cells.

Chapter 2 describes RPL screenings with the anti-HEL MAb, D1.3 (124). The purpose of the screenings was to identify a cross-reactive peptide that could be optimized and used as a marker to identify the presence of D1.3 or D1.3-like Abs in sera from HEL-immunized mice. Based on a consensus sequence that emerged from the RPL screening with Dl.3 MAb, two sublibraries were constructed and an optimized peptide, E3 (ASQPNCDGLVCNRWH), was identified and selected for further characterization (Table 2.4, page 49). Although the E3 peptide bears no sequence alignment to HEL, an Ala replacement scan of the phage-displayed peptide revealed that it shares CBRs in common with its cognate, discontinuous HEL epitope (underlined) (122) (125, 128) (Table 2.14, page70). Because D1.3 MAb is so close in sequence to its germline genes (it bears only five replacement somatic mutations), and BALB/c mice are inbred, it was assumed that D1.3 is commonly produced amongst HEL-immunized mice (168). Direct ELISA analysis of anti-HEL sera from different mice, however, showed no reactivity against the peptide, suggesting that either D1.3 is not commonly made or it is present at too low a titer for detection (Table 2.7, page 59).

Under the assumption that D1.3 Ab is commonly produced (but at a low titer) amongst HEL-immunized BALB/c mice, a prime-boost immunization strategy was undertaken with HEL and the E3 peptide. It was hypothesized that a priming immunization with HEL would elicit a pcAb response, including a subpopulation of D1.3 or D1.3-like Abs, and that the peptide could be

used in boosting immunization(s) to specifically amplify this subpopulation of Abs. The prime-boost immunization, however, did not yield Abs that cross-react with HEL and the E3 peptide (Table 2.12 and Table 2.13, page 66). The failure may either have been due to the fact that the E3 peptide is not an immunogenic mimic of the discontinuous D1.3 epitope (direct immunization with the peptide did not elicit Abs that cross-react with HEL) or because D1.3 Abs were not elicited in the priming immunization with HEL and, therefore, could not be amplified in the boosting immunizations with the peptide.

In order to test the concept of prime-boost immunization, RPL screenings were undertaken with pcAbs from the sera of HEL-immunized mice in an attempt to identify peptide markers for commonly produced anti-HEL Ab specificities amongst BALB/c mice. It was hypothesized that such peptide markers could be identified because screenings with immune human IgG have identified peptide markers for Abs commonly elicited in response to Lyme disease (177), HIV-1 (176), Hepatitis B (180) (63) and Hepatitis C (179) infection, and even rheumatoid arthritis (178). As far as we are aware, this is the first identification of a cross-reactive peptide marker for commonly produced murine Ab against a target Agn. For the screenings undertaken with immune human IgG, the Ab samples were not affinity-purified on Agn prior to the screenings. The BALB/c mouse Ab repertoire, however, is the product of many polyreactive B cells (181), including a high proportion of B1 cells (210). Thus, it was necessary to purify the Abs on HEL prior to the screenings. Indeed, preliminary screening studies with IgG enriched Abs from the sera of seven HEL-immunized mice (data not shown) identified several IgG peptide markers that did not cross-react with HEL.

Chapter 3 describes the screening of RPLs with anti-HEL Abs purified from the sera of three immunized mice (Table 3.1, page 83), and the reactivity of those peptides, along with a set of linear HEL peptides, with sera from different mice (Table 3.13, page 100). Although 22 unique cross-reactive peptides were identified in the RPL screening, only one of them, 3D, was commonly recognized by serum from different HEL-immunized mice (Table 3.8, page 91). Interestingly, the 3D peptide (TCIHGLPPSECH) was also the only one that bore any similarity to the linear sequence of HEL (underlined). The remaining peptide sequences could only be aligned to consensus groups amongst one another. Competition ELISA ultimately showed that of all 22 peptides only three HEL epitopes were represented. Also, except for phage clone 3D, the reactivity of the cross-reactive phage was limited to one of the three screening Abs (AH6) used to select them. Possible reasons for this are provided in the Results of Chapter 3 (section 3.3.4, page 89). Interestingly, anti-HEL serum samples from different mice showed very similar patterns of

reactivity against a set of 10-mer overlapping HEL peptides, indicating that the Ab response in different mice targets common HEL epitopes (Figure 3.6, page 98).

It is possible that the overlapping 10-mer HEL peptides are recognized by Abs elicited against linear HEL epitopes, or that the peptides represent contiguous segments of discontinuous epitopes and are thus recognized by Abs derived against complex HEL epitopes. The broad reactivity of the anti-HEL sera against the 10-mer peptides, however, begs the question of why an abundance of phage clones that align to linear epitopes were not enriched in the screening? The types of peptides enriched in the RPLs screenings are influenced by two factors. The first is the representation of peptide sequences amongst the phage clones and the second is the competition that occurs amongst the purified screening Abs. With respect to the RPLs, not all potential Ab-binding peptide sequences will be represented. Regarding the screening Abs, those that are present at higher concentration and/or those that are more inclined to cross-react with peptide ligands may out compete other Ab specificities. Moreover, the serum samples were purified on HEL prior to the screening and this may have biased the type of Ab used in the screening. Whereas the overlapping peptides were probed with serum samples that may have included Ab specificities against denatured HEL protein, the purification of Ab on HEL probably enriched for Abs against conformational epitopes.

A preliminary immunization of BALB/c mice with recombinant 3D phage has shown that the peptide is immunogenic, but after two immunizations there was no evidence of Abs that cross-react with HEL (Figure 3.5, page 96). Thus, like the E3 peptide, the 3D peptide is not an immunogenic mimic of its cognate HEL epitope. A prime-boost immunization study with HEL and 3D phage is currently being conducted. Similar to the E3 peptide study, mice are being primed with HEL to elicit a pcAb response against HEL and boosted with recombinant 3D phage in an attempt to amplify a subpopulation of the Abs. It is possible, however, that instead of amplifying a target subpopulation of Abs, that the peptide will elicit "anti-peptide-like" Abs (49, 53) that do not cross-react with HEL.

One of the most comprehensive analyses of B cell responses to peptides is a body of work by Kanury V.S. Rao and colleagues (211) (212) (213) (214) (215) (216) (217) (218). Employing both recombinant and synthetic peptide model Agns (such as PS1CT3, a chimeric Agn derived from a 15 residue B cell epitope of the hepatitis B virus surface Agn and a promiscuous T cell epitope from the malaria parasite *Plasmodium falciparum*) and mouse models, they have shown that anti-peptide IgM specificities generated in the primary immunization with peptide are heterogeneous in nature but that class switching to IgG is

associated with the selection of a limited subset of the Ab specificities. Interestingly, in the case of the chimeric Agn PS1CT3, the IgG response was mostly directed against a tetrapeptide segment of the sequence. They also demonstrated that the success or failure of a particular IgG specificity is associated with its ability to acquire T cell help. Thus, with respect to the 3D, it is impossible to determine, *a priori*, the nature of the B cell epitope(s) that it comprises. For example, if HGL are CBRs for the peptide and they are shared by its cognate HEL epitope, will those residues even constitute a B cell epitope in the context of the peptide? Or, will BCRs be selected with residues of the peptide that bear no significance to its cross-reactivity with HEL?

Because epitopes and paratopes are relational entities, an epitope-targeted vaccine involving a cross-reactive peptide, could also be considered a "paratope-targeted" vaccine – the vaccine is targeting the production of a particular Ab or restricted subset of Abs. In all likelihood, a cross-reactive peptide is optimized for binding the Ab molecule used in its selection (*i.e.*, it is idiotype specific) but it is not an optimized mimic of its cognate epitope, especially if the peptide cross-reacts with a conformational epitope. In contrast, a linear peptide derived from a protein, or even a peptide mimic of a linear epitope, may bear multiple B cell epitopes in common with the cognate protein making it more likely that the peptide will elicit cross-reactive Ab specificities.

In order for the immune system to produce a particular circulating, TD Ab response, several conditions must be met: (i) the individual must bear the genes encoding a particular surface Ig and the rearrangement of those genes into germline configuration may be influenced by organization/location of those genes within the genome, (ii) the germline configuration of the BCR must be present in the repertoire expressed at the time of Agn stimulation, (iii) the B cell must receive secondary stimulation either directly or indirectly from an *activated* T cell, (iv) the B cell must survive interclonal competition based on competition for a limited supply of Agn, and (v) the B cell must survive intraclonal competition within a GC as it undergoes affinity maturation *via* somatic mutations, and (vi) if the target Ab is highly mutated, the "germline" Ab may have to undergo, and survive, multiple rounds of somatic hypermutation (98) (77) (219) (220) (79) (78) (81) (80). Despite the high level of competition involved in Ab production and the vast size of the human Ig repertoire, estimated to be greater than 10^{11} specificites (72), there is evidence of immunodominant gene usage in protective Ab responses against pathogens including human cytomegalovirus (221), rotavirus (222), *Streptococcus pneumoniae* (223) and *Haemophilus influenzae* (224). Thus, for these pathogens it might be possible to develop an effective prime-boost immunization strategy.

Many questions remain regarding the immunogenic mimicry of cross-reactive peptides as well as the nature of the Abs that they elicit. For example, are the peptides structural mimics of their cognate epitope? Further, what is the gene usage of the Abs elicited against the peptides? Is it possible that completely differently Ab specificities (different germline gene usage, or different somatic mutation profiles) were elicited by the peptide but they were able to cross-react with the cognate epitope? Also, what is the breadth of the Ab response against the cross-reactive peptide and what proportion of the Ab specificities bind the cognate epitope (26)? Work in this thesis demonstrates obstacles in developing epitope-targeted vaccines with peptide ligands. First of all, it is very unlikely that direct immunization with a cross-reactive peptide ligand will yield Abs that bind a cognate discontinuous protein epitope. Moreover, differences in Ab specificities produced amongst individuals present limitations for the prime-boost immunization strategy should it work. Lastly, genetic differences in the Ab repertoires (and other immune response genes) of various animal models *versus* humans, is an obstacle in developing epitope-targeted vaccines with cross-reactive peptides. Prime-boost immunization strategies for targeting the production of Abs against conformational epitopes, however, should be further explored as a means of combating pathogens such as HIV-1 for which traditional vaccine design has thus far failed.

REFERENCES

1. Delves, P.J., and I.M. Roitt. 2000. The immune system. First of two parts. *N Engl J Med* 343:37-49.

2. Delves, P.J., and I.M. Roitt. 2000. The immune system. Second of two parts. *N Engl J Med* 343:108-117.

3. Takada, A., H. Feldmann, T.G. Ksiazek, and Y. Kawaoka. 2003. Antibody-dependent enhancement of Ebola virus infection. *J Virol* 77:7539-7544.

4. Nussbaum, G., W. Cleare, A. Casadevall, M.D. Scharff, and P. Valadon. 1997. Epitope location in the Cryptococcus neoformans capsule is a determinant of antibody efficacy. *J Exp Med* 185:685-694.

5. Joiner, K.A., R. Scales, K.A. Warren, M.M. Frank, and P.A. Rice. 1985. Mechanism of action of blocking immunoglobulin G for Neisseria gonorrhoeae. *J Clin Invest* 76:1765-1772.

6. Zinkernagel, R.M. 2000. What is missing in immunology to understand immunity? *Nat Immunol* 1:181-185.

7. Zinkernagel, R.M. 2003. On natural and artificial vaccinations. *Annu Rev Immunol* 21:515-546.

8. Burton, D.R., and P.W. Parren. 2000. Vaccines and the induction of functional antibodies: time to look beyond the molecules of natural infection? *Nat Med* 6:123-125.

9. Burton, D.R., R.A. Williamson, and P.W. Parren. 2000. Antibody and virus: binding and neutralization. *Virology* 270:1-3.

10. Nara, P.L., and R. Garrity. 1998. Deceptive imprinting: a cosmopolitan strategy for complicating vaccination. *Vaccine* 16:1780-1787.

11. Robinson, H.L. 2002. New hope for an AIDS vaccine. *Nat Rev Immunol* 2:239-250.

12. Richman, D.D., T. Wrin, S.J. Little, and C.J. Petropoulos. 2003. Rapid evolution of the neutralizing antibody response to HIV type 1 infection. *Proc Natl Acad Sci U S A* 100:4144-4149.

13. Wei, X., J.M. Decker, S. Wang, H. Hui, J.C. Kappes, X. Wu, J.F. Salazar-Gonzalez, M.G. Salazar, J.M. Kilby, M.S. Saag, N.L. Komarova, M.A. Nowak, B.H. Hahn, P.D. Kwong, and G.M. Shaw. 2003. Antibody neutralization and escape by HIV-1. *Nature* 422:307-312.

14. Weiss, R.A., P.R. Clapham, R. Cheingsong-Popov, A.G. Dalgleish, C.A. Carne, I.V. Weller, and R.S. Tedder. 1985. Neutralization of human T-lymphotropic virus type III by sera of AIDS and AIDS-risk patients. *Nature* 316:69-72.

15. Parren, P.W., J.P. Moore, D.R. Burton, and Q.J. Sattentau. 1999. The neutralizing antibody response to HIV-1: viral evasion and escape from humoral immunity. *Aids* 13:S137-162.

16. Collis, A.V., A.P. Brouwer, and A.C. Martin. 2003. Analysis of the antigen combining site: correlations between length and sequence composition of the hypervariable loops and the nature of the antigen. *J Mol Biol* 325:337-354.

17. Haynes, B.F., J. Fleming, E.W. St Clair, H. Katinger, G. Stiegler, R. Kunert, J. Robinson, R.M. Scearce, K. Plonk, H.F. Staats, T.L. Ortel, H.X. Liao, and S.M. Alam. 2005. Cardiolipin polyspecific autoreactivity in two broadly neutralizing HIV-1 antibodies. *Science* 308:1906-1908.

18. Calarese, D.A., C.N. Scanlan, M.B. Zwick, S. Deechongkit, Y. Mimura, R. Kunert, P. Zhu, M.R. Wormald, R.L. Stanfield, K.H. Roux, J.W. Kelly, P.M. Rudd, R.A. Dwek, H. Katinger, D.R. Burton, and I.A. Wilson. 2003. Antibody domain exchange is an immunological solution to carbohydrate cluster recognition. *Science* 300:2065-2071.

19. Zwick, M.B., L.L. Bonnycastle, A. Menendez, M.B. Irving, C.F. Barbas, 3rd, P.W. Parren, D.R. Burton, and J.K. Scott. 2001. Identification and characterization of a peptide that specifically binds the human, broadly neutralizing anti-human immunodeficiency virus type 1 antibody b12. *J Virol* 75:6692-6699.

20. Menendez, A., K.C. Chow, O.C. Pan, and J.K. Scott. 2004. Human immunodeficiency virus type 1-neutralizing monoclonal antibody 2F5 is multispecific for sequences flanking the DKW core epitope. *J Mol Biol* 338:311-327.

21. Beale, J. 1982. Synthetic peptides as the basis for future vaccines. *Nature* 298:14-15.

22. Lerner, R.A. 1982. Tapping the immunological repertoire to produce antibodies of predetermined specificity. *Nature* 299:593-596.

23. Sundberg, E.J., and R.A. Mariuzza. 2002. Molecular recognition in antibody-antigen complexes. *Adv Protein Chem* 61:119-160.

24. Geysen, H.M., J.A. Tainer, S.J. Rodda, T.J. Mason, H. Alexander, E.D. Getzoff, and R.A. Lerner. 1987. Chemistry of antibody binding to a protein. *Science* 235:1184-1190.

25. Fack, F., B. Hugle-Dorr, D. Song, I. Queitsch, G. Petersen, and E.K. Bautz. 1997. Epitope mapping by phage display: random versus gene-fragment libraries. *J Immunol Methods* 206:43-52.

26. Matthews, L.J., R. Davis, and G.P. Smith. 2002. Immunogenically fit subunit vaccine components via epitope discovery from natural peptide libraries. *J Immunol* 169:837-846.

27. Scott, J.K., and L. Craig. 1994. Random peptide libraries. *Curr Opin Biotechnol* 5:40-48.

28. Ben-Yedidia, T., and R. Arnon. 1997. Design of peptide and polypeptide vaccines. *Curr Opin Biotechnol* 8:442-448.

29. Casal, J.I., J.P. Langeveld, E. Cortes, W.W. Schaaper, E. van Dijk, C. Vela, S. Kamstrup, and R.H. Meloen. 1995. Peptide vaccine against canine parvovirus: identification of two neutralization subsites in the N terminus of VP2 and optimization of the amino acid sequence. *J Virol* 69:7274-7277.

30. Steward, M.W., C.M. Stanley, and O.E. Obeid. 1995. A mimotope from a solid-phase peptide library induces a measles virus-neutralizing and protective antibody response. *J Virol* 69:7668-7673.

31. Chargelegue, D., O.E. Obeid, S.C. Hsu, M.D. Shaw, A.N. Denbury, G. Taylor, and M.W. Steward. 1998. A peptide mimic of a protective epitope of respiratory syncytial virus selected from a combinatorial library induces virus-neutralizing antibodies and reduces viral load in vivo. *J Virol* 72:2040-2046.

32. Yu, M.W., J.K. Scott, A. Fournier, and P.J. Talbot. 2000. Characterization of murine coronavirus neutralization epitopes with phage-displayed peptides. *Virology* 271:182-196.

33. Grabowska, A.M., R. Jennings, P. Laing, M. Darsley, C.L. Jameson, L. Swift, and W.L. Irving. 2000. Immunisation with phage displaying peptides representing single epitopes of the glycoprotein G can give rise to partial protective immunity to HSV-2. *Virology* 269:47-53.

34. Schellekens, G.A., E. Lasonder, M. Feijlbrief, D.G. Koedijk, J.W. Drijfhout, A.J. Scheffer, S. Welling-Wester, and G.W. Welling. 1994. Identification of the core residues of the epitope of a monoclonal antibody raised against glycoprotein D of herpes simplex virus type 1 by screening of a random peptide library. *Eur J Immunol* 24:3188-3193.

35. Westerink, M.A., P.C. Giardina, M.A. Apicella, and T. Kieber-Emmons. 1995. Peptide mimicry of the meningococcal group C capsular polysaccharide. *Proc Natl Acad Sci U S A* 92:4021-4025.

36. Arnon, R., R. Tarrab-Hazdai, and M. Steward. 2000. A mimotope peptide-based vaccine against Schistosoma mansoni: synthesis and characterization. *Immunology* 101:555-562.

37. Mitchison, N.A. 1971. The carrier effect in the secondary response to hapten-protein conjugates. II. Cellular cooperation. *Eur J Immunol* 1:18-27.

38. Greenwood, J., A.E. Willis, and R.N. Perham. 1991. Multiple display of foreign peptides on a filamentous bacteriophage. Peptides from Plasmodium falciparum circumsporozoite protein as antigens. *J Mol Biol* 220:821-827.

39. de la Cruz, V.F., A.A. Lal, and T.F. McCutchan. 1988. Immunogenicity and epitope mapping of foreign sequences via genetically engineered filamentous phage. *J Biol Chem* 263:4318-4322.

40. Kneissel, S., I. Queitsch, G. Petersen, O. Behrsing, B. Micheel, and S. Dubel. 1999. Epitope structures recognised by antibodies against the major coat protein (g8p) of filamentous bacteriophage fd (Inoviridae). *J Mol Biol* 288:21-28.

41. Panina-Bordignon, P., A. Tan, A. Termijtelen, S. Demotz, G. Corradin, and A. Lanzavecchia. 1989. Universally immunogenic T cell epitopes: promiscuous binding to human MHC class II and promiscuous recognition by T cells. *Eur J Immunol* 19:2237-2242.

42. Sinigaglia, F., M. Guttinger, J. Kilgus, D.M. Doran, H. Matile, H. Etlinger, A. Trzeciak, D. Gillessen, and J.R. Pink. 1988. A malaria T-cell epitope recognized in association with most mouse and human MHC class II molecules. *Nature* 336:778-780.

43. Amzel, L.M., and R.J. Poljak. 1979. Three-dimensional structure of immunoglobulins. *Annu Rev Biochem* 48:961-997.

44. Kabat, E.A., T.T. Wu, and H. Bilofsky. 1977. Unusual distributions of amino acids in complementarity-determining (hypervariable) segments of heavy and light chains of immunoglobulins and their possible roles in specificity of antibody-combining sites. *J Biol Chem* 252:6609-6616.

45. Wilson, I.A., and R.L. Stanfield. 1994. Antibody-antigen interactions: new structures and new conformational changes. *Curr Opin Struct Biol* 4:857-867.

46. MacCallum, R.M., A.C. Martin, and J.M. Thornton. 1996. Antibody-antigen interactions: contact analysis and binding site topography. *J Mol Biol* 262:732-745.

47. Chothia, C., A.M. Lesk, A. Tramontano, M. Levitt, S.J. Smith-Gill, G. Air, S. Sheriff, E.A. Padlan, D. Davies, W.R. Tulip, and et al. 1989. Conformations of immunoglobulin hypervariable regions. *Nature* 342:877-883.

48. Padlan, E.A. 1990. On the nature of antibody combining sites: unusual structural features that may confer on these sites an enhanced capacity for binding ligands. *Proteins* 7:112-124.

49. Vargas-Madrazo, E., F. Lara-Ochoa, and J.C. Almagro. 1995. Canonical structure repertoire of the antigen-binding site of immunoglobulins suggests strong geometrical restrictions associated to the mechanism of immune recognition. *J Mol Biol* 254:497-504.

50. Webster, D.M., J. Pedersen, D. Staunton, A. Jones, and A.R. Rees. 1994. Antibody-combining sites. Extending the natural limits. *Appl Biochem Biotechnol* 47:119-132; discussion 132-114.

51. Jones, S., and J.M. Thornton. 1996. Principles of protein-protein interactions. *Proc Natl Acad Sci U S A* 93:13-20.

52. Wilson, I.A., and R.L. Stanfield. 1994. Antibody-antigen interactions: new structures and new conformational changes. *Curr Opin Struct Biol* 4:857-867.

53. Lara-Ochoa, F., J.C. Almagro, E. Vargas-Madrazo, and M. Conrad. 1996. Antibody-antigen recognition: a canonical structure paradigm. *J Mol Evol* 43:678-684.

54. Almagro, J.C. 2004. Identification of differences in the specificity-determining residues of antibodies that recognize antigens of different size: implications for the rational design of antibody repertoires. *J Mol Recognit* 17:132-143.

55. Stanfield, R.L., T.M. Fieser, R.A. Lerner, and I.A. Wilson. 1990. Crystal structures of an antibody to a peptide and its complex with peptide antigen at 2.8 A. *Science* 248:712-719.

56. Davies, D.R., and G.H. Cohen. 1996. Interactions of protein antigens with antibodies. *Proc Natl Acad Sci U S A* 93:7-12.

57. Barlow, D.J., M.S. Edwards, and J.M. Thornton. 1986. Continuous and discontinuous protein antigenic determinants. *Nature* 322:747-748.

58. Lo Conte, L., C. Chothia, and J. Janin. 1999. The atomic structure of protein-protein recognition sites. *J Mol Biol* 285:2177-2198.

59. Mariuzza, R.A., and R.J. Poljak. 1993. The basics of binding: mechanisms of antigen recognition and mimicry by antibodies. *Curr Opin Immunol* 5:50-55.

60. Dall'Acqua, W., E.R. Goldman, E. Eisenstein, and R.A. Mariuzza. 1996. A mutational analysis of the binding of two different proteins to the same antibody. *Biochemistry* 35:9667-9676.

61. Goldman, E.R., W. Dall'Acqua, B.C. Braden, and R.A. Mariuzza. 1997. Analysis of binding interactions in an idiotope-antiidiotope protein-protein complex by double mutant cycles. *Biochemistry* 36:49-56.

62. Weiss, G.A., C.K. Watanabe, A. Zhong, A. Goddard, and S.S. Sidhu. 2000. Rapid mapping of protein functional epitopes by combinatorial alanine scanning. *Proc Natl Acad Sci U S A* 97:8950-8954.

63. Meola, A., P. Delmastro, P. Monaci, A. Luzzago, A. Nicosia, F. Felici, R. Cortese, and G. Galfre. 1995. Derivation of vaccines from mimotopes. Immunologic properties of human hepatitis B virus surface antigen mimotopes displayed on filamentous phage. *J Immunol* 154:3162-3172.

64. Felici, F., A. Luzzago, A. Folgori, and R. Cortese. 1993. Mimicking of discontinuous epitopes by phage-displayed peptides, II. Selection of clones recognized by a protective monoclonal antibody against the Bordetella pertussis toxin from phage peptide libraries. *Gene* 128:21-27.

65. Jemmerson, R. 1987. Antigenicity and native structure of globular proteins: low frequency of peptide reactive antibodies. *Proc Natl Acad Sci U S A* 84:9180-9184.

66. Meffre, E., R. Casellas, and M.C. Nussenzweig. 2000. Antibody regulation of B cell development. *Nat Immunol* 1:379-385.

67. Snapper, C.M. 1996. Cytokine Regulation of humoral immunity: basic and clinical aspects. John Wiley and Sons Ltd., West Sussex.

68. O'Connor, B.P., M. Cascalho, and R.J. Noelle. 2002. Short-lived and long-lived bone marrow plasma cells are derived from a novel precursor population. *J Exp Med* 195:737-745.

69. Slifka, M.K., R. Antia, J.K. Whitmire, and R. Ahmed. 1998. Humoral immunity due to long-lived plasma cells. *Immunity* 8:363-372.

70. Manz, R.A., M. Lohning, G. Cassese, A. Thiel, and A. Radbruch. 1998. Survival of long-lived plasma cells is independent of antigen. *Int Immunol* 10:1703-1711.

71. Manz, R.A., S. Arce, G. Cassese, A.E. Hauser, F. Hiepe, and A. Radbruch. 2002. Humoral immunity and long-lived plasma cells. *Curr Opin Immunol* 14:517-521.

72. Janeway, C.A., Travers, P. , Walport, M., Shlomchik, M. 2001. Immunobiology: The Immune System in Health and Disease. Garland Publishing, New York.

73. McHeyzer-Williams, M.G. 1989. Combinations of interleukins 2, 4 and 5 regulate the secretion of murine immunoglobulin isotypes. *Eur J Immunol* 19:2025-2030.

74. Hardy, R.R. 2003. B-cell commitment: deciding on the players. *Curr Opin Immunol* 15:158-165.

75. Cariappa, A., and S. Pillai. 2002. Antigen-dependent B-cell development. *Curr Opin Immunol* 14:241-249.

76. Spriggs, M.K., R.J. Armitage, L. Strockbine, K.N. Clifford, B.M. Macduff, T.A. Sato, C.R. Maliszewski, and W.C. Fanslow. 1992. Recombinant human CD40 ligand stimulates B cell proliferation and immunoglobulin E secretion. *J Exp Med* 176:1543-1550.

77. Jacob, J., R. Kassir, and G. Kelsoe. 1991. In situ studies of the primary immune response to (4-hydroxy-3-nitrophenyl)acetyl. I. The architecture and dynamics of responding cell populations. *J Exp Med* 173:1165-1175.

78. McHeyzer-Williams, M.G., M.J. McLean, P.A. Lalor, and G.J. Nossal. 1993. Antigen-driven B cell differentiation in vivo. *J Exp Med* 178:295-307.

79. Lalor, P.A., G.J. Nossal, R.D. Sanderson, and M.G. McHeyzer-Williams. 1992. Functional and molecular characterization of single, (4-hydroxy-3-nitrophenyl)acetyl (NP)-specific, IgG1+ B cells from antibody-secreting and memory B cell pathways in the C57BL/6 immune response to NP. *Eur J Immunol* 22:3001-3011.

80. McHeyzer-Williams, L.J., and M.G. McHeyzer-Williams. 2005. Antigen-specific memory B cell development. *Annu Rev Immunol* 23:487-513.

81. McHeyzer-Williams, L.J., D.J. Driver, and M.G. McHeyzer-Williams. 2001. Germinal center reaction. *Curr Opin Hematol* 8:52-59.

82. McHeyzer-Williams, M.G., and R. Ahmed. 1999. B cell memory and the long-lived plasma cell. *Curr Opin Immunol* 11:172-179.

83. Oliver, A.M., F. Martin, and J.F. Kearney. 1997. Mouse CD38 is down-regulated on germinal center B cells and mature plasma cells. *J Immunol* 158:1108-1115.

84. Lai, L., N. Alaverdi, L. Maltais, and H.C. Morse, 3rd. 1998. Mouse cell surface antigens: nomenclature and immunophenotyping. *J Immunol* 160:3861-3868.

85. Calame, K.L. 2001. Plasma cells: finding new light at the end of B cell development. *Nat Immunol* 2:1103-1108.

86. Calame, K.L., K.I. Lin, and C. Tunyaplin. 2003. Regulatory mechanisms that determine the development and function of plasma cells. *Annu Rev Immunol* 21:205-230.

87. Orfao, A., and A. Ruiz-Arguelles. 1996. General concepts about cell sorting techniques. *Clin Biochem* 29:5-9.

88. Weaver, J.L. 2000. Introduction to flow cytometry. *Methods* 21:199-201.

89. Newman, J., J.S. Rice, C. Wang, S.L. Harris, and B. Diamond. 2003. Identification of an antigen-specific B cell population. *J Immunol Methods* 272:177-187.

90. Townsend, S.E., C.C. Goodnow, and R.J. Cornall. 2001. Single epitope multiple staining to detect ultralow frequency B cells. *J Immunol Methods* 249:137-146.

91. Collins, A.M., W.A. Sewell, and M.R. Edwards. 2003. Immunoglobulin gene rearrangement, repertoire diversity, and the allergic response. *Pharmacol Ther* 100:157-170.

92. Nemazee, D., and K.A. Hogquist. 2003. Antigen receptor selection by editing or downregulation of V(D)J recombination. *Curr Opin Immunol* 15:182-189.

93. Mainville, C.A., K.M. Sheehan, L.D. Klaman, C.A. Giorgetti, J.L. Press, and P.H. Brodeur. 1996. Deletional mapping of fifteen mouse VH gene families reveals a common organization for three Igh haplotypes. *J Immunol* 156:1038-1046.

94. Kofler, R., S. Geley, H. Kofler, and A. Helmberg. 1992. Mouse variable-region gene families: complexity, polymorphism and use in non-autoimmune responses. *Immunol Rev* 128:5-21.

95. Almagro, J.C., I. Hernandez, M.C. Ramirez, and E. Vargas-Madrazo. 1998. Structural differences between the repertoires of mouse and human germline genes and their evolutionary implications. *Immunogenetics* 47:355-363.

96. Williams, G.S., A. Martinez, A. Montalbano, A. Tang, A. Mauhar, K.M. Ogwaro, D. Merz, C. Chevillard, R. Riblet, and A.J. Feeney. 2001. Unequal VH gene rearrangement frequency within the large VH7183 gene family is not due to recombination signal sequence variation, and mapping of the genes shows a bias of rearrangement based on chromosomal location. *J Immunol* 167:257-263.

97. Yancopoulos, G.D., and F.W. Alt. 1986. Regulation of the assembly and expression of variable-region genes. *Annu Rev Immunol* 4:339-368.

98. Kraj, P., S.P. Rao, A.M. Glas, R.R. Hardy, E.C. Milner, and L.E. Silberstein. 1997. The human heavy chain Ig V region gene repertoire is biased at all stages of B cell ontogeny, including early pre-B cells. *J Immunol* 158:5824-5832.

99. May, R.J., D.O. Beenhouwer, and M.D. Scharff. 2003. Antibodies to keyhole limpet hemocyanin cross-react with an epitope on the polysaccharide capsule of Cryptococcus neoformans and other carbohydrates: implications for vaccine development. *J Immunol* 171:4905-4912.

100. Ofek, G., M. Tang, A. Sambor, H. Katinger, J.R. Mascola, R. Wyatt, and P.D. Kwong. 2004. Structure and mechanistic analysis of the anti-human immunodeficiency virus type 1 antibody 2F5 in complex with its gp41 epitope. *J Virol* 78:10724-10737.

101. Benjamin, D.C., J.A. Berzofsky, I.J. East, F.R. Gurd, C. Hannum, S.J. Leach, E. Margoliash, J.G. Michael, A. Miller, E.M. Prager, and et al. 1984. The antigenic structure of proteins: a reappraisal. *Annu Rev Immunol* 2:67-101.

102. Hill, S.W., and E.E. Sercarz. 1975. Fine specificity of the H-2 linked immune response gene for the gallinaceous lysozymes. *Eur J Immunol* 5:317-324.

103. Metzger, D.W., L.K. Ch'ng, A. Miller, and E.E. Sercarz. 1984. The expressed lysozyme-specific B cell repertoire. I. Heterogeneity in the monoclonal anti-hen egg white lysozyme specificity repertoire, and its difference from the in situ repertoire. *Eur J Immunol* 14:87-93.

104. Maizels, R.M., J.A. Clarke, M.A. Harvey, A. Miller, and E.E. Sercarz. 1980. Epitope specificity of the T cell proliferative response to lysozyme: proliferative T cells react predominantly to different determinants from those recognized by B cells. *Eur J Immunol* 10:509-515.

105. Tainer, J.A., E.D. Getzoff, Y. Paterson, A.J. Olson, and R.A. Lerner. 1985. The atomic mobility component of protein antigenicity. *Annu Rev Immunol* 3:501-535.

106. Takagaki, Y., A. Hirayama, H. Fujio, and T. Amano. 1980. Antibodies to a continuous region at residues 38-54 of hen egg white lysozyme found in a small fraction of anti-hen egg white lysozyme antibodies. *Biochemistry* 19:2498-2505.

107. Hirayama, A., Y. Takagaki, and F. Karush. 1985. Interaction of monoclonal anti-peptide antibodies with lysozyme. *J Immunol* 134:3241-3247.

108. Fujio, H., Takgaki, Y., Mei, X., Kim, Y.U., Sakato, N. 1989. The Immune Response to Structurally Defined Proteins: The Lysozyme Model. Adenine Press, Guilderland. 325-340 pp.

109. Miller, A., Hsu, D.H., Benjamin, C., Ch'ng, L.K., Harvey, M.A., Kaplan, M.A., Kawahara, D. Keller, M.A., Metzger, D.W., Wicker, L.S., Sercarz, E. 1989. The Immune Response to Structurally Defined Proteins: The Lysozyme Model. Adenine Press, Inc., Guilderlalnd. 341-351 pp.

110. Arnon, R., E. Maron, M. Sela, and C.B. Anfinsen. 1971. Antibodies reactive with native lysozyme elicited by a completely synthetic antigen. *Proc Natl Acad Sci U S A* 68:1450-1455.

111. Arnon, R., Sela, M., Pecht, I. 1989. The Immune Response to Structurally Defined Proteins: The Lysozyme Model. Adenine Press, Inc., Guilderland. 315-323 pp.

112. Mozes, E., E. Maron, R. Arnon, and M. Sela. 1971. Strain-dependent differences in the specificity of antibody responses toward lysozyme. *J Immunol* 106:862-864.

113. Ibrahimi, I.M., J. Eder, E.M. Prager, A.C. Wilson, and R. Arnon. 1980. The effect of a single amino acid substitution on the antigenic specificity of the loop region of lysozyme. *Mol Immunol* 17:37-46.

114. Newman, M.A., C.R. Mainhart, C.P. Mallett, T.B. Lavoie, and S.J. Smith-Gill. 1992. Patterns of antibody specificity during the BALB/c immune response to hen eggwhite lysozyme. *J Immunol* 149:3260-3272.

115. Smith-Gill, S.J., T.B. Lavoie, and C.R. Mainhart. 1984. Antigenic regions defined by monoclonal antibodies correspond to structural domains of avian lysozyme. *J Immunol* 133:384-393.

116. Goldbaum, F.A., A. Cauerhff, C.A. Velikovsky, A.S. Llera, M.M. Riottot, and R.J. Poljak. 1999. Lack of significant differences in association rates and affinities of antibodies from short-term and long-term responses to hen egg lysozyme. *J Immunol* 162:6040-6045.

117. Eisen, H.N., and G.W. Siskind. 1964. Variations in Affinities of Antibodies During the Immune Response. *Biochemistry* 155:996-1008.

118. Weigert, M.G., I.M. Cesari, S.J. Yonkovich, and M. Cohn. 1970. Variability in the lambda light chain sequences of mouse antibody. *Nature* 228:1045-1047.

119. Mukherjee, J., A. Casadevall, and M.D. Scharff. 1993. Molecular characterization of the humoral responses to Cryptococcus neoformans infection and

glucuronoxylomannan-tetanus toxoid conjugate immunization. *J Exp Med* 177:1105-1116.

120. Roost, H.P., M.F. Bachmann, A. Haag, U. Kalinke, V. Pliska, H. Hengartner, and R.M. Zinkernagel. 1995. Early high-affinity neutralizing anti-viral IgG responses without further overall improvements of affinity. *Proc Natl Acad Sci U S A* 92:1257-1261.

121. Bachmann, M.F., U. Kalinke, A. Althage, G. Freer, C. Burkhart, H. Roost, M. Aguet, H. Hengartner, and R.M. Zinkernagel. 1997. The role of antibody concentration and avidity in antiviral protection. *Science* 276:2024-2027.

122. Amit, A.G., R.A. Mariuzza, S.E. Phillips, and R.J. Poljak. 1986. Three-dimensional structure of an antigen-antibody complex at 2.8 A resolution. *Science* 233:747-753.

123. Boulot, G., J.L. Eisele, G.A. Bentley, T.N. Bhat, E.S. Ward, G. Winter, and R.J. Poljak. 1990. Crystallization and preliminary X-ray diffraction study of the bacterially expressed Fv from the monoclonal anti-lysozyme antibody D1.3 and of its complex with the antigen, lysozyme. *J Mol Biol* 213:617-619.

124. Harper, M., F. Lema, G. Boulot, and R.J. Poljak. 1987. Antigen specificity and cross-reactivity of monoclonal anti-lysozyme antibodies. *Mol Immunol* 24:97-108.

125. England, P., R. Nageotte, M. Renard, A.L. Page, and H. Bedouelle. 1999. Functional characterization of the somatic hypermutation process leading to antibody D1.3, a high affinity antibody directed against lysozyme. *J Immunol* 162:2129-2136.

126. Bhat, T.N., G.A. Bentley, T.O. Fischmann, G. Boulot, and R.J. Poljak. 1990. Small rearrangements in structures of Fv and Fab fragments of antibody D1.3 on antigen binding. *Nature* 347:483-485.

127. Hawkins, R.E., S.J. Russell, M. Baier, and G. Winter. 1993. The contribution of contact and non-contact residues of antibody in the affinity of binding to antigen. The interaction of mutant D1.3 antibodies with lysozyme. *J Mol Biol* 234:958-964.

128. Dall'Acqua, W., E.R. Goldman, W. Lin, C. Teng, D. Tsuchiya, H. Li, X. Ysern, B.C. Braden, Y. Li, S.J. Smith-Gill, and R.A. Mariuzza. 1998. A mutational analysis of binding interactions in an antigen-antibody protein-protein complex. *Biochemistry* 37:7981-7991.

129. Goldbaum, F.A., C.A. Velikovsky, W. Dall'Acqua, C.A. Fossati, B.A. Fields, B.C. Braden, R.J. Poljak, and R.A. Mariuzza. 1997. Characterization of anti-anti-idiotypic antibodies that bind antigen and an anti-idiotype. *Proc Natl Acad Sci U S A* 94:8697-8701.

130. Jerne, N.K. 1974. Towards a network theory of the immune system. *Ann Immunol (Paris)* 125C:373-389.

131. Russel, M. 1991. Filamentous phage assembly. *Mol Microbiol* 5:1607-1613.

132. Russel, M., H. Whirlow, T.P. Sun, and R.E. Webster. 1988. Low-frequency infection of F- bacteria by transducing particles of filamentous bacteriophages. *J Bacteriol* 170:5312-5316.

133. Russel, M., N.A. Linderoth, and A. Sali. 1997. Filamentous phage assembly: variation on a protein export theme. *Gene* 192:23-32.

134. Gao, C., S. Mao, C.H. Lo, P. Wirsching, R.A. Lerner, and K.D. Janda. 1999. Making artificial antibodies: a format for phage display of combinatorial heterodimeric arrays. *Proc Natl Acad Sci U S A* 96:6025-6030.

135. Jespers, L.S., J.H. Messens, A. De Keyser, D. Eeckhout, I. Van den Brande, Y.G. Gansemans, M.J. Lauwereys, G.P. Vlasuk, and P.E. Stanssens. 1995. Surface expression and ligand-based selection of cDNAs fused to filamentous phage gene VI. *Biotechnology (N Y)* 13:378-382.

136. Fransen, M., P.P. Van Veldhoven, and S. Subramani. 1999. Identification of peroxisomal proteins by using M13 phage protein VI phage display: molecular evidence that mammalian peroxisomes contain a 2,4-dienoyl-CoA reductase. *Biochem J* 340 (Pt 2):561-568.

137. Barbas III, C.F., D.R. Burton, J.K. Scott, and G.J. Silverman. 2001. Phage Display: A Laboratory Manual. Cold Spring Harbour Laboratory Press, Plainview, New York.

138. Devlin, J.J., L.C. Panganiban, and P.E. Devlin. 1990. Random peptide libraries: a source of specific protein binding molecules. *Science* 249:404-406.

139. Scott, J.K., and G.P. Smith. 1990. Searching for peptide ligands with an epitope library. *Science* 249:386-390.

140. Cwirla, S.E., E.A. Peters, R.W. Barrett, and W.J. Dower. 1990. Peptides on phage: a vast library of peptides for identifying ligands. *Proc Natl Acad Sci U S A* 87:6378-6382.

141. Malik, P., T.D. Terry, L.R. Gowda, A. Langara, S.A. Petukhov, M.F. Symmons, L.C. Welsh, D.A. Marvin, and R.N. Perham. 1996. Role of capsid structure and membrane protein processing in determining the size and copy number of peptides displayed on the major coat protein of filamentous bacteriophage. *J Mol Biol* 260:9-21.

142. Petrenko, V.A., G.P. Smith, X. Gong, and T. Quinn. 1996. A library of organic landscapes on filamentous phage. *Protein Eng* 9:797-801.

143. Parmley, S.F., and G.P. Smith. 1988. Antibody-selectable filamentous fd phage vectors: affinity purification of target genes. *Gene* 73:305-318.

144. Bonnycastle, L.L., J.S. Mehroke, M. Rashed, X. Gong, and J.K. Scott. 1996. Probing the basis of antibody reactivity with a panel of constrained peptide libraries displayed by filamentous phage. *J Mol Biol* 258:747-762.

145. Zwick, M.B., J. Shen, and J.K. Scott. 1998. Phage-displayed peptide libraries. *Curr Opin Biotechnol* 9:427-436.

146. Zwick, M.B., J. Shen, and J.K. Scott. 2000. Homodimeric peptides displayed by the major coat protein of filamentous phage. *J Mol Biol* 300:307-320.

147. Craig, L., P.C. Sanschagrin, A. Rozek, S. Lackie, L.A. Kuhn, and J.K. Scott. 1998. The role of structure in antibody cross-reactivity between peptides and folded proteins. *J Mol Biol* 281:183-201.

148. Glaser, S.M., D.E. Yelton, and W.D. Huse. 1992. Antibody engineering by codon-based mutagenesis in a filamentous phage vector system. *J Immunol* 149:3903-3913.

149. Jin, L., B.M. Fendly, and J.A. Wells. 1992. High resolution functional analysis of antibody-antigen interactions. *J Mol Biol* 226:851-865.

150. Van Regenmortel, M.H. 2001. Antigenicity and immunogenicity of synthetic peptides. *Biologicals* 29:209-213.

151. Zwick, M.B., L.L. Bonnycastle, K.A. Noren, S. Venturini, E. Leong, C.F. Barbas, 3rd, C.J. Noren, and J.K. Scott. 1998. The maltose-binding protein as a scaffold for monovalent display of peptides derived from phage libraries. *Anal Biochem* 264:87-97.

152. Smith, G.P., and J.K. Scott. 1993. Libraries of peptides and proteins displayed on filamentous phage. *Methods Enzymol* 217:228-257.

153. Menendez, A., and J.K. Scott. 2005. The nature of target-unrelated peptides recovered in the screening of phage-displayed random peptide libraries with antibodies. *Anal Biochem* 336:145-157.

154. Sambrook, J., Fritsch, E.F., Maniatis, T. 1989. Molecular Cloning: A Laboratory Manual. Cold Spring Harbour Laboratory Press, Plainview, New York.

155. Neu, H.C., and L.A. Heppel. 1965. The release of enzymes from Escherichia coli by osmotic shock and during the formation of spheroplasts. *J Biol Chem* 240:3685-3692.

156. Blake, R.C., 2nd, A.R. Pavlov, and D.A. Blake. 1999. Automated kinetic exclusion assays to quantify protein binding interactions in homogeneous solution. *Anal Biochem* 272:123-134.

157. Zhong, G., G.P. Smith, J. Berry, and R.C. Brunham. 1994. Conformational mimicry of a chlamydial neutralization epitope on filamentous phage. *J Biol Chem* 269:24183-24188.

158. Brinkley, M. 1992. A brief survey of methods for preparing protein conjugates with dyes, haptens, and cross-linking reagents. *Bioconjug Chem* 3:2-13.

159. Schagger, H., H. Aquila, and G. Von Jagow. 1988. Coomassie blue-sodium dodecyl sulfate-polyacrylamide gel electrophoresis for direct visualization of polypeptides during electrophoresis. *Anal Biochem* 173:201-205.

160. Morrissey, J.H. 1981. Silver stain for proteins in polyacrylamide gels: a modified procedure with enhanced uniform sensitivity. *Anal Biochem* 117:307-310.

161. Menendez, A., Bonnycastle, L.C., Pan, O.C.C. and Scott, J.K. 2001. Phage Display: A Laboratory Manual. Cold Spring Harbour Laboratory Press, New York.

162. Chirinos-Rojas, C.L., M.W. Steward, and C.D. Partidos. 1999. A phage-displayed mimotope inhibits tumour necrosis factor-alpha-induced cytotoxicity more effectively than the free mimotope. *Immunology* 96:109-113.

163. Delmastro, P., A. Meola, P. Monaci, R. Cortese, and G. Galfre. 1997. Immunogenicity of filamentous phage displaying peptide mimotopes after oral administration. *Vaccine* 15:1276-1285.

164. Rudbach, J.A., Cantrell, J.L., Ulrich, J.T. 1988. Technological Advances in Vaccine Development. Liss, Inc., New York. 443-454 pp.

165. Chothia, C., A.M. Lesk, M. Levitt, A.G. Amit, R.A. Mariuzza, S.E. Phillips, and R.J. Poljak. 1986. The predicted structure of immunoglobulin D1.3 and its comparison with the crystal structure. *Science* 233:755-758.

166. Braden, B.C., B.A. Fields, X. Ysern, W. Dall'Acqua, F.A. Goldbaum, R.J. Poljak, and R.A. Mariuzza. 1996. Crystal structure of an Fv-Fv idiotope-anti-idiotope complex at 1.9 A resolution. *J Mol Biol* 264:137-151.

167. Freire, E. 1999. The propagation of binding interactions to remote sites in proteins: analysis of the binding of the monoclonal antibody D1.3 to lysozyme. *Proc Natl Acad Sci U S A* 96:10118-10122.

168. England, P., F. Bregegere, and H. Bedouelle. 1997. Energetic and kinetic contributions of contact residues of antibody D1.3 in the interaction with lysozyme. *Biochemistry* 36:164-172.

169. Berman, H.M., J. Westbrook, Z. Feng, G. Gilliland, T.N. Bhat, H. Weissig, I.N. Shindyalov, and P.E. Bourne. 2000. The Protein Data Bank. *Nucleic Acids Res* 28:235-242.

170. Niman, H.L., R.A. Houghten, L.E. Walker, R.A. Reisfeld, I.A. Wilson, J.M. Hogle, and R.A. Lerner. 1983. Generation of protein-reactive antibodies by short peptides is an event of high frequency: implications for the structural basis of immune recognition. *Proc Natl Acad Sci U S A* 80:4949-4953.

171. Bastien, N., M. Trudel, and C. Simard. 1997. Protective immune responses induced by the immunization of mice with a recombinant bacteriophage displaying an epitope of the human respiratory syncytial virus. *Virology* 234:118-122.

172. Meloen, R.H., J.P. Langeveld, W.M. Schaaper, and J.W. Slootstra. 2001. Synthetic peptide vaccines: unexpected fulfillment of discarded hope? *Biologicals* 29:233-236.

173. Arnon, R., R. Tarrab-Hazdai, and T. Ben-Yedidia. 2001. Peptide-based synthetic recombinant vaccines with anti-viral efficacy. *Biologicals* 29:237-242.

174. Steward, M.W. 2001. The development of a mimotope-based synthetic peptide vaccine against respiratory syncytial virus. *Biologicals* 29:215-219.

175. El Kasmi, K.C., S. Fillon, D.M. Theisen, H. Hartter, N.H. Brons, and C.P. Muller. 2000. Neutralization of measles virus wild-type isolates after immunization with a synthetic peptide vaccine which is not recognized by neutralizing passive antibodies. *J Gen Virol* 81:729-735.

176. Scala, G., X. Chen, W. Liu, J.N. Telles, O.J. Cohen, M. Vaccarezza, T. Igarashi, and A.S. Fauci. 1999. Selection of HIV-specific immunogenic epitopes by screening random peptide libraries with HIV-1-positive sera. *J Immunol* 162:6155-6161.

177. Kouzmitcheva, G.A., V.A. Petrenko, and G.P. Smith. 2001. Identifying diagnostic peptides for lyme disease through epitope discovery. *Clin Diagn Lab Immunol* 8:150-160.

178. Dybwad, A., O. Forre, J.B. Natvig, and M. Sioud. 1995. Structural characterization of peptides that bind synovial fluid antibodies from RA patients: a novel strategy for identification of disease-related epitopes using a random peptide library. *Clin Immunol Immunopathol* 75:45-50.

179. Prezzi, C., M. Nuzzo, A. Meola, P. Delmastro, G. Galfre, R. Cortese, A. Nicosia, and P. Monaci. 1996. Selection of antigenic and immunogenic mimics of hepatitis C virus using sera from patients. *J Immunol* 156:4504-4513.

180. Folgori, A., R. Tafi, A. Meola, F. Felici, G. Galfre, R. Cortese, P. Monaci, and A. Nicosia. 1994. A general strategy to identify mimotopes of pathological antigens using only random peptide libraries and human sera. *Embo J* 13:2236-2243.

181. Rousseau, P.G., C.P. Mallett, and S.J. Smith-Gill. 1989. A substantial proportion of the adult BALB/c available B cell repertoire consists of multireactive B cells. *Mol Immunol* 26:993-1006.

182. Palmer, M.a.S.E. 1989. The Immune Response to Structurally Defined Proteins: The Lysozyme Model. Adenine Press, Guilderland. 285-288 pp.

183. Wicker, L.S., C.D. Benjamin, A. Miller, and E.E. Sercarz. 1984. Immunodominant protein epitopes. II. The primary antibody response to hen egg white lysozyme

requires and focuses upon a unique N-terminal epitope. *Eur J Immunol* 14:447-453.

184. McHeyzer-Williams, M.G., G.J. Nossal, and P.A. Lalor. 1991. Molecular characterization of single memory B cells. *Nature* 350:502-505.

185. Jerne, N.K., and A.A. Nordin. 1963. Plaque formation in agar by single antibody-producing cells. *Science* 140:405.

186. Cunningham, A.J., and A. Szenberg. 1968. Further improvements in the plaque technique for detecting single antibody-forming cells. *Immunology* 14:599-600.

187. Roitt, I., Brostoff, J., Male, D. 1998. Immunology. Mosby, London.

188. Czerkinsky, C.C., L.A. Nilsson, H. Nygren, O. Ouchterlony, and A. Tarkowski. 1983. A solid-phase enzyme-linked immunospot (ELISPOT) assay for enumeration of specific antibody-secreting cells. *J Immunol Methods* 65:109-121.

189. Sedgwick, J.D., and P.G. Holt. 1983. A solid-phase immunoenzymatic technique for the enumeration of specific antibody-secreting cells. *J Immunol Methods* 57:301-309.

190. Snapper, C.M., and W.E. Paul. 1987. Interferon-gamma and B cell stimulatory factor-1 reciprocally regulate Ig isotype production. *Science* 236:944-947.

191. Snapper, C.M., and W.E. Paul. 1987. B cell stimulatory factor-1 (interleukin 4) prepares resting murine B cells to secrete IgG1 upon subsequent stimulation with bacterial lipopolysaccharide. *J Immunol* 139:10-17.

192. Purkerson, J.M., M. Newberg, G. Wise, K.R. Lynch, and P.C. Isakson. 1988. Interleukin 5 and interleukin 2 cooperate with interleukin 4 to induce IgG1 secretion from anti-Ig-treated B cells. *J Exp Med* 168:1175-1180.

193. Loughnan, M.S., and G.J. Nossal. 1989. Interleukins 4 and 5 control expression of IL-2 receptor on murine B cells through independent induction of its two chains. *Nature* 340:76-79.

194. Takahashi, Y., A. Ametani, M. Totsuka, and S. Kaminogawa. 1996. The direct cloning of the immunoglobulin VH genes from primary cultured B cells specific for a short peptide. *J Biotechnol* 49:201-210.

195. Morrison, D.C. 1990. Diversity of mammalian macromolecules which bind to bacterial lipopolysaccharides. *In* Cellular and Molecular Aspects of Endotoxin Reactions. Elsevier, Amsterdam. 183-189.

196. Snapper, C.M., H. Yamada, D. Smoot, R. Sneed, A. Lees, and J.J. Mond. 1993. Comparative in vitro analysis of proliferation, Ig secretion, and Ig class switching by murine marginal zone and follicular B cells. *J Immunol* 150:2737-2745.

197. Erickson, L.D., T.M. Foy, and T.J. Waldschmidt. 2001. Murine B1 B cells require IL-5 for optimal T cell-dependent activation. *J Immunol* 166:1531-1539.

198. Babcook, J.S., K.B. Leslie, O.A. Olsen, R.A. Salmon, and J.W. Schrader. 1996. A novel strategy for generating monoclonal antibodies from single, isolated lymphocytes producing antibodies of defined specificities. *Proc Natl Acad Sci U S A* 93:7843-7848.

199. Berzofsky, J.A., J.D. Ahlers, J. Janik, J. Morris, S. Oh, M. Terabe, and I.M. Belyakov. 2004. Progress on new vaccine strategies against chronic viral infections. *J Clin Invest* 114:450-462.

200. Burton, D.R., R.C. Desrosiers, R.W. Doms, W.C. Koff, P.D. Kwong, J.P. Moore, G.J. Nabel, J. Sodroski, I.A. Wilson, and R.T. Wyatt. 2004. HIV vaccine design and the neutralizing antibody problem. *Nat Immunol* 5:233-236.

201. Mascola, J.R., G. Stiegler, T.C. VanCott, H. Katinger, C.B. Carpenter, C.E. Hanson, H. Beary, D. Hayes, S.S. Frankel, D.L. Birx, and M.G. Lewis. 2000. Protection of macaques against vaginal transmission of a pathogenic HIV-1/SIV chimeric virus by passive infusion of neutralizing antibodies. *Nat Med* 6:207-210.

202. Baba, T.W., V. Liska, R. Hofmann-Lehmann, J. Vlasak, W. Xu, S. Ayehunie, L.A. Cavacini, M.R. Posner, H. Katinger, G. Stiegler, B.J. Bernacky, T.A. Rizvi, R. Schmidt, L.R. Hill, M.E. Keeling, Y. Lu, J.E. Wright, T.C. Chou, and R.M. Ruprecht. 2000. Human neutralizing monoclonal antibodies of the IgG1 subtype protect against mucosal simian-human immunodeficiency virus infection. *Nat Med* 6:200-206.

203. Green, N., H. Alexander, A. Olson, S. Alexander, T.M. Shinnick, J.G. Sutcliffe, and R.A. Lerner. 1982. Immunogenic structure of the influenza virus hemagglutinin. *Cell* 28:477-487.

204. Wilson, I.A., H.L. Niman, R.A. Houghten, A.R. Cherenson, M.L. Connolly, and R.A. Lerner. 1984. The structure of an antigenic determinant in a protein. *Cell* 37:767-778.

205. Arnon, R., and M.H. Van Regenmortel. 1992. Structural basis of antigenic specificity and design of new vaccines. *Faseb J* 6:3265-3274.

206. Watanabe, K., K. Yoshioka, H. Ito, M. Ishigami, K. Takagi, S. Utsunomiya, M. Kobayashi, H. Kishimoto, M. Yano, and S. Kakumu. 1999. The hypervariable region 1 protein of hepatitis C virus broadly reactive with sera of patients with chronic hepatitis C has a similar amino acid sequence with the consensus sequence. *Virology* 264:153-158.

207. Moynihan, J.S., D.H. Jones, G.H. Farrar, and C.R. Howard. 2001. A novel microencapsulated peptide vaccine against hepatitis B. *Vaccine* 19:3292-3300.

208. Demangel, C., P. Lafaye, and J.C. Mazie. 1996. Reproducing the immune response against the Plasmodium vivax merozoite surface protein 1 with mimotopes selected from a phage-displayed peptide library. *Mol Immunol* 33:909-916.

209. Van Regenmortel, M.H.V. 1996. Mapping Epitope Structure and Activity: From One-Dimensional Prediction to Four-Dimensional Description of Antigenic Specificity. *Methods* 9:465-472.

210. Foy, T.M., and T.J. Waldschmidt. 1993. Switching capacity of Fc epsilon RII-positive and -negative murine B cells. *Eur J Immunol* 23:3208-3216.

211. Agarwal, A., S. Sarkar, C. Nazabal, G. Balasundaram, and K.V. Rao. 1996. B cell responses to a peptide epitope. I. The cellular basis for restricted recognition. *J Immunol* 157:2779-2788.

212. Agarwal, A., and K.V. Rao. 1997. B cell responses to a peptide epitope: III. Differential T helper cell thresholds in recruitment of B cell fine specificities. *J Immunol* 159:1077-1085.

213. Vijayakrishnan, L., S. Sarkar, R.P. Roy, and K.V. Rao. 1997. B cell responses to a peptide epitope: IV. Subtle sequence changes in flanking residues modulate immunogenicity. *J Immunol* 159:1809-1819.

214. Agarwal, A., B.P. Nayak, and K.V. Rao. 1998. B cell responses to a peptide epitope. VII. Antigen-dependent modulation of the germinal center reaction. *J Immunol* 161:5832-5841.

215. Vijayakrishnan, L., V. Manivel, and K.V. Rao. 1998. B cell responses to a peptide epitope. VI. The kinetics of antigen recognition modulates B cell-mediated recruitment of T helper subsets. *J Immunol* 161:4661-4670.

216. Nayak, B.P., A. Agarwal, P. Nakra, and K.V. Rao. 1999. B cell responses to a peptide epitope. VIII. Immune complex-mediated regulation of memory B cell generation within germinal centers. *J Immunol* 163:1371-1381.

217. Vijayakrishnan, L., K. Natarajan, V. Manivel, S. Raisuddin, and K.V. Rao. 2000. B cell responses to a peptide epitope. IX. The kinetics of antigen binding differentially regulates costimulatory capacity of activated B cells. *J Immunol* 164:5605-5614.

218. Nakra, P., V. Manivel, R.A. Vishwakarma, and K.V. Rao. 2000. B cell responses to a peptide epitope. X. Epitope selection in a primary response is thermodynamically regulated. *J Immunol* 164:5615-5625.

219. Nossal, G.J. 1992. The molecular and cellular basis of affinity maturation in the antibody response. *Cell* 68:1-2.

220. Nossal, G.J. 1994. Differentiation of the secondary B-lymphocyte repertoire: the germinal center reaction. *Immunol Rev* 137:173-183.

221. McLean, G.R., O.A. Olsen, I.N. Watt, P. Rathanaswami, K.B. Leslie, J.S. Babcook, and J.W. Schrader. 2005. Recognition of human cytomegalovirus by human primary immunoglobulins identifies an innate foundation to an adaptive immune response. *J Immunol* 174:4768-4778.

222. Weitkamp, J.H., N. Kallewaard, K. Kusuhara, E. Bures, J.V. Williams, B. LaFleur, H.B. Greenberg, and J.E. Crowe, Jr. 2003. Infant and adult human B cell responses to rotavirus share common immunodominant variable gene repertoires. *J Immunol* 171:4680-4688.

223. Zhou, J., K.R. Lottenbach, S.J. Barenkamp, A.H. Lucas, and D.C. Reason. 2002. Recurrent variable region gene usage and somatic mutation in the human antibody response to the capsular polysaccharide of Streptococcus pneumoniae type 23F. *Infect Immun* 70:4083-4091.

224. Adderson, E.E., P.G. Shackelford, A. Quinn, and W.L. Carroll. 1991. Restricted Ig H chain V gene usage in the human antibody response to Haemophilus influenzae type b capsular polysaccharide. *J Immunol* 147:1667-1674.